Role of endothelial β1 integrin in adaptive peripheral and coronary vascular growth

Inaugural-Dissertation

zur Erlangung des Doktorgrades
der Mathematisch-Naturwissenschaftlichen Fakultät
der Heinrich-Heine-Universität Düsseldorf

vorgelegt von

Anna Branopolski
aus Nowokusnezk (Russische Föderation)

Düsseldorf, Juni 2021

aus dem Institut für Stoffwechselphysiologie
der Heinrich-Heine-Universität Düsseldorf

Gedruckt mit der Genehmigung der
Mathematisch-Naturwissenschaftlichen Fakultät der
Heinrich-Heine-Universität Düsseldorf

Berichterstatter:
1. Prof. Dr. Eckhard Lammert
2. Prof. Dr. Malte Kelm

Tag der mündlichen Prüfung: 14. September 2021

Table of Contents

Summary

Cardiovascular disease (CVD) represents the leading cause of death worldwide and predominantly affects industrialized countries. In consequence of an arterial stenosis or occlusion - a characteristic phenomenon in most CVDs - alterations in blood flow and, hence, in biomechanical forces can stimulate collateral vessel growth in the particular tissue. While the extent of collateral circulation varies between individuals, in an ideal case, it is potentially capable of restoring sufficient blood supply to ischemic territories and thereby preventing tissue necrosis, e.g. in the heart, the brain or in lower extremities. Therefore, with regard to prevention and treatment of acute ischemic events, it is important to explore factors underlying adaptive vascular growth in adults.

In general, adequate vascular response to altered biomechanical forces relies on the sensation and the transduction of mechanical stimuli by endothelial cells. In this context, important players could be mechanosensitive integrins, which are heterodimeric transmembrane glycoproteins. Given the evidence for the central role of β1 subunit containing integrins in endothelial mechanotransduction, the present study focused on the role of this subunit in adult ischemia-induced vascular growth. We analyzed peripheral and coronary vascular growth by using mouse models of hindlimb ischemia (HI) and repetitive myocardial ischemia/reperfusion (RepI/R), respectively, which were combined with pharmacological or genetic manipulations of β1 integrin. Our results demonstrate that endothelial β1 integrin is essential for both HI- and RepI/R-induced vascular growth. In addition, using MRI-based techniques, we examined RepI/R for cardioprotective effects and found a contributing role for endothelial β1 integrin in RepI/R-mediated protection from myocardial infarction. Finally, we performed *in vitro* experiments using primary human cardiac endothelial cells, and found that β1 integrin is essential for mechanically induced cell proliferation as a central component of vascular growth. Moreover, our *in vitro* data provide a potential link between β1 integrin in human cardiac endothelial cells and AKT signaling, endothelial nitric oxide synthase (eNOS) and hepatocyte growth factor (HGF), all of which represent important factors in vascular growth and cardioprotection.

All in all, the present study identifies the key role of endothelial β1 integrin in adaptive vascular growth. This suggests that therapeutic targeting of β1 integrin signaling could represent a potential strategy to stimulate collateral vascular growth as part of prevention or treatment of acute ischemic events in individuals with CVD and/or insufficient collateralization.

Zusammenfassung

Kardiovaskuläre Erkrankungen stellen weltweit die häufigste Todesursache dar und betreffen vor allem Industriestaaten. Als Folge einer arteriellen Stenose oder eines arteriellen Verschlusses - ein charakteristisches Phänomen bei den meisten kardiovaskulären Erkrankungen - können Veränderungen des Blutflusses und damit der biomechanischen Kräfte das Kollateralgefäßwachstum im entsprechenden Gewebe stimulieren. Während das Ausmaß der Kollateralzirkulation von Individuum zu Individuum variiert, ist sie im Idealfall potenziell in der Lage, eine ausreichende Blutversorgung ischämischer Territorien wiederherzustellen und dadurch Gewebsnekrosen zu verhindern, z. B. im Herzen, im Gehirn oder in den unteren Extremitäten. Im Hinblick auf die Prävention und Behandlung von akuten Ischämien in Patienten mit kardiovaskulären Erkrankungen ist es daher wichtig, die Faktoren zu erforschen, die dem adaptiven Gefäßwachstum bei erwachsenen Individuen zugrunde liegen.

Im Allgemeinen beruht eine adäquate vaskuläre Reaktion auf veränderte biomechanische Kräfte auf der Wahrnehmung und Transduktion mechanischer Reize durch Endothelzellen. Wichtige Akteure in diesem Zusammenhang könnten mechanosensitive Integrine sein, bei welchen es sich um heterodimere transmembrane Glykoproteine handelt. Angesichts der Hinweise auf die zentrale Rolle der β1-Integrine bei der endothelialen Mechanotransduktion, konzentrierte sich die vorliegende Studie auf die Rolle dieser Integrine beim adulten Ischämie-induzierten Gefäßwachstum. In Kombination mit pharmakologischer oder genetischer Manipulation von β1-Integrin analysierten wir das periphere und koronare Gefäßwachstum mit Hilfe von Mausmodellen der Hinterlauf-Ischämie (HI) bzw. der repetitiven myokardialen Ischämie/Reperfusion (RepI/R). Unsere Ergebnisse zeigen, dass endotheliales β1-Integrin sowohl für HI- als auch für RepI/R-induziertes Gefäßwachstum essentiell ist. Darüber hinaus untersuchten wir RepI/R mit Hilfe von MRT-basierten Techniken auf kardioprotektive Effekte und entdeckten, dass endotheliales β1-Integrin zum RepI/R-vermittelten Schutz beiträgt. Schließlich führten wir *in vitro* Experimente mit primären humanen kardialen Endothelzellen durch und fanden heraus, dass β1-Integrin essentiell für die mechanisch induzierte Proliferation dieser Zellen ist. Darüber hinaus liefern unsere *in vitro* Daten eine potentielle Verbindung zwischen β1-Integrin in humanen kardialen Endothelzellen und dem AKT-Signalweg, der endothelialen Stickstoffmonoxid-Synthase (eNOS) und dem Hepatozyten-Wachstumsfaktor (HGF), welche wichtige Faktoren des vaskulären Wachstums und der Kardioprotektion darstellen.

Zusammengefasst identifiziert die vorliegende Studie die Schlüsselrolle des endothelialen β1-Integrins beim adaptiven Gefäßwachstum. Dies deutet darauf hin, dass therapeutische Manipulation des β1-Integrin-Signalwegs eine potenzielle Strategie

darstellen könnte, welche der Stimulierung von Kollateralgefäßwachstum im Rahmen der Vorbeugung oder Behandlung von akuter Ischämie bei Individuen mit kardiovaskulären Erkrankungen und/oder unzureichender Kollateralisierung dient.

1. Introduction

1.1 Vascular mechanobiology

1.1.1 Architecture of the blood vasculature

The cardiovascular system is an essential circulatory system consisting of the heart and the blood vasculature. The latter is a hierarchically organized network of vessels, transporting blood on a route of around 100,000 km throughout the human body and thereby supplying all tissues and organs with oxygen and nutrients to maintain their vital functions (Bondareva and Sheikh, 2020; Milnor, 1990).

Blood vessels vary in diameter and composition, depending on their location and function, and are classified into three main groups: arteries, veins and capillaries (Fig. 1.1 a). In the systemic circulation, arteries carry oxygenated blood from the left ventricle of the heart via the aorta to the myocardium itself and to other organs and tissues of the body at high pressure. Arteries repeatedly branch into the smallest arteries called arterioles, which, due to their small diameter, generate a high resistance and are hence involved in the regulation of the blood flow and pressure. Moreover, arterioles give rise to capillary beds, i.e. networks of smallest blood vessels, where gases, nutrients, hormones and metabolic byproducts are exchanged between the blood and the surrounding tissues. Deoxygenated blood is then collected by the smallest veins called venules and carried by large veins back to the heart for reoxygenation in the lungs (Lammert and Axnick, 2012; Lammert and Zeeb, 2014; Schmidt et al., 2011; van Thiel et al., 2017; Willerson et al., 2007).

Both arteries and veins are composed of three tunics (Fig. 1.1 b). The *tunica intima* lines the vascular lumen and consists of a single endothelial cell (EC) monolayer or endothelium. Subendothelial connective tissue and a basal layer of elastic tissue, called internal elastic lamina, surround the endothelium. The adjacent *tunica media* is regarded as the muscular layer of the blood vessels, as it is mainly composed of vascular smooth muscle cells (VSMCs) and elastic fibers. The *tunica externa* represents the outer layer of the blood vascular wall. This layer is mainly composed of collagen and infiltrated with fibroblasts as well as nerve fibers (Lammert and Zeeb, 2014; van Thiel et al., 2017; Zaromitidou et al., 2016). Compared to veins, arteries display a more prominent *tunica media*, which is rich in VSMCs and elastic fibers. Such characteristics provide arteries with sufficient capacity of vasoconstriction and vasodilation to regulate the blood flow and pressure. Unlike arterioles and larger, muscular venules, post-capillary venules represent an exception from the typical composition, since their *tunica media* is composed of an incomplete layer of occasional VSMCs and vascular pericytes. The latter are contractile cells, involved in blood vessel stability and regulation of microvascular blood flow. In contrast to arteries and veins,

capillary walls consist of a single endothelial monolayer with surrounding basal lamina and, depending on the type and location, can be covered by vascular pericytes (McMillan and Harris, 2018; van Thiel et al., 2017; Zhao and Chappell, 2019).

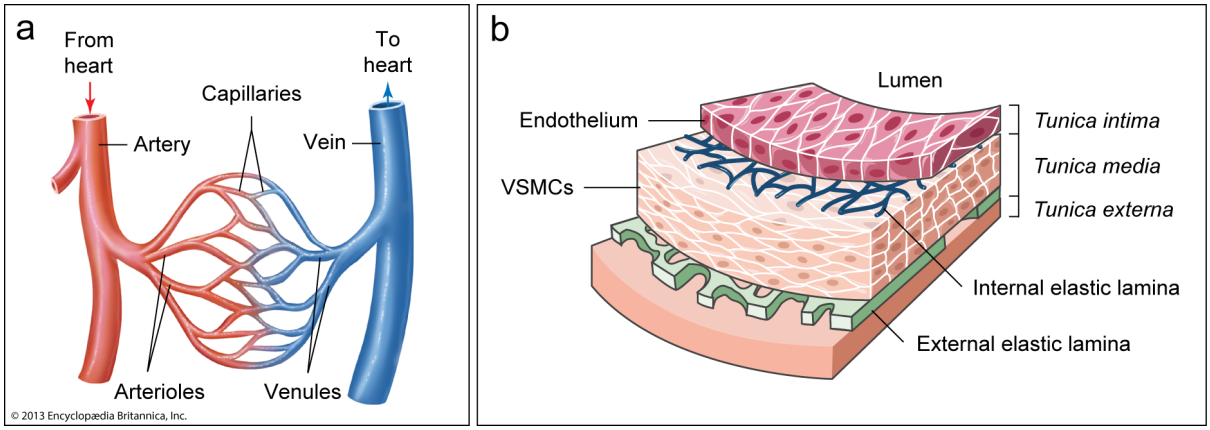

Figure 1.1: Schematic illustration of the vascular architecture.
(a) Hierarchy of blood vessels, represented by a simplified overview of the network, including an artery, arterioles, capillaries, venules and a vein. **(b)** Composition of the arterial wall: *Tunica intima,* lining the vascular lumen and consisting of an endothelial monolayer and internal elastic lamina; *Tunica media,* composed of vascular smooth muscle cells (VSMCs) and external elastic lamina; *Tunica externa*, the outer layer, mainly composed of collagen and infiltrated with fibroblasts and nerve fibers. Modified from Encyclopaedia Britannica Inc. (section: "Anatomy & Physiology") and Servier Medical ART (section: "Cardiovascular System").

1.1.2 Interplay of mechanical forces in the blood vasculature

A tight regulation of blood flow is essential for an adequate perfusion of all tissues under dynamic physiological conditions, and mechanical forces play a fundamental role in this context (Baeyens et al., 2016; Bondareva and Sheikh, 2020; Hahn and Schwartz, 2009). In spite of their diversity, all vertebrate blood vessels contain an EC monolayer. Due to the direct contact to the circulating blood, ECs are permanently exposed to fluid shear stress (FSS) and its changes (Fig. 1.2 a). More specifically, this mechanical force arises from the friction of flowing blood against the endothelium and acts parallel to the luminal surface of the vessel. FSS is directly proportional to blood flow velocity and viscosity and is inversely related to the cube of the vessel radius (Cai and Schaper, 2008; Hoefer et al., 2013; Ma and Bai, 2020). In straight regions of the arterial tree, the blood flow is usually unidirectional, pulsatile and characterized by laminar patterns. In contrast, at bifurcations and curvatures, the blood flow is disturbed by recirculation, leading to heterogeneously distributed low shear stress levels and flow reversal (Chiu and Chien, 2011; Hahn and Schwartz, 2009; Hoefer et al., 2013; Urner et al., 2018). In veins, the flow is generally steadier, and its velocity is lower than in the arteries, as the venous system is less affected by alterations in pressure during

the cardiac cycle and additionally relies on the control of blood flow by venous valves and muscle contractions (Bazigou and Makinen, 2013; Secomb, 2016).

In general, increases in blood flow and hence in FSS are observed under physiological conditions of high demand, e.g. during exercise training. Such increases induce acute vasodilation, counterbalancing the elevated FSS and normalizing it to homeostatic values (Celermajer et al., 1992; Gaenzer et al., 2001; Goto et al., 2007; Pohl et al., 1986; Schretzenmayr, 1933). This adaptive response requires an intact endothelium, which was demonstrated for the first time in 1986 on the canine femoral artery (FA), a conduit artery that provides blood to lower extremities (Pohl et al., 1986). Further studies have proposed that endothelium-derived vasodilators including prostaglandins, hyperpolarizing factors and nitric oxide (NO) are involved in flow-dependent vasodilation (Feletou and Vanhoutte, 1996; Friebel et al., 1995; Rubanyi et al., 1986). The role of NO in this response has been addressed in several human studies by non-invasive measurements of flow-mediated dilation (FMD) in conduit arteries induced by a transient cuff occlusion (Green et al., 2014; Heiss et al., 2005; Kooijman et al., 2008). According to a meta-analysis based on 20 published studies, NO mediates approximately half of the FMD response in humans and is therefore considered as a major regulator of this phenomenon (Green et al., 2014). Mechanistically, increased shear stress triggers the production of NO from L-arginine by the endothelial nitric oxide synthase 3 (eNOS) in the endothelium. eNOS is a membrane protein localized in the caveolae of the plasma membrane or on the Golgi apparatus, and its activity is regulated by post-translational modifications including acetylation and phosphorylation. Once released by ECs, NO diffuses to the adjacent VSMCs, resulting in smooth muscle relaxation and, thereby, vasodilation (Balligand et al., 2009; Kooijman et al., 2008; Qian and Fulton, 2013).

In consequence of vasodilation, the vascular wall experiences stretch perpendicular to blood flow direction, resulting in increased circumferential wall stress (CWS) (Fig. 1.2 b), another relevant mechanical force in vascular mechanobiology (Hoefer et al., 2013; Lu and Kassab, 2011). CWS is not only generated by FSS-induced vasodilation, but also by increased blood pressure levels due to mechanical distention of the blood vessel wall, and is around one thousand-fold larger compared to FSS. Importantly, in contrast to FSS, which acts on and is sensed exclusively by the endothelium, CWS affects all layers of the vascular wall and might thereby directly stimulate other cell types as well (Ma and Bai, 2020; Schaper, 2009; Thondapu et al., 2017).

In addition, it is known that arteries are permanently exposed to low levels of longitudinal wall stress (LWS), deriving from bidirectional longitudinal or axial stretch of the vessel wall due to the cyclic nature of cardiac motion and blood flow (Fig. 1.2 a). Although longitudinal stretch is less characterized and technically difficult to measure, it is assumed to

contribute, together with circumferential stretch, to the distribution of the vessel wall stretch in the vascular system (Cinthio et al., 2006; Ma and Bai, 2020; Thondapu et al., 2017).

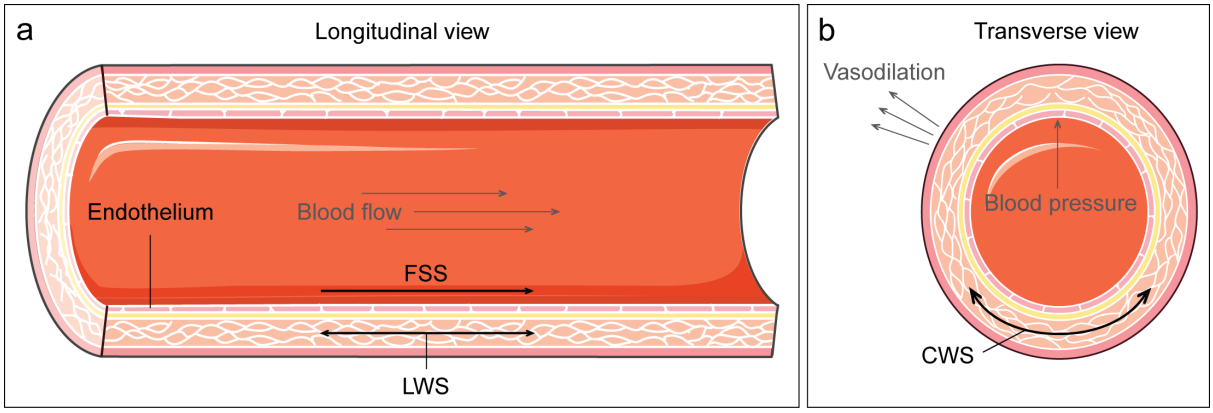

Figure 1.2: Schematic overview of mechanical forces in the blood vasculature.
(a) Illustration of an artery in longitudinal view. Indicated are the blood flow direction and the resulting fluid shear stress (FSS) acting on the endothelium as well as the distribution of longitudinal wall stress (LWS) affecting all layers of the vascular wall. **(b)** Illustration of an artery in transverse view. Indicated is the distribution of circumferential wall stress (CWS) within the vascular wall in consequence of vasodilation and increased blood pressure. Modified from Servier Medical ART (section: "Cardiovascular System"), based on the review by Ma and Bai, 2020.

1.1.3 Endothelial mechanotransduction by β1 integrin

Mechanical forces play a central role in the regulation of vascular development and homeostasis (Baeyens et al., 2016; Baeyens and Schwartz, 2016). To maintain a physiological balance between the distinct forces and the vascular response, the blood vasculature relies on an adequate sensation and transmission of mechanical stimuli. Although the question how different mechanical stimuli are sensed by and transduced in the endothelium has gained much attention during the last decades, the underlying molecular mechanisms are not completely identified. Among several proposed mechanosensors and mechanotransducers, including ion channels, guanine nucleotide-binding proteins (G-proteins) and platelet endothelial cell adhesion molecule-1 (PECAM-1), integrins have emerged as potent players in endothelial mechanotransduction (Baeyens et al., 2016; Baeyens and Schwartz, 2016; Ingber, 1991; Lorenz et al., 2018; Ross et al., 2013; Urner et al., 2018). Integrins are ubiquitously expressed heterodimeric transmembrane receptors. They act as key mediators of interactions between a cell and its microenvironment, including the extracellular matrix (ECM) and surrounding cells, and thereby regulate fundamental cellular processes such as adhesion and migration. Integrins are composed of non-covalently associated α- and β-subunits. To date, 18 types of α-subunits and 8 types of β-subunits have been described that combine to form at least 24 different heterodimers, 12 of which contain the β1-subunit. Each subunit has a large extracellular domain, a single

transmembrane α-helix and a short intracellular domain, except for the large cytoplasmic domain of the β4-subunit. Extracellularly, the heterodimers bind to several extracellular ligands, including fibronectin, laminin and collagen, while intracellularly, they are connected to the cytoskeleton via structural adaptor proteins, such as filamin and talin (Anderson et al., 2014; Hynes, 2002; Kechagia et al., 2019; Legate and Fassler, 2009; Sun et al., 2019).

Integrins are well known for their unique ability to transmit signals bidirectionally, although they lack any intrinsic enzymatic activity. On the one hand, integrin activity is regulated by biochemical interactions of the intracellular domain with the cytosolic adaptor proteins, which is defined as “inside-out” signaling. In particular, integrin activation involves the binding of talin to the cytoplasmic domain of the β-subunit, resulting in profound conformational changes in the heterodimer, and is proposed to occur in three phases. The “bent-closed” or inactive conformer, characterized by a low affinity to the extracellular ligands, shifts to the “extended-closed” state with a low to intermediate affinity and, finally, to the “extended-open” conformer exhibiting the highest ligand affinity (Kechagia et al., 2019; Li and Springer, 2017; Li et al., 2017b; Shattil et al., 2010). On the other hand, in the “outside-in” signaling, integrin binding to extracellular ligands induces conformational changes, contributing to integrin clustering and resulting in the activation of downstream signaling pathways, such as the phosphoinositide 3-kinase (PI3K)/AKT pathway. This activation involves catalytic adaptor proteins, including kinases of the Src and focal adhesion kinase (FAK) families (Anderson et al., 2014; Legate and Fassler, 2009; Shattil et al., 2010).

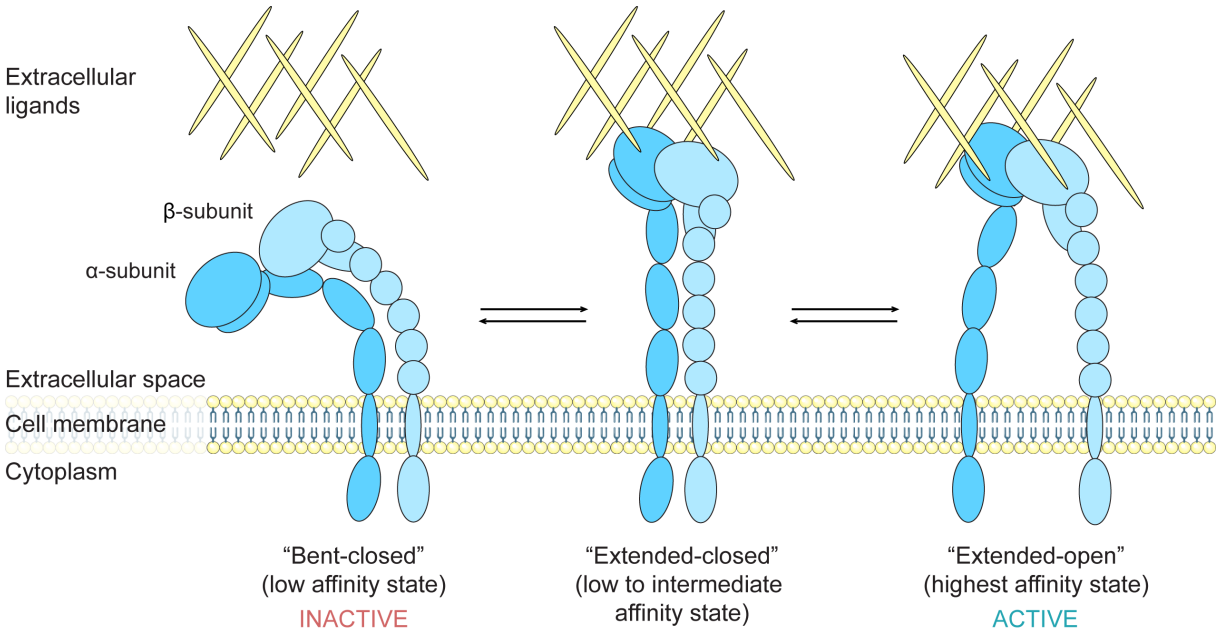

Figure 1.3: Simplified illustration of integrin activation.
In the “bent-closed” or inactive conformation, integrin heterodimer has a low affinity to extracellular ligands. Mechanically or biochemically induced activation of the integrin implies major conformational changes to the “extended-closed” state and to the high-affinity, “extended-open” or active state. Modified from the doctoral dissertation of Dr. Jennifer Axnick (Axnick, 2016), based on the review by Sun et al., 2019

In addition to the above-described biochemical interactions, force application promotes integrin activation and clustering as well (Kechagia et al., 2019; Shattil et al., 2010). Accordingly, several studies showed that mechanical stimuli, exerted on the endothelium, are transmitted into intracellular biochemical signals and converted into cellular responses in an integrin-dependent manner (Jalali et al., 2001; Lorenz et al., 2018; Planas-Paz et al., 2012; Tzima et al., 2001). In this regard, the subunit β1, one of the most abundantly expressed integrin subunits, was shown to be required for mechanically induced activation of vascular endothelial growth factor receptor-3 (VEGFR3) and proliferation of lymphatic ECs (Planas-Paz et al., 2012). Of note, recently published data indicate that this β1 integrin-mediated VEGFR3 activation implies a dissociation of the adaptor protein ILK from the integrin allowing the latter to physically interact with VEGFR3 (Urner et al., 2019). Moreover, the relevance of endothelial mechanosensing by β1 integrin was recently demonstrated in studies on developing and adult murine liver as well as on primary human hepatic ECs. Among others, it was shown that this integrin plays an important role in mechanically induced production and/or release of the hepatocyte growth factor (HGF) as an angiocrine factor involved in liver growth and regeneration (Lorenz et al., 2018). Finally, our recently published data demonstrated that an endothelium-specific deletion of β1 integrin impairs the FMD response of the FA in the hindlimb of adult mice, indicating that mechanosensing by β1 integrin is required for the acute vascular response to hemodynamic changes (Henning et al., 2019). Interestingly, previous *in vitro* studies revealed that application of FSS on bovine aortic ECs (BAECs) triggers the activation of AKT and its downstream target eNOS in a β1 integrin-dependent manner. This finding points to a possible functional interaction between the integrin and eNOS via AKT in the context of hemodynamic changes (Yang and Rizzo, 2013).

A global β1 integrin deficiency results in early embryonic lethality, revealing a crucial role for this integrin subunit in mouse embryonic development in general (Fassler and Meyer, 1995; Stephens et al., 1995). Moreover, in accordance with its critical function in mechanotransduction in ECs, endothelial β1 integrin has been shown to have important functions in the development of the blood vascular system. In particular, its expression was found to be required for developmental angiogenesis, i.e. sprouting of new capillaries from pre-existing vessels, as well as for the formation of patent arteriolar lumen and stable, non-leaky blood vessels (Carlson et al., 2008; Silva et al., 2008; Tanjore et al., 2008; Yamamoto et al., 2015; Zovein et al., 2010). Strikingly, its homozygous deletion was shown to result in embryonic lethality, accompanied by a general developmental delay and smaller embryo sizes (Lei et al., 2008). In addition, concerning adult blood vasculature, it was observed that a heterozygous endothelium-specific β1 integrin deletion leads to an abnormal vascular remodeling in response to blood flow changes after external carotid artery ligation (Lei et al., 2008). Moreover, chronically elevated FSS *in vivo* has been associated with an increased

expression of the heterodimer α5β1 in the vascular wall (Cai et al., 2009). Together, these findings support a crucial role for endothelial β1 integrin in the long-term adaptive processes in adult vascular system under physiological and pathological conditions.

1.2 Collateral growth

1.2.1 Mechanisms of collateral growth

Apart from flow-induced acute vasodilation, conditions of chronically elevated FSS are known to promote a compensatory vascular remodeling reducing it to homeostatic levels (Ma and Bai, 2020). Such sustained increases are observed under physiological conditions, for instance, during pregnancy, normal growth or during frequent exercise training, as well as under pathological conditions of cardiovascular disease (CVD), outlined in 1.3.2 in more detail (Hoefer et al., 2013; Lu and Kassab, 2011). In the year 1980, Kamiya and Togawa provided the first experimental evidence for the adaptive response of an artery to chronically elevated blood flow and hence FSS (Kamiya and Togawa, 1980). More specifically, the researchers constructed an arteriovenous shunt to create increased blood flow in the canine carotid artery and, after a period of about 6 months, observed an increased diameter of this artery. Such blood flow-induced vascular enlargement can also occur in the collateral circulation, a network of small, pre-existing collateral arterioles directly connecting parallel arteries or two different regions of one artery, and found in the heart, the cerebrum and lower extremities of various mammals, including humans. The growth of these collateral arterioles to functional collateral vessels is called arteriogenesis. In the last decades, this process has attracted scientific attention, since functional collateral vessels provide alternative routes for the blood supply, thereby serving as a natural, protective “bypass” system in the setting of arterial occlusive disease (Faber et al., 2014; Gloekler and Seiler, 2007; Liebeskind, 2003; Schaper, 2009; Seiler and Meier, 2014).

It is generally assumed, that an arterial occlusion reduces the pressure in the vessels distal to the occlusion generating a pressure gradient across the collateral network, which remained in a quiescent state until then. As a consequence, the blood flow and FSS increase in bypassing collateral vessels, directly affecting their endothelium and inducing NO-dependent vasodilation (Cai and Schaper, 2008; Mees et al., 2007; Rosenthal and Guyton, 1968; Simons and Eichmann, 2015). Such FSS-mediated activation of ECs is considered as a fundamental step of arteriogenesis that implies an upregulation of genes encoding e.g. monocyte chemoattractant protein-1 (MCP-1) and adhesion molecules leading to recruitment of circulating inflammatory cells. Both activated ECs and recruited inflammatory cells secrete various growth factors, e.g. fibroblast growth factor (FGF),

vascular endothelial growth factor (VEGF) and platelet-derived growth factor (PDGF), as well as proteolytic enzymes including matrix metalloproteases (MMPs) 2 and 9. The former promote proliferation of ECs and SMCs, whereas the latter mediate degradation and remodeling of external elastic lamina and ECM components, facilitating collateral vessel growth (Cai and Schaper, 2008; Heil and Schaper, 2004).

An alternative, more recently suggested type of collateral network development is the *de novo* formation of new arterial vessels (Mac Gabhann and Peirce, 2010; Simons and Eichmann, 2015; Zhang and Faber, 2015). In particular, capillary arterialization was proposed as a possible mechanism of *de novo* arteriogenesis that involves the growth of capillaries and the acquisition of the medial layer, e.g. by the recruitment of VSMCs (Mac Gabhann and Peirce, 2010; Simons and Eichmann, 2015). In addition, a recent work has identified a novel mechanism of arteriogenesis in neonatal mouse hearts, in particular via arterial reassembly (Das et al., 2019). More specifically, in response to a coronary occlusion, arterial ECs were found to migrate away from arteries to capillaries and to reassemble to collateral arteries. This mechanism, however, was not mainly responsible for collateral formation observed in adult mouse hearts (Das et al., 2019). Regardless of the different possible origins of collateral vessels, it is very likely, that EC proliferation is required for all types of the vascular growth in response to arterial occlusion (Das et al., 2019; Moraes et al., 2014; Seiler, 2003).

Arteriogenesis is independent of oxygen levels and usually occurs in normoxic tissues, which fundamentally distinguishes it from angiogenesis that is mainly induced by hypoxia-inducible factor-1α (HIF-1α) under conditions of hypoxia, e.g. in hypoperfused, ischemic territories distal to the occlusion (Heil and Schaper, 2004; Ito et al., 1997). While biomechanical forces are believed to be the key triggers of arteriogenesis, the impact of individual force components is not completely understood. Interestingly, initially increased FSS and the consequent vasodilation seem to have distinct effects. For instance, cyclic stretching of *in vitro* cultured ECs was shown to induce MCP-1 expression, whereas exposure of those cells to FSS had no significant effects (Demicheva et al., 2008). Besides, since FSS decreases with increasing vessel radius in the third power and has been reported to return to homeostatic levels before the process of growth and remodeling is accomplished, other factors such as sustained circumferential stretching, deriving from the radial growth, might be involved in later stages of collateral development (Cai and Schaper, 2008; Ma and Bai, 2020; Rosenthal and Guyton, 1968; Tulis et al., 1998; Unthank et al., 1996). Of note, increased LWS has been suggested as a potent stimulus inducing vascular length adaptation, as indicated by a rapid remodeling in the rabbit carotid artery after an arterial excision, leading to a complete normalization of the longitudinal tension by 7 days. Considering that well-developed collateral vessels display a pronounced corkscrew-shape, longitudinal growth is another major aspect in collateral growth (Jackson et al., 2002; Ma

and Bai, 2020). Although the critical role of biomechanical forces in collateral development is widely recognized, there are still open questions, e.g. regarding the contribution of the particular type of mechanical stimuli and of integrin-dependent mechanotransduction.

1.2.2 Experimental models of adult collateral growth

In order to better characterize collateral expansion and to investigate the underlying mechanisms, several animal models of adult vascular growth have been established and applied during the last decades. Initially, researchers from the cardiovascular field focused on large animal models of arterial occlusion, i.e. canine and porcine models, taking advantage of their blood vessel size. For instance, the vasculature of these species can be visualized by the commonly applied technique of angiography. Moreover, large animals are suitable for measurements of vascular and hemodynamic properties, allowing analyses of both the acute and chronic vascular responses to arterial occlusions in the limb or in the heart (Hoefer et al., 2006; Pohl et al., 1986; Rosenthal and Guyton, 1968; Schaper et al., 1976). Because of high similarity between the human and porcine coronary circulation, the pig is accepted as the most suitable species for preclinical studies related to CVD (Lelovas et al., 2014). Despite these translational advantages, for reasons of availability, handling and associated costs, rodent models of arterial occlusion have been introduced in following years, which brought advantages such as lower costs, higher reproduction rates and availability. For instance, rabbits have been intensively used to analyze the influence of compounds on vascular growth (Bauters et al., 1994; Ito et al., 1997; Pu et al., 1993). However, due to the relatively low availability of transgenic rabbits and specific reagents, rabbit models provide only limited information about involved signaling pathways and cell types (Hoefer et al., 2006; Santini et al., 2020). Therefore, more recently, murine models of arterial occlusion were introduced and have become the tool of choice to investigate mechanistic details of vascular growth, due to accessibility of transgenic mice (Hoefer et al., 2006; Lavine et al., 2013; Limbourg et al., 2009; Moraes et al., 2014; Zhang and Faber, 2015).

Currently, the most commonly used model of peripheral arteriogenesis is the murine model of hindlimb ischemia (HI), which involves a permanent ligation of the FA with a suture. Similar to humans, the murine limb is characterized by the presence of pre-existent collateral blood vessels in the proximal region. These vessels have been shown to experience hemodynamic changes and to undergo luminal expansion following FA ligation, thus reflecting aspects of collateral growth in the context of arterial occlusions in human lower extremities (Henning et al., 2019; Limbourg et al., 2009; Meisner et al., 2013). Given the fact that FA ligation results in a prolonged hypoperfusion and hence ischemia in the lower limb, thereby inducing a HIF-1α-dependent angiogenic response, the model of HI is also suitable

to examine angiogenesis (Bosch-Marce et al., 2007; Couffinhal et al., 1998; Limbourg et al., 2009). Moreover, along with the development of more accurate ultrasound-based imaging, non-invasive *in vivo* measurements of hemodynamics and the diameter of the murine FA have been established in recent years with the aim to investigate the acute vascular response to ischemia-induced hemodynamic changes as a central aspect in the initiation of arteriogenesis (Henning et al., 2019; Schuler et al., 2014).

In addition to HI, murine models of myocardial ischemia have been used in recent years to examine, among others, coronary vascular growth. While all of these models involve an occlusion of the left anterior descending coronary artery (LAD), arising from the left coronary artery (LCA), the type of the occlusion can be categorized as a permanent and a transient one. These two types represent two possible clinical scenarios concerning the success of the reperfusion therapy after an arterial occlusion (Das et al., 2019; Lavine et al., 2013; Lindsey et al., 2018; Zhang and Faber, 2015). The transient occlusion, also termed ischemia and reperfusion (I/R), can be performed in either an open-chest or closed-chest surgery (Kim et al., 2012; Michael et al., 1995; Nossuli et al., 2000). The latter implies a pre-surgery for the implantation of an occluder system, followed by a recovery period. In this way, the occlusion itself does not require thoracotomy, which minimizes the associated local and systemic inflammatory effects and hence better reflects the pathophysiology of clinical myocardial ischemia (Kim et al., 2012; Mitsos et al., 2009). Moreover, with this technique, it is possible to induce ischemic events repeatedly (RepI/R), which is of particular interest when studying aspects of ischemia-induced cardioprotection such as vascular growth, as outlined in 1.3.2 in more detail (Lavine et al., 2013).

While both permanent and transient LAD occlusions have been reported to induce vascular growth in mouse hearts, the nature of the resulting blood vessels differs depending on the chosen conditions. For instance, large-caliber collateral vessels have been detected after a permanent ligation, but not when the LAD was occluded transiently, which was rather found to induce changes on the microvascular level (Das et al., 2019; He et al., 2017; Lavine et al., 2013; Miquerol et al., 2015; Zhang and Faber, 2015). Thus, considering distinct effects of the described occlusion types as well as their respective advantages and disadvantages, an accurate selection of the appropriate mouse model is essential to answer a particular scientific question.

1.3 Cardiovascular disease (CVD)

1.3.1 Pathophysiology of CVD

CVD is the leading cause of death around the globe and accounts for around 30% of all worldwide deaths and even for more than 40% of those in Europe (Di Angelantonio et al., 2019; Timmis et al., 2020). Arterial stenoses or occlusions are characteristic for most CVDs and occur as a consequence of atherosclerosis, i.e. formation of atherosclerotic plaques in arteries. In general, human atherosclerosis is considered as a natural process of ageing which begins in the early teenage years and is accelerated in the presence of additional risk factors such as smoking, hyperlipidemia, hypertension, diabetes mellitus as well as individual genetic predisposition. Endothelial dysfunction is a commonly known condition that precedes and promotes plaque formation and is characterized by an impairment of the regulatory function of the endothelium in vascular homeostasis, such as modulation of vascular diameter (Heiss et al., 2015; Insull, 2009; Wang and Bennett, 2012).

Although the mechanisms of atherosclerosis are still not completely understood, there is evidence that a complex interaction of cellular, molecular and biomechanical factors is responsible for this phenomenon (Kwak et al., 2014; Tyrrell and Goldstein, 2020). In particular, it is known that atherosclerotic plaques form as a result of the accumulation of atherogenic lipoproteins, lipids, inflammatory cells, ECM components and other biomaterials in the blood vascular wall, and that this accumulation predominantly occurs in regions with disturbed flow patterns (Kwak et al., 2014; Wang and Bennett, 2012). Such patterns are characterized by an inhomogeneous distribution of low and low/oscillatory shear stresses with flow reversal and are usually observed near branches, bifurcations and curvatures of the blood vasculature (Chiu and Chien, 2011; Hahn and Schwartz, 2009; Kwak et al., 2014; Steinman, 2002; Traub and Berk, 1998; Urner et al., 2018). Of note, ECs located in regions with disturbed flow, i.e. in atherosclerosis-prone regions, have been reported to exhibit elevated expression levels of inflammatory factors and apoptosis rates as well as a reduced proliferative capacity as signs of endothelial dysfunction (Kwak et al., 2014; Wang and Bennett, 2012). Moreover, disturbed flow was found to reduce eNOS expression in ECs and to promote the production of reactive oxygen species (ROS) by ECs, both of which are also associated with endothelial dysfunction and, thereby, likely contribute to the high susceptibility of the above-mentioned arterial segments for atherogenesis (Balaguru et al., 2016; Harding et al., 2018; Heo et al., 2011; Won et al., 2007). Indeed, experimental studies involving apolipoprotein E knockout mice ($ApoE^{-/-}$) as a model for atherosclerosis could show that disturbed flow generated in the carotid artery induces endothelial dysfunction and atherosclerosis, suggesting a key role for low and low/oscillatory shear stresses in this respect (Cheng et al., 2006; Nam et al., 2009). As opposed to atherogenic effects of low and low/oscillatory shear stresses, high laminar shear stress has been shown to act in an

atheroprotective manner, which probably explains the protection of straight arterial regions from plaque formation observed in humans (Nam et al., 2009; Pan, 2009).

A major reason why endothelial dysfunction plays a crucial role in the initiation of atherosclerosis is the impaired barrier integrity of dysfunctional endothelium. This impairment implies an increase in endothelial permeability, which leads to subendothelial retention of cholesterol-rich apolipoprotein B-containing lipoproteins, e.g. low-density lipoprotein (LDL) that is subsequently oxidized to oxLDL (Gimbrone and Garcia-Cardena, 2016; Mundi et al., 2018). As an atherogenic factor, oxLDL stimulates ECs and VSMCs to recruit monocytes into the subendothelial space, where these monocytes differentiate into macrophages. Finally, oxLDL is internalized by macrophages transforming them to foam cells, which recruit further inflammatory cells and promote oxidative modification of LDL (Bentzon et al., 2014; Gimbrone and Garcia-Cardena, 2016). The resulting fatty streak can regress or evolve to an atherosclerotic plaque, depending on the molecular environment (Fig. 1.4). For instance, some lipoproteins are known to act in an atheroprotective manner, e.g. high-density lipoproteins (HDL) promote the removal of cholesterol from the vascular wall and reduce inflammation and oxidative stress. Thus, HDL counteracts the atherogenic effects of LDL, thereby preventing or attenuating further plaque progression (Bentzon et al., 2014; Linton et al., 2000). In addition, given its essential role in the maintenance of vascular homeostasis, functional eNOS is discussed to play a key role in atheroprotection, whereas dysfunction of eNOS leads to formation of ROS, thereby contributing to LDL oxidation and inflammation (Hong et al., 2019).

Atherosclerotic plaques develop over decades and result in luminal narrowing or stenosis, obstructing the blood flow and giving rise to transient ischemic events in the affected tissue (Bentzon et al., 2014; Lavine et al., 2013). At the same time, altered biomechanics in the affected collateral network induce collateral growth, as described in 1.2.1 in more detail. Arterial stenosis can affect the heart (coronary artery disease or CAD), the brain (cerebral ischemic disease) or the extremities, mostly the legs (peripheral artery disease or PAD). CAD is the most common form of CVD, and its manifestation is usually indicated by transient episodes of chest pain, a symptom that is called stable *angina pectoris* (Fujita et al., 1987; Lavine et al., 2013).

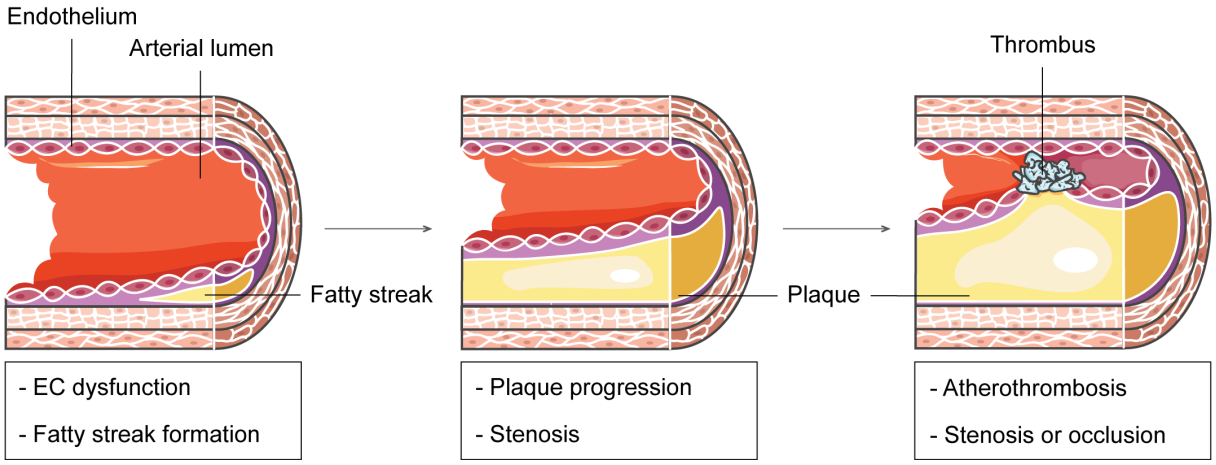

Figure 1.4: Simplified overview of atherosclerotic plaque formation.
Endothelial dysfunction in atherosclerosis susceptible regions leads to an enhanced retention of atherogenic apolipoprotein B-containing proteins (e.g. low-density lipoprotein, LDL) in the subendothelial space, initiating the formation of fatty streaks as precursors of atherosclerotic plaques (left). Further lipoprotein accumulation and inflammation promote plaque progression, resulting in arterial stenosis (middle). Atherothrombosis is defined as thrombus formation in later stages of atherosclerosis, which can result in stenosis or a fatal complete occlusion of the artery (right). Modified from Servier Medical ART (section: “Cardiovascular System”), based on the reviews by Bentzon et al., 2014 and Linton et al., 2000.

Later stages of atherosclerosis are characterized by an increased risk for atherothrombosis, i.e. formation of intraluminal thrombi, which is most frequently caused by plaque rupture (Fig. 1.4). These thrombi may further narrow the arterial lumen or even result in a complete, sustained arterial occlusion, severe ischemia and, finally, tissue necrosis in the heart (myocardial infarction (MI)), the brain (ischemic stroke) or lower extremities (Bentzon et al., 2014).

As a logical consequence of the known risk factors for atherosclerosis, current prevention strategies involve lowering of LDL-cholesterol levels, antihypertensive and antidiabetic therapies, reduction or elimination of smoking and unhealthy dietary behaviors, and promotion of physical activity. In fact, these strategies have decreased the risk of cardiovascular events, and the optimized thrombolytic and reperfusion therapies have improved the overall prognosis of patients with CVD in the last years (Insull, 2009; Mensah et al., 2017). However, this disease remains the leading death cause worldwide, arousing the need to identify new targets for developing additional preventive and therapeutic approaches.

1.3.2 Relevance of vascular growth in CVD

The existence of collateral vessels in the human heart was documented by the anatomist Richard Lower of Amsterdam about 350 years ago for the first time (Lower, 1669; Seiler and Meier, 2014). A report by Herrik from 1912 describing a patient who survived an

acute coronary occlusion in the presence of such vessels provided the first indication of their protective role in the setting of CAD (Herrick, 1983; Seiler and Meier, 2014). Following *post mortem* examinations in the 50ies of the last century revealed that coronary collateral vessels are present at birth and that their number and diameter are increased in hearts displaying signs of CAD (Baroldi et al., 1956). Few years later, Fulton found a positive correlation between the amount of large-caliber collateral vessels and the duration of *angina pectoris* (Fulton, 1963). In accordance, more recent clinical studies have shown that one third of patients with CAD exhibit functionally sufficient collateral network to prevent myocardial ischemia during brief coronary balloon occlusions by restoring blood flow to the affected tissue, whereas only one fifth to one quarter of individuals with normal coronary arteries display this feature (Pohl et al., 2001; Wustmann et al., 2003). These findings collectively suggest that collateral growth is particularly triggered in the presence of arterial stenosis or occlusion(s). Of note, the latter observation indicates that functionally sufficient coronary collateral vessels, which are missing in the majority of humans without CAD, can develop under physiological conditions as well. For instance, exercise training was reported to enhance the collateral circulation in patients both with and without CAD (Mobius-Winkler et al., 2016; Zbinden et al., 2004; Zbinden et al., 2007). On the other hand, individual genetic background is discussed to influence the capability of tissues to collateralize (Chittenden et al., 2006). Moreover, arteriogenesis was shown to be impaired under conditions of diabetes resulting in poorly developed collateral network (Abaci et al., 1999; Shen et al., 2018).

A number of clinical investigations focusing on the compensatory role of collateral vessels in the setting of CVD demonstrated their protective effects in the myocardium, cerebrum and lower extremities (Habib et al., 1991; Liebeskind et al., 2011; Ziegler et al., 2010). For instance, it was shown that a well-developed coronary collateral circulation is capable of reducing the infarct size, preserving cardiac function and even increasing survival rates after an acute coronary occlusion, as compared to poorly developed ones (Fig. 1.5) (Elias et al., 2017; Elsman et al., 2004; Gloekler and Seiler, 2007; Habib et al., 1991; Hatada et al., 2001; Sabia et al., 1992; Yoon et al., 2009). Given these protective effects of collateral vessels, it is likely that poor collateralization may contribute to the increased risk of and impaired outcomes after MI, ischemic stroke and peripheral artery occlusion observed among patients with diabetes (Thiruvoipati, 2015).

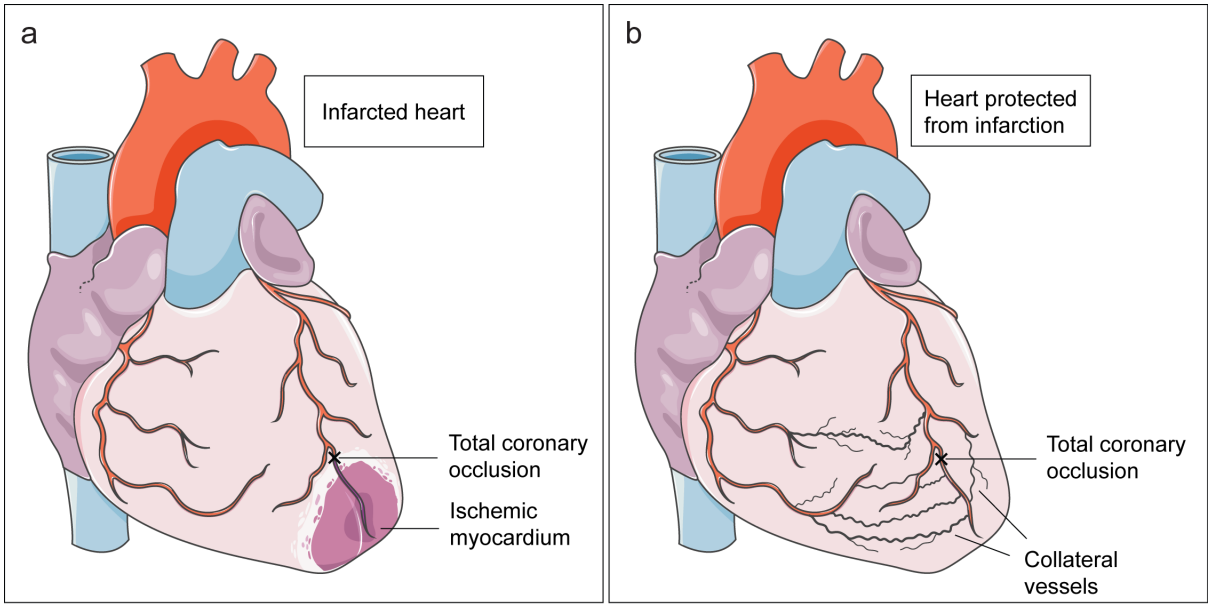

Figure 1.5: Simplified presentation of the protective role of coronary collateral vessels. **(a)** In absence of functional collateral network, obstructed coronary flow due to a total arterial occlusion results in critical ischemia and MI (indicated in purple). **(b)** In the ideal situation, functional collateral network compensates for the flow obstruction, supplying tissue downstream of the occlusion, and protects the heart from critical ischemia and MI. Modified from Servier Medical ART (section: "Cardiovascular System"), based on the article by Gloekler and Seiler, 2007.

Considering that the enhancement of tissue perfusion through collateral expansion may be protective in the context of CVD, stimulation of vascular growth has become an attractive tool in both prevention and treatment of severe ischemic events, especially in individuals with insufficient collateral network. However, clinical trials addressing this process have provided inconsistent results with no, or modest beneficial effects (Brakenhielm and Richard, 2019; van Royen et al., 2009). Thus, until now, an approved arteriogenic therapy is missing, underlining the need for further investigations on the mechanisms underlying adult vascular growth to identify novel molecular targets in this respect (Brakenhielm and Richard, 2019; Henry et al., 2003; van Royen et al., 2009; Ziegler et al., 2010; Zimarino et al., 2014).

1.4 Aims of the study

Although there is growing evidence for the importance of β1 integrin in endothelial mechanotransduction, which is a pivotal component in vascular remodeling processes, to our knowledge, the role of this integrin subunit in peripheral and coronary vascular adaptation to ischemia has not been investigated yet. Therefore, the major aim of this study was to investigate whether endothelial β1 integrin is involved in adaptive peripheral and coronary vascular growth.

For studies of peripheral vascular growth, we employed the mouse model of HI as a model for PAD. First, we examined the subcellular localization of β1 integrin in ECs of mouse hindlimb arteries and the impact of HI on its expression. Afterwards, we analyzed the calf and the thigh muscles for capillary and arteriole formation as well as investigated the impact of an EC-specific β1 integrin deletion on both processes.

In order to study aspects of coronary growth, we applied the mouse model of RepI/R, which is supposed to reflect the transient ischemic events occurring in patients with CAD. We first analyzed the hearts for cardiac EC proliferation and arteriole formation after RepI/R, particularly differentiating between ischemic and non-ischemic myocardium. Next, we investigated the effects of pharmacological inhibition and an EC-specific deletion of β1 integrin on RepI/R-induced coronary growth.

We further wished to investigate the role of β1 integrin in ischemia-induced cardioprotection. To this end, we first analyzed the effect of RepI/R on the outcome after an additional MI (60 min I/R), as evaluated by MRI-based analyses of the infarct size and the cardiac function. Afterwards, we examined the effects of pharmacological and genetic manipulation of β1 integrin in this respect.

Further, we aimed to find out whether a link exists between β1 integrin and proliferation of primary human cardiac ECs. Therefore, we analyzed the proliferation of these cells upon siRNA-mediated silencing of β1 integrin. To address further aspects related to vascular growth and cardioprotection, we analyzed the expression of eNOS in and the secretion of HGF by human cardiac ECs dependent on β1 integrin expression and activation, respectively.

Finally, we aimed to investigate the role of β1 integrin-mediated mechanotransduction in mechanically stimulated proliferation of human cardiac ECs. We first explored the effects of transient exposure of these cells to increased FSS and stretching on cell proliferation. Afterwards, we analyzed the impact of siRNA-mediated β1 integrin silencing on mechanically induced phosphorylation of the kinase AKT, a downstream effector of integrins, as well as on cell proliferation.

By filling the gap in knowledge on the role of endothelial β1 integrin in adaptive peripheral and coronary vascular growth, this study contributes to the understanding of endothelium-dependent mechanisms underlying this clinically relevant process.

The following chapter contains parts described in our publications Henning et al., 2019 and Henning et al., 2021.

2. Experimental procedures

2.1 *In vivo* methods

2.1.1 Mouse lines

For *in vivo* studies presented in this thesis, adult mouse lines with different background were used. For experiments with pharmacological inhibition of β1 integrin, 10 to 15 weeks old, male wild-type C57BL/6J mice (Janvier) were intravenously injected with 100 µl β1 integrin blocking antibody (BD Bioscience, 555002) or control antibody (BD Bioscience, 553957) at a concentration of 1 mg/ml one day before each 15 minute-ischemia/reperfusion (I/R). For endothelium-specific deletion of the *Itgb1* gene (*Itgb1*^{iECKO}), *Cdh5-Cre*^{ERT2}; homozygous *Itgb1*-loxP mice were crossed with homozygous *Itgb1*-loxP mice (Benedito et al., 2009; Potocnik et al., 2000; Wang et al., 2010). For knockout induction, *Cdh5-Cre*^{ERT2}; homozygous *Itgb1*-loxP mice received intraperitoneal tamoxifen injections of 100 µl (75 mg/kg bodyweight) for 5 consecutive days. Age-matched, male *Cdh5-Cre*^{ERT2} mice were equally treated with tamoxifen and were used as controls. All experiments were performed according to the German animal protection laws (Animal Ethics Committee of the Landesamt für Natur, Umwelt und Verbraucherschutz, North-Rhine-Westphalia).

2.1.2 Genotyping

For genotyping, mouse tail tips were incubated in 100 µl lysis buffer (78 µl dH_2O, 20 µl 5x Go Taq Flexi buffer (Promega) and 2 µl Proteinase K (740 mAnsonU/ml, PanReac AppliChem)) at 56°C and 300 rpm overnight. The lysates were centrifuged at 13.000 rpm for 10 minutes, and the supernatants were used for polymerase chain reaction (PCR). PCR samples were prepared as follows:

PCR sample component	Volume
dH_2O	12.8 µl
Go Taq Flexi buffer (5x, Promega)	4 µl
$MgCl_2$ (25 mM, Promega)	1.2 µl
dNTPs (10 mM, Sigma)	0.4 µl
Primer forward (100 pmol/µl, Eurofins)	0.2 µl
Primer reverse (100 pmol/µl, Eurofins)	0.2 µl
Taq Polymerase (5 U/µl, MPI-CGB)	0.2 µl
Lysate	1 µl

Primer sequences and PCR product sizes are listed in the following table:

Mouse line	Primer sequence (5'→3')	Product size
Cdh5-Cre^{ERT2}	Forward: GCCTGCATTACCGGTCGATGCAACGA; Reverse: GTGGCAGATGGCGCGGCAACACCATT	Cre-positive: ~700 bp
Itgb1-loxP	Forward: AGGTGCCCTTCCCTCTAGA; Reverse: GTGAAGTAGGTGAAAGGTAAC	Wt: ~350 bp; Homo: 450 bp; Het: ~350 bp and ~450 bp

PCR was performed using a Professional Trio Thermocycler (Biometra) according to the following protocols:

Cdh5-Cre^{ERT2}	***Itgb1-loxP***
94°C, 5 min	94°C, 2 min
35x 94°C, 30 s	35x 94°C, 1 min
58°C, 30 s	58°C, 1 min
72°C, 1 min	72°C, 1 min
72°C, 5 min	72°C, 10 min
10°C, ∞	10°C, ∞

For separation of PCR products, the samples were loaded on a 1% agarose (Bio-Budget Technologies) gel containing 3% SYBR® Safe DNA Gel Stain (Invitrogen). Subsequently, gel electrophoresis was run at 120 V for 20-30 minutes using a Power PAC 1000 or a 3000 System (BioRad). The gel images were acquired by using a Chemidoc^{TM} XRS Imaging System (BioRad).

2.1.3 Induction of hindlimb ischemia (HI)

To investigate the aspects of peripheral vascular growth, the mouse hindlimb ischemia model (HI) was used, as previously described (Henning et al., 2019). For anaesthesia, the mice were intraperitoneally injected with ketamine (100 mg/kg bodyweight, KetanestS®, Pfizer Pharma GmbH) and xylazine (10 mg/kg bodyweight, Rompun TM, Bayer Healthcare). The mice were fixed on a pre-heated surgery table and kept at 37°C during throughout the procedure. Respiration was ensured by ventilation with oxygen-enriched room air (O_2 40%) and isoflurane (1.5%-2% vol., Piramal Healthcare) via a ventilation mask. Following hindlimb hair removal and skin disinfection with Octenisept (Schülke), a vertical longitudinal incision was made in the region between the groin and the knee on the inside of the thigh. The vascular plexus including the femoral artery (FA) was exposed. The FA was carefully prepared, ensuring that the vein and the nerve remained intact. Subsequently, the FA was ligated distal to the origin of the *arteria profunda femoris* with two sutures (Prolene 5/0, Ethicon) and cut between the two sutures. After closing the wound, the animal was allowed to recover.

2.1.4 Induction of myocardial ischemia/reperfusion (RepI/R)

For studies of coronary growth, an established closed-chest model of repetitive myocardial ischemia (RepI/R) was applied (Dewald et al., 2004; Henning et al., 2021; Lavine et al., 2013; Nossuli et al., 2000). In the first step, an occluder system was implanted around the LAD. For this, mice were intraperitoneally anaesthetized with ketamine (100 mg/kg bodyweight, KetanestS®, Pfizer Pharma GmbH) and xylazine (10 mg/kg bodyweight, RompunTM, Bayer Healthcare), intubated and ventilated with oxygen-enriched air (40% O_2) and isoflurane (2% vol., Piramal Healthcare). Mice were transferred in a supine position on a preheated surgery table, which was constantly kept at 37°C. After hair removal in the thoracic region and skin disinfection, the heart was exposed by opening the skin as well as widening the muscles and the ribs. The pericardium was removed, and a 7/0 prolene suture (Ethicon) was carefully positioned underneath the proximal left anterior descending coronary artery (LAD). Both suture ends were threaded through a 1 mm polyethylene (PE) tube, serving as an occluder in later steps. The thorax was closed, and the suture ends were placed into a subcutaneous pocket.

After recovery (2 days for proliferation studies with pharmacological inhibition and cardioprotection studies; 7 days for remaining analyses), mice were anesthetized with isoflurane (3% vol., Piramal Healthcare) and oxygen-enriched air (40% O_2). Subsequently, the isoflurane dosage was reduced to 2%, the skin was disinfected, and ECG electrodes were fixed on the paws. After opening the skin, the suture ends were fixed to two magnets.

LAD occlusion was introduced by exerting tension on the suture for 15 minutes, and reperfusion was achieved by releasing the tension. Induction of ischemia and the following reperfusion were verified by detection of ST-segment elevation in ECG. Introduction of 15-minute I/R was performed each second day. For analysis of RepI/R-mediated cardioprotection, an experimental myocardial infarction (MI) was additionally performed by inducing I/R for 60 minutes, according to the protocol described for 15-minute I/R.

2.1.5 Implantation of osmotic pumps

In order to label proliferating cells *in vivo*, osmotic pumps (Alzet, model 1002) were filled with 20 mg/ml 5-bromo-2'-deoxyuridine (BrdU, Sigma) in phosphate buffer saline (PBS) and implanted in the first 15-minute I/R episode. For this, abdominal skin hair was removed, the skin was disinfected and an incision was made in the skin and the peritoneum. Afterwards, one osmotic pump was placed intraperitoneally. The skin was closed, and the pumps remained in mice until heart isolation.

2.1.6 Magnetic resonance imaging (MRI)

To determine the infarct size and left-ventricular (LV) myocardial function after 60-minute I/R, ^{1}H MR imaging was performed at 400,13 MHz using a Bruker AVANCE III 9.4 T Wide Bore NMR spectrometer (Bruker), controlled by ParaVision 5.1 software, as previously described (Bonner et al., 2014; Haberkorn et al., 2017). Therefore, mice were anaesthetized with isoflurane (1.5% vol., Piramal Healthcare) and were kept at body temperature throughout the procedure. The forepaws and the left hindpaw were attached to ECG electrodes (Klear-Trace; CAS Medical Systems). For detection of respiration, a pneumatic pillow was placed at the back of the mouse. Vital parameters were monitored by means of the M1025 system (SA Instruments, Stony Brook) and used for synchronization of the measurements with cardiac and respiratory motions. For late-gadolinium-enhancement (LGE) imaging, which was applied to visualize infarcted tissue on the first day after MI, mice were intraperitoneally treated with a gadolinium-based contrast agent (Gd-DTPA, 0.2 mmol per kg body weight) immediately prior to the measurement. For analysis of cardiac function, ^{1}H cine MR-loops in short axis orientation were acquired by means of an ECG- and respiration-triggered segmented fast gradient echo cine sequence with steady state precession (FISP). LV ejection fraction, which is defined as the difference between the end-diastolic and the end-systolic volumes divided by the end-diastolic volume, was quantified by manually selecting the ventricular borders using the ParaVision region-of-interest (ROI) tool (Bruker). Infarct size was determined by manual selection of LGE-positive area, related to the calculated LV volume.

2.1.7 Hindlimb and heart isolation

For isolation of hindlimbs and hearts, mice were intraperitoneally anaesthetized with ketamine (100 mg/kg bodyweight, Ketanest ®, Pfizer Pharma GmbH) and xylazin (10 mg/kg bodyweight, Rompun TM, Bayer Healthcare). In dorsal position, the hearts were exposed via thoracotomy. To wash and to fix the myocardia and the hindlimbs, the left and the right ventricles were perfused with ice-cold $PBS^{Ca2+,Mg2+}$ containing 1 µM adenosine (Sigma) and subsequently with 4% PFA. Afterwards, the isolated hindlimbs and hearts were prepared for cryosectioning (see 2.5.1).

2.2 *In vitro* methods

2.2.1 Primary human cell culture and transfection

In vitro experiments were performed with primary human coronary artery endothelial cells (HCAECs, PB-CH-182-2011) and human cardiac microvascular endothelial cells (HCMVECs, PB-CH-151-4011), purchased from PELOBiotech and cultured in microvascular endothelial cell growth medium kit enhanced (PELOBiotech) at 37 °C and 5% CO_2 in a humidified incubator. HCAECs were plated on 6-, 12-, 24-well plates, stretch or flow chambers and were used up to passage 6. All used cell culture dishes were pre-coated with speed coating solution (PELOBiotech).

To induce a knockdown of the *ITGB1* gene (β1 integrin) *in vitro*, HCAECs were transfected with one of the following *ITGB1*-siRNAs (β1-siRNA) (Invitrogen) via electroporation (4D-NucleofectorTM System, LONZA):

β1-siRNA1: 5′-CCUAAGUCAGCAGUAGGAACAUUAU-3′;
β1-siRNA2: 5′-UGCGAGUGUGGUGUCUGUAAGUGUA-3′;
β1-siRNA3: 5′-GGGAGCCACAGACAUUUACAUUAAA-3′.

As control for non-specific effects of siRNA transfection, a non-targeting siRNA (Invitrogen) with a similar GC content was used. Both the targeting and the control siRNAs were used at a concentration of 250 nM. Transfected cells were incubated for 48 h prior to lysis or mechanical stretching. Knockdown efficiencies were analyzed by quantitative real-time PCR (qPCR) and Western blotting.

2.2.2 Mechanical stimulation of HCAECs by stretching or shear stress

To expose HCAECs to mechanical stretch, non-transfected or siRNA-transfected cells were first plated on STREX stretch chambers (BioCat, ST-CH-04-BR) and allowed to grow for 24 to 48 h. Afterwards, stretch of 25% was performed manually (STREX Inc.). To analyze β1 integrin activation, HCAECs were stretched for 15 minutes and immediately fixed for further immunofluorescence staining (see 2.5.2). To detect AKT phosphorylation, the cells were stretched for 30 minutes and immediately lysed for Western blotting analysis (see 2.4). In the case of proliferation studies, the cells were stretched for 30 minutes, incubated under unstretched conditions for further 90 minutes and stained for proliferation markers (see 2.2.3 and 2.5.2).

In vitro flow chamber studies were performed by means of the ibidi® pump system according to the manufacturer's protocol. Therefore, the cells were carefully seeded on slides (µ-Slide $I^{0.4}$ Luer, ibidi®) without creating air bubbles. After cell attachment, shear stress was applied at a rate between 5 and 20 dynes/cm^2.

2.2.3 *In vitro* BrdU proliferation assay

For proliferation studies without mechanical stimulation, HCAECs were grown on cover glasses (VWR) in 24-well plates. After incubation with 10 µM BrdU for 2 h, the cells were immediately washed with cold PBS and fixed with a fixative solution (70% ethanol, 30% glycine 50 mM) for 20 minutes on ice for BrdU-staining.

To determine the proliferation rate after stretching, BrdU was added into stretching chambers immediately prior to stretching. Subsequently, the cells were unstretched, incubated for further 90 minutes and immediately fixed with the fixative solution. In case of flow chamber experiments, BrdU was added and the shear stress was simultaneously increased 2- to 4-fold for 30 minutes and reset to the basal condition. After a 90-minute incubation under basal shear stress, the cells were fixed.

Fixed cells were pre-treated with 2 M HCl for 20 minutes at room temperature (RT) and subsequently neutralized with 0.1 M sodiumtetraborate for 2 minutes at RT. Cells were washed with washing buffer containing 0.5% BSA and 0.02% NaN_3 (1%, Sigma-Aldrich) in PBS. Immunofluorescence staining was performed using mouse anti-BrdU antibody (BD Bioscience, 555627) as primary and anti-mouse antibody conjugated with AlexaFluor488 (Invitrogen Molecular probes) as secondary antibodies. All antibodies were diluted in washing buffer. Cell nuclei were counterstained with DAPI (Sigma). Alternatively, proliferating ECs were labeled with Ki67 (see 2.5.2).

2.2.4 Activation of β1 integrin in HCMVECs and detection of hepatocyte growth factor (HGF) in the supernatant

Antibody-mediated stimulation of β1 integrin and HGF secretion studies were performed with HCMVECs. For this, HCMVECs grown on cover glasses in 24-well plates were incubated with 1 µl/ml β1 integrin activating antibody (R&D, MAB17782) or isotype control antibody (R&D, MAB002) in serum-free medium for 90 minutes. The supernatants were centrifuged for 10 minutes at maximum speed and 4°C, collected and directly used for enzyme-linked immunosorbent assay (ELISA). The assay was performed by means of the human HGF Quantikine® HGF ELISA Kit (DHG00, R&D) according to the manufactrurer's protocol.

2.3 Quantitative real-time PCR

Total RNA extraction from cultured HCAECs was performed using RNeasy Mini Kit (QIAGEN) according to the manufacturer's protocol. RNA-concentrations and quality were measured by means of Bio Mate 3 (Thermo Fisher Scientific). Equal amounts of RNA were applied for cDNA-synthesis, performed with SuperScript® II Reverse Transcriptase (Invitrogen) according to the manufacturer's protocol. The samples used for quantitative real-time PCR (qPCR) were prepared as follows:

Sample component	Volume
2x Brilliant III Ultra-Fast SYBR® Green QPCR Master Mix	5 µl
Primer mix (3 µM forward primer; 3 µM reverse primer)	1 µl
dH_2O	1 µl
cDNA (diluted 1:10 in dH_2O)	3 µl

qPCR was performed by means of the thermal cycler Stratagene Mx3000P (Agilent Technologies). Primer sequences and the applied thermal profile are described in the following tables.

Gene	Primer sequence (5'→3')
human *ITGB1*	Forward: CATCTGCGAGTGTGGTGTCT; Reverse: GGGGTAATTTGTCCCGACTT
human *RPLP0*	Forward: GCAGCATCTACAACCCTGAAG; Reverse: CACTGGCAACATTGCGGAC
human *HPRT*	Forward: TGACACTGGCAAAACAATGCA; Reverse: GGTCCTTTTCACCAGCAAGCT
human *B2M*	Forward: TTTCATCCATCCGACATTGA; Reverse: CCTCCATGATGCTGCTTACA

Thermal profile
95°C, 2 min 40x 95°C, 5 s 60°C, 20 s 95°C, 1 min 55°C, 30 s 95°C, 30 s

All samples were analyzed in triplicates. The knockdown efficiency of β1 integrin was calculated based on the ΔΔCT method, where *RPLP0*, *HPRT* and *B2M* were used as housekeeping genes for normalization (Livak and Schmittgen, 2001).

2.4 Western blotting

For protein expression and phosphorylation studies, Western blotting was performed. Therefore, cultured HCAECs were carefully washed with cold PBS and subsequently lysed in RIPA buffer, containing following components:

RIPA buffer component	Concentration
Tris/HCl (pH 7.4)	50 mM
NaCl	150 mM
IGEPAL	1%
Na-deoxycholate	0.25%
EDTA	1 mM
Protease inhibitors (cOmplete Protease Inhibitor Cocktail Tablets, Roche)	1x
Phosphatase inhibitors (Phosphatase Inhibitor Cocktail Tablets, Roche)	1x

For SDS-PAGE, the protein lysates were mixed with 4x Laemmli buffer (Bio-Rad) and β-Mercaptoethanol (Roth), heated at 95°C for 5 minutes and loaded on a 4-15% SDS-gel (Bio-Rad). The protein separation was run at 200 Volt for 1 to 1.5 h using 1x Tris/Glycine/SDS running buffer (Bio-Rad) and Mini PROTEAN Tetra Cell (Bio-Rad). After protein transfer with Trans-Blot Turbo Transfer System (Bio-Rad) at 2.5 A for 24 minutes, the

polyvinylidene fluoride (PVDF) membranes were blocked with blocking solution ($PBS^{Ca2+, Mg2+}$ containing 5% BSA (AppliChem) and 0.5% Tween-20 (AppliChem)) for 1 h at RT. The membranes were then incubated with primary antibodies, diluted in blocking solution, overnight at 4°. The used primary antibodies are listed in the following table.

Primary antibody	Dilution
rabbit anti-GAPDH (Abcam, ab9485)	1:5000
rabbit anti-phospho(S473)-AKT (Cell Signaling, 4060)	1:1000
rabbit anti-AKT (Cell Signaling, 4691)	1:2000
goat anti-β1 integrin (Santa Cruz, sc-6622)	1:2000

Secondary antibodies, listed below, were diluted in blocking solution and incubated for 1 h at RT.

Secondary antibody	Dilution
HRP-conjugated donkey anti-rabbit (Cell Signaling Technologies, 7074)	1:2000
HRP-conjugated donkey anti-goat (Jackson ImmunoResearch, 705-035-147)	1:5000

For protein expression and phosphorylation studies, a semi-quantitative band density analysis was performed (FIJI, ImageJ NIH), where GAPDH was used as housekeeping protein for normalization.

2.5 Immunofluorescence staining and analysis

2.5.1 Immunohistochemistry of hindlimb and cardiac cryosections

Isolated hindlimbs and hearts were fixed in 4% PFA overnight at 4°C, followed by a stepwise equilibration with 15% and 30% sucrose solved in $PBS^{Ca2+,Mg2+}$, overnight at 4°C. After embedding in Tissue-Tek O.C.T. compound (Sakura Finetek GmbH), tissues were stored at -80°C and used for preparation of 12 µm transversal cryosections by means of a cryostat (Microtome HM 560, Thermo Fisher Scientific). Obtained cryosections were collected on SuperFrost-slides (Thermo Fisher Scientific).

For immunofluorescence staining, the cryosections were first blocked with blocking solution consisting of $PBS^{Ca2+,Mg2+}$ with 5% normal donkey serum (NDS, Jackson ImmunoResearch), 3% bovine serum albumin (BSA, Applichem) and 0.2% Triton X-100

(AppliChem) for 1 h at RT in humidified chambers. Primary antibodies, listed in the following table, were diluted in blocking solution and incubated for 1 h at RT or overnight at 4°C.

Primary antibody	Dilution
Mouse anti-αSMA Cy3 (Sigma, C6198)	1:200
Goat anti-CD31 (R&D, AF3628)	1:20
Rat anti-β1 integrin (Merck Millipore, MAB1997)	1:200
Rat anti-IgG2b (isotype control, Abcam, ab18541)	1:100
Rat anti-BrdU (Abcam, ab6326)	1:200

The slides were then washed and incubated with DAPI (1:1000) and secondary antibodies, diluted in blocking solution, for 45 minutes at RT in the dark. Used secondary antibodies are listed in the following table.

Secondary antibody	Dilution
Donkey anti-goat/rat/mouse AlexaFluor488 (Invitrogen Molecular Probes)	1:500
Donkey anti-rat/mouse AlexaFluor555 (Invitrogen Molecular Probes)	1:500
Donkey anti-goat/rat/mouse Cy5 (Invitrogen Molecular Probes)	1:500
Donkey anti-goat NL557 (R&D, NL001)	1:200

The slides were washed, mounted with Fluoroshield (Sigma) and dried for 30 minutes at RT before imaging or storage at 4°C.

Apoptotic ECs were detected by means of an *in situ* cell death detection kit (TUNEL) according to the manufacturer's protocol (12156792910, Roche).

In the case of BrdU labeling, cryosections of BrdU-treated mice were incubated with 2 M HCl for 30 minutes at 37°C, neutralized with 0.1 M sodiumtetraborate and subsequently immunostained as described above.

2.5.2 Immunofluorescence staining of cultured ECs

For immunofluorescence staining, the cells grown either on coverslips, in flow chambers or stretching chambers were briefly washed with cold PBS, fixed with 4% PFA for 30 minutes at RT and stored at 4°C. After blocking with 1% BSA, 5% NDS, 0.2% Triton-X100 in PBS for 1 h at RT, the cells were incubated with primary antibodies overnight at 4°C and subsequently treated with DAPI and secondary antibodies for 1 h at RT. The used primary antibodies are listed in the following table, and the secondary antibodies are listed above (see 2.5.1).

Primary antibody	Dilution
mouse anti-act. β1 integrin (Merck Millipore, MAB2079Z)	1:100
Rabbit anti-Ki67 (Abcam, ab15580)	1:500

Coverslips or the bottoms of stretch chambers were placed on slides and mounted with Fluoroshield. In the case of flow experiment, the cells were mounted directly in the ibidi® flow chambers, which are suitable for imaging.

2.5.3 Microscopy and analysis

Immunofluorescence images were acquired by confocal fluorescence microscopy with a laser-scanning microscope (either with Zeiss LSM 710 or Leica TCS SP8) and analyzed with the open-source software FIJI (ImageJ, NIH). To identify capillaries and arterioles, hindlimb and cardiac sections were stained for PECAM-1 as a marker for ECs and for αSMA as a marker for smooth muscle cells.

For quantification, hindlimb capillaries and arterioles were counted manually. Capillaries were related to the number of muscle fibers, whereas arterioles were normalized to tissue area (in mm^2), determined by means of the freehand selection tool in FIJI. Coronary arterioles and proliferating cardiac ECs were also counted manually and related to tissue area (in mm^2). Cryosections located at papillary muscle level and below the occlusion were used for coronary growth studies. Hearts with considerable tissue damage and myocardial areas containing part of the occlusion system were excluded from analysis. Proliferating HCAECs were counted manually and normalized to total nuclei number.

2.6 Statistics

Statistical analysis was performed in Prism (GraphPad Software Inc.). To compare two groups, a paired or an unpaired two-tailed Student's *t*-test was applied. For multiple comparisons, a one-way ANOVA and a subsequent Dunnett's post-hoc test were performed. Differences with $p \leq 0.05$ were considered as statistically significant. Exact values are shown for $p \leq 0.1$. All quantitative data are shown as the mean ± standard error of the mean (SEM).

2.7 Personal contributions

Anna Branopolski was supervised by Prof. Dr. Lammert and performed the experiments presented in the following figures without other contributors: 3.4, 3.5, 3.23, 3.24, 3.26, 3.27, 3.28, 3.29, 3.30, 3.31.

Hindlimb ischemia experiments: Dr. Carina Henning performed hindlimb ischemia surgeries in wild-type mice and a part of immunohistochemical analyses. Dr. Dominik Schuler performed hindlimb ischemia surgeries in adult Itgb1^{iECKO} mice and corresponding control mice. Dr. Jelle Postma supported the imaging at Leica TCS SP8 for studies of subcellular localization of β1 integrin. Anna Branopolski performed most of immunohistochemical analyses of hindlimb sections.

Myocardial ischemia experiments: Dr. Carina Henning performed myocardial ischemia surgeries as well as the analyses of MR images and BrdU incorporation. Anna Branopolski performed MR imaging and immunohistochemical analyses of cardiac sections (except for BrdU incorporation).

In vitro experiments: Dr. Carina Henning performed Western blotting for eNOS-expression in transfected human cardiac ECs. Anna Branopolski performed cell culture, transfections and remaining analyses of ECs.

Anna Branopolski and Dr. Carina Henning were both involved in the project and share several data sets for their theses. Anna Branopolski and Dr. Carina Henning contributed to equal amounts to figures 3.6, 3.7, 3.8, 3.9, 3.14, 3.15, 3.20, 3.21 and 3.25. Anna Branopolski contributed to one-quarter and Dr. Carina Henning to three-quarter to figures 3.16, 3.17 and 3.22. Dr. Carina Henning completely contributed to figures 3.12, 3.13, 3.18 and 3.19.

The following chapter contains parts described in our publications Henning et al., 2019 and Henning et al., 2021.

3. Results

3.1 Expression of endothelial β1 integrin in murine hindlimb under physiological and pathological conditions

Blood vascular endothelium is directly exposed to hemodynamic changes under both physiological and pathological conditions such as in the setting of arterial stenosis or occlusion. Endothelial mechanosensation and mechanotransduction are critical for an adequate vascular response to these changes (Baeyens and Schwartz, 2016). Considering the important role of β1 integrin for mechanotransduction in endothelial cells (ECs) (Lorenz et al., 2018; Planas-Paz et al., 2012; Yang and Rizzo, 2013), we aimed to investigate its potential regulatory role in adaptive vascular response to an arterial occlusion in adult mice. Therefore, we first analyzed the expression of β1 integrin in the wild-type mouse hindlimb at baseline conditions with regard to its localization in ECs. Afterwards, we studied the influence of pathological conditions on the expression of endothelial β1 integrin using mouse hindlimb ischemia (HI) model of peripheral artery disease (PAD).

3.1.1 Subcellular localization of endothelial β1 integrin in the murine hindlimb

A large number of studies proposed that integrins act as mechanosensors exclusively at the basal side of the endothelium, although they are also expressed at the apical side to a small extent (Katsumi et al., 2004). However, more recent *in vitro* studies revealed that apically localized integrins can be activated by mechanical forces as well (Xanthis et al., 2019; Yang and Rizzo, 2013). In order to address the question on which side of murine vascular endothelium β1 integrin may act as mechanosensor, we immunohistochemically assessed its subcellular localization in the hindlimb, taking advantage of the large-diameter arteries present in the murine thigh muscle. For this, adjacent cross-sections of the thigh were stained with an antibody against β1 integrin, and the staining specificity was evaluated using an isotype-matched control antibody. Qualitative examination of the signal pattern revealed β1 integrin staining at both the basal and apical surfaces of ECs in the investigated artery (Fig. 3.1 a-d). Importantly, control antibody application did not result in any considerable signal, thus verifying the staining specificity of the used antibody against β1 integrin (Fig. 3.1 e-h).

In conclusion and in line with previous studies, these observations indicate that β1 integrin is localized at both the basal and apical surfaces of ECs in mouse hindlimb arteries and thus may be involved in flow sensing on both sides.

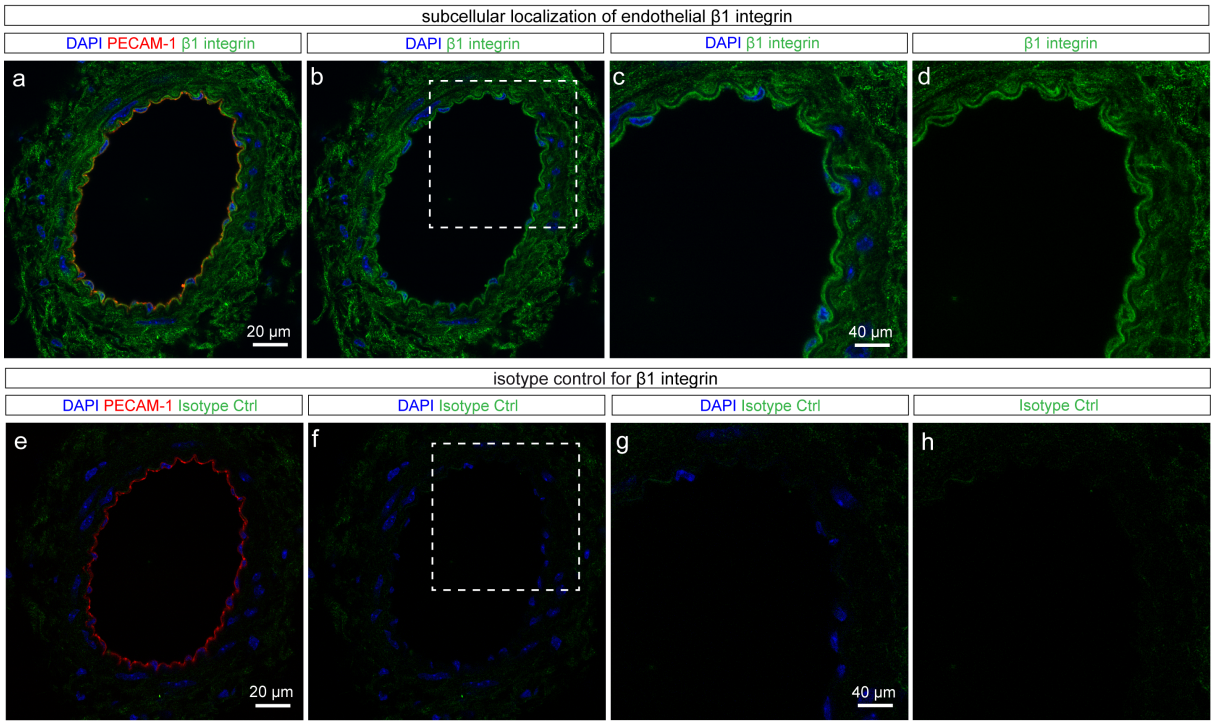

Figure 3.1: β1 integrin is localized at the basal and apical surfaces of ECs in murine hindlimb. Immunohistochemical assessment of the expression pattern of endothelial β1 integrin by using two adjacent transversal sections through murine thigh. **(a-h)** Representative immunofluorescence images of adjacent sections through an artery in the thigh. Sections were stained for DAPI (cell nuclei, blue), platelet endothelial cell adhesion molecule-1 (PECAM-1, red), **(a-d)** β1 integrin (green) or **(e-h)** IgG2b as isotype control (Isotype Ctrl, green). Anna Branopolski performed, and Dr. Jelle Postma supported the presented experiment.

3.1.2 Expression of β1 integrin upon femoral artery (FA) ligation

Vascular adaptation to ischemia can be classified into an acute and a chronic response. As part of this project, non-invasive *in vivo* measurements of flow-mediated dilation (FMD) revealed endothelial β1 integrin to be required for the acute vascular response to hemodynamic changes. More specifically, mice lacking endothelial β1 integrin showed a reduced FMD in the femoral artery (FA), induced by a transient cuff occlusion of the distal hindlimb, compared to control mice (Henning et al., 2019). Given this finding, we aimed to investigate the role of this integrin in the chronic or long-term vascular adaptation to an arterial occlusion. Therefore, the well-established mouse model of HI was used, which is suitable for evaluating the vascular response in form of angiogenesis and arteriogenesis (Limbourg et al., 2009). Here, a permanent ligation of the FA with a suture (Fig. 3.2 a) results in ischemia of the tissue distal to the occlusion, and, in hemodynamic changes in the

vascular network of the hindlimb (Meisner et al., 2013; Schaper, 2009). With respect to the potential function of endothelial β1 integrin as a mechanosensor in the vascular response to these changes, we examined whether its expression is affected by FA ligation in the thigh and the calf (Fig. 3.2 b). For this, murine hindlimbs were exposed to either a permanent FA ligation or a sham surgery and harvested at day 7 post-surgery. The obtained transversal sections of the thighs and the calves were analyzed for the mean intensity of β1 integrin immunostaining in the endothelium defined as PECAM-1-positive area.

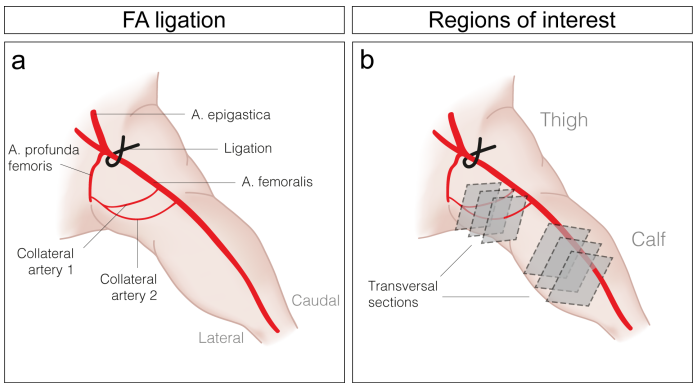

Figure 3.2: Schematic overview of femoral artery (FA) ligation and analyzed regions.
(a) Schematic illustration of the arterial tree in the mouse hindlimb, including the arteria epigastica, arteria profunda femoris, arteria femoralis (FA) and two collateral arteries as well as the position of the surgical knot for ligation of the FA. **(b)** Differentiation between the thigh and the calf regions for the preparation and analysis of hindlimb sections, indicated by the dashed squares. Illustration is modified from Henning et al., 2019.

The analysis of the thigh muscles showed a slight HI-induced upregulation of endothelial β1 integrin expression, as indicated by a non-significant increase of the mean intensity of the integrin staining in ECs by 22% after FA ligation compared to sham surgery (Fig. 3.3 a-d, i). In the calf muscles, the upregulation of β1 integrin expression seemed to be stronger, as indicated by a significantly increased mean intensity by 35% upon FA ligation compared to sham surgery (Fig. 3.3 e-h, j). Consistently, the integrin heterodimer α5β1 was reported to be upregulated in collateral vessels upon FA ligation in rabbits, however, without specifying the cell type (Cai et al., 2009). Interestingly, the differential upregulation of endothelial β1 integrin in the calf and thigh muscles correlates with the observation of a more prolonged perfusion reduction in the calf muscle compared to the thigh muscle, as shown by Laser-Doppler measurements and near-infrared imaging (Henning, 2019). This correlation points to a possible hypoxia-dependent upregulation of the integrin, which is supported by previously published data suggesting a hypoxia-inducible factor-1α (HIF-1α)-dependent induction of β1 integrin expression in fibroblasts by hypoxia *in vitro* (Keely et al., 2009).

Taken together, the results indicate that HI results in an upregulation of endothelial β1 integrin expression in the entire hindlimb, with a stronger induction in the hypoxic calf,

thereby pointing to a possible role of endothelial β1 integrin in the chronic vascular adaptation in response to HI.

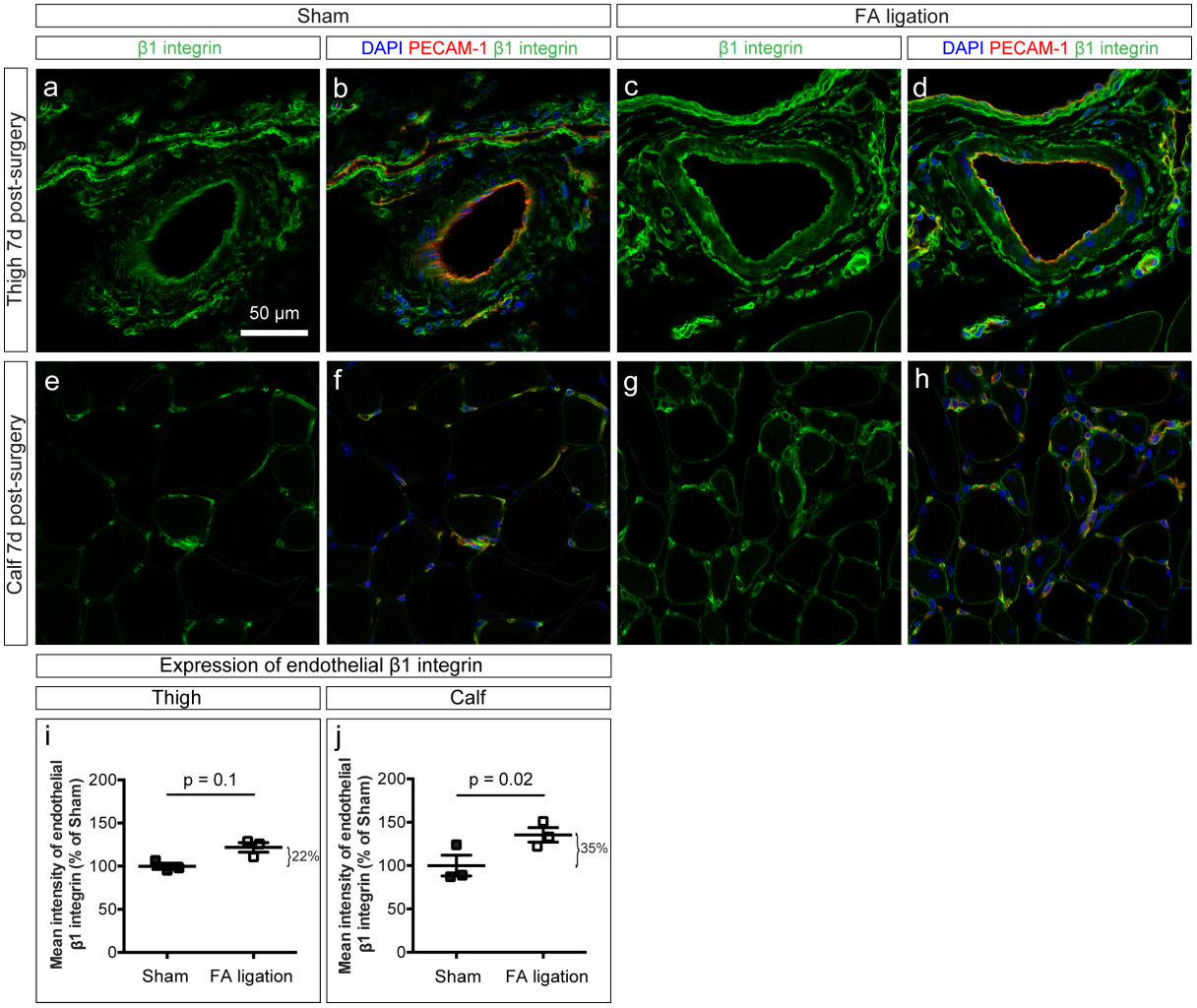

Figure 3.3: HI results in an increased expression of endothelial β1 integrin.
Analysis of endothelial β1 integrin expression in the thigh and calf muscles 7 days after FA ligation. **(a-h)** Representative LSM images of vessels in **(a-d)** the thigh and **(e-h)** the calf of WT mice 7 days after **(a, b, e, f)** sham operation and **(c, d, g, h)** FA ligation. Sections were stained for DAPI (cell nuclei, blue), PECAM-1 (ECs, red) and β1 integrin (green). **(i, j)** Quantification of endothelial β1 integrin expression in **(i)** thigh and **(j)** calf, represented by the mean intensity of β1 integrin staining within PECAM-1 positive areas, shown as percentage of sham hindlimb. All values are mean ± standard error of the mean (SEM) with n = 3 per condition; statistical significance was determined using paired, two-tailed Student's t-test. Anna Branopolski and Carina Henning performed the presented experiment.

3.2 Role of endothelial β1 integrin in peripheral vascular growth

Integrins containing the β1 subunit were shown to play an essential role in embryonic and postnatal vascular development (Carlson et al., 2008; Silva et al., 2008; Tanjore et al., 2008; Yamamoto et al., 2015; Zovein et al., 2010). However, there is still a lack of knowledge on the role of β1 integrin in the adult vascular growth as a result of chronic

adaptation to ischemia. Based on the findings that endothelial β1 integrin is required for the acute response to ischemia and that its expression is increased upon a permanent FA ligation, we next aimed to investigate its role in ischemia-induced vascular growth by studying the impact of EC-specific β1 integrin deletion on capillary and arteriole densities after HI (Henning et al., 2019).

3.2.1 Assessment of EC-specific knockout of β1 integrin in *Itgb1*^{iECKO} mice

For deletion of the *Itgb1* gene in ECs, we employed transgenic mice expressing tamoxifen-inducible *Cre* recombinase only in the endothelium. More specifically, *Cdh5-Cre*^{ERT2}; homozygous *Itgb1*-loxP mice were crossed with homozygous *Itgb1*-loxP mice (Benedito et al., 2009; Potocnik et al., 2000; Wang et al., 2010). To obtain EC-specific knockout of the *Itgb1* gene (referred to as *Itgb1*^{iECKO}), *Cdh5-Cre*^{ERT2}; homozygous *Itgb1*-loxP mice, were intraperitoneally injected with tamoxifen. Regarding possible off-target effects of *Cre* recombinase, *Cdh5-Cre*^{ERT2} mice were also treated with tamoxifen and were used as controls for *Itgb1*^{iECKO} mice.

For assessment of the knockout efficiency, overall three different methods were applied. A successful *Cre*-mediated recombination in *Itgb1*^{iECKO} mice was first confirmed by means of an X-Gal staining for β-Galactosidase activity (Henning et al., 2019). Second, a qPCR analysis of ECs sorted by Magnetic Activated Cell Sorting (MACS) revealed a statistically non-significant reduction of *Itgb1*-mRNA by 52% in *Itgb1*^{iECKO} mice as compared to control mice (Henning et al., 2019). In addition, the knockout induction was assessed by immunohistochemical staining of hindlimb cross-sections. The analysis of β1 integrin staining in the endothelium revealed a statistically significant reduction of the mean intensity by 28% in *Itgb1*^{iECKO} mice compared to control mice, additionally supporting a successful knockout induction in ECs of the hindlimb (Fig. 3.4).

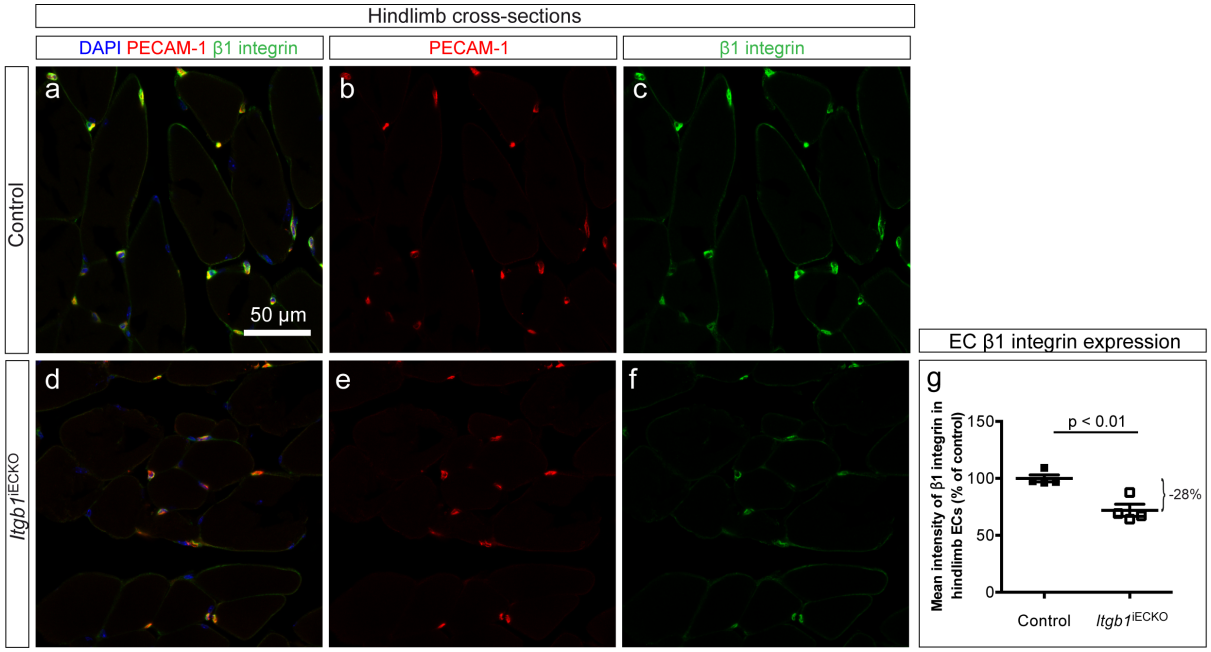

Figure 3.4: Endothelial β1 integrin expression is reduced in the hindlimb of tamoxifen-treated *Itgb1*^{iECKO} mice.
Immunohistochemical assessment of β1 integrin expression in *Itgb1*^{iECKO} and control mice after tamoxifen treatment. **(a-f)** Representative LSM images of **(a-c)** control and **(d-f)** *Itgb1*^{iECKO} hindlimb sections stained for DAPI (cell nuclei, blue), PECAM-1 (ECs, red) and β1 integrin (green). **(g)** Quantification of endothelial β1 integrin expression in the hindlimb represented by the mean intensity of β1 integrin staining within PECAM-1 positive areas and shown as percentage of control hindlimbs. All values are mean ± standard error of the mean (SEM) with n = 4 per condition; statistical significance was determined using paired, two-tailed Student's t-test. Anna Branopolski performed the presented experiment.

In order to exclude possible alterations in EC viability due to *Itgb1* gene deletion, which may interfere with results obtained from studies of vascular growth, ECs from the hindlimb were examined for apoptosis, determined by TUNEL immunostaining (Fig. 3.5 a-h). The quantification of TUNEL positive ECs revealed an average rate of about 10% in both control and *Itgb1*^{iECKO} mice after tamoxifen treatment, indicating that endothelium-specific deletion of the *Itgb1* gene neither induced nor inhibited basal EC apoptosis (Fig 3.5 i).

Based on these results, we conclude that β1 integrin was successfully deleted in ECs of *Itgb1*^{iECKO} mice following tamoxifen treatment and that this deletion did not have any considerable influence on EC viability at baseline conditions, thereby providing a reliable basis for studies addressing the functions of endothelial β1 integrin.

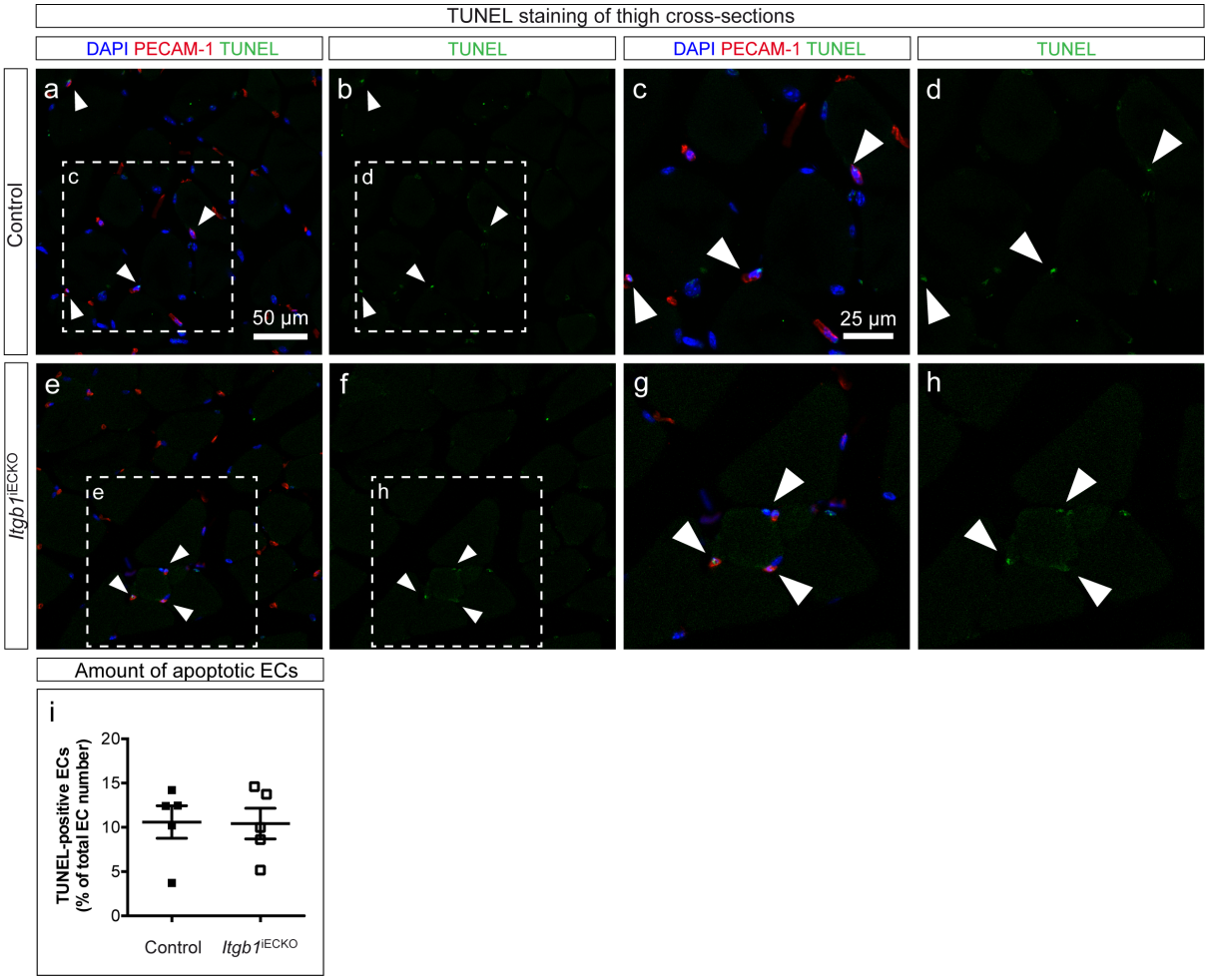

Figure 3.5: Deletion of the *Itgb1* gene in the endothelium does not induce EC apoptosis. Analysis of apoptotic ECs in the hindlimb control and *Itgb1*^{iECKO} mice after tamoxifen treatment by TUNEL immunostaining. **(a-h)** Representative LSM images of hindlimb sections of **(a-d)** control mice and **(e-h)** *Itgb1*^{iECKO} mice stained for DAPI (cell nuclei, blue), PECAM-1 (ECs, red) and TUNEL (apoptotic cells, green). Arrowheads indicate TUNEL-positive ECs. **(i)** Quantification of TUNEL-positive ECs related to the total EC number in hindlimbs of control and *Itgb1*^{iECKO} mice. All values are mean ± standard error of the mean (SEM) with n = 5 per condition; statistical significance was determined using paired, two-tailed Student's t-test. Anna Branopolski performed the presented experiment.

3.2.2 Endothelial β1 integrin expression is required for vascular growth in the murine hindlimb upon FA ligation

In order to determine the impact of the endothelial β1 integrin deletion on the long-term vascular response to ischemia, control and *Itgb1*^{iECKO} mice were equally treated with tamoxifen and subjected to sham surgery or HI. Calves and thighs were harvested 7 and 14 days following the surgery and analyzed for quantitative changes in the microvasculature by immunohistochemistry. Arterioles were identified by positive staining for PECAM-1 and αSMA, and normalized to the tissue area in mm^2 to determine arteriole density. For capillary density, PECAM-1-positive vessels were related to the number of muscle fibers.

First, the effects of HI on the microvasculature in control mice were assessed, with a differentiation between the thigh and the calf muscles. As revealed by quantification of arterioles and capillaries in the thigh at day 7 after the surgery, HI resulted in a significant increase of arteriole density of around 42% (Fig. 3.6 a-c), while only a trend towards a greater capillarization was observed (Fig. 3.6 d-f) when compared to the sham surgery, respectively.

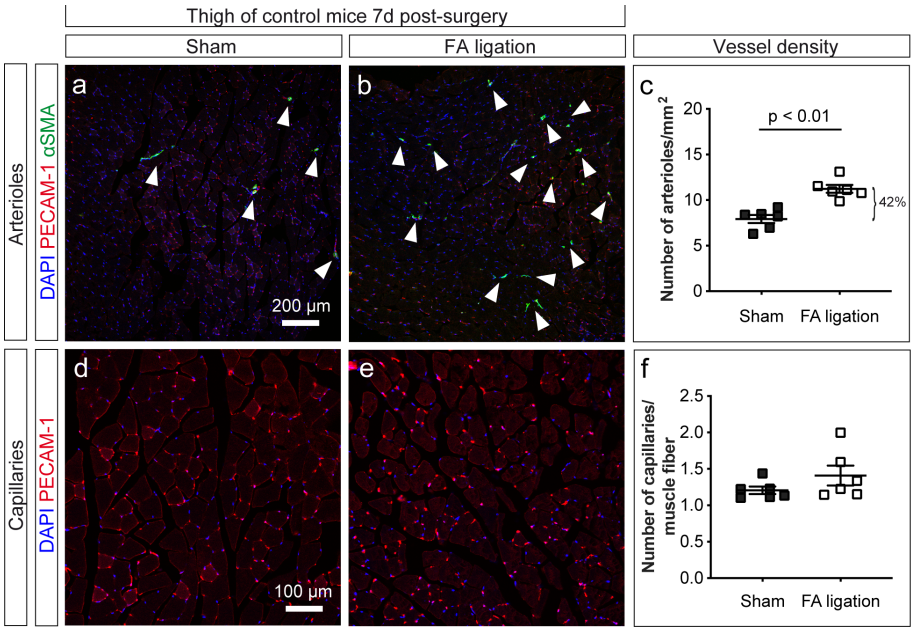

Figure 3.6: HI leads to a significant increase in arteriole density and a slight non-significant increase in capillary density in the thigh of control mice.
Analysis of arteriole and capillary densities in the thighs of tamoxifen-treated control mice 7 days following FA ligation. **(a, b)** Representative LSM images of arterioles in the thigh muscle after **(a)** sham surgery or **(b)** FA ligation. Sections were stained for DAPI (cell nuclei, blue), PECAM-1 (ECs, red) and αSMA (smooth muscle cells, green). Arrowheads point to arterioles identified as vessels positive for PECAM-1 and αSMA. **(c)** Quantification of arteriole density represented by the number of arterioles per mm^2. **(d, e)** Representative LSM images of capillaries in the thigh muscle after **(d)** sham surgery or **(e)** FA ligation. Sections were stained for DAPI (cell nuclei, blue) and PECAM-1 (ECs, red). **(f)** Quantification of capillary density, represented by the number of capillaries per muscle fiber. All values are mean ± standard error of the mean (SEM) with n = 6 per condition; statistical significance was determined using paired, two-tailed Student's t-test. Anna Branopolski, Carina Henning and Dominik Schuler performed the presented experiment.

The quantitative analyses of microvascular changes in the calf also revealed an increase in average arteriole density of about 47% when compared to the sham condition, which was, however, statistically not significant (Fig. 3.7 a-c). In contrast to the minor angiogenic response to HI in the thigh, the calf exhibited a significant rise in capillary density of around 31% after FA ligation, compared to the sham surgery (Fig. 3.7 d-f), which is in line with previously reported HI-induced angiogenesis in the lower leg (Limbourg et al., 2009). Although the thigh and the calf muscles were analyzed at distinct time points, the apparent differential angiogenic response to HI in the thigh and the calf seemed to correlate with the

already mentioned more prolonged reduction of perfusion in the calf upon FA ligation, suggesting predominantly hypoxia-driven angiogenesis in the context of HI.

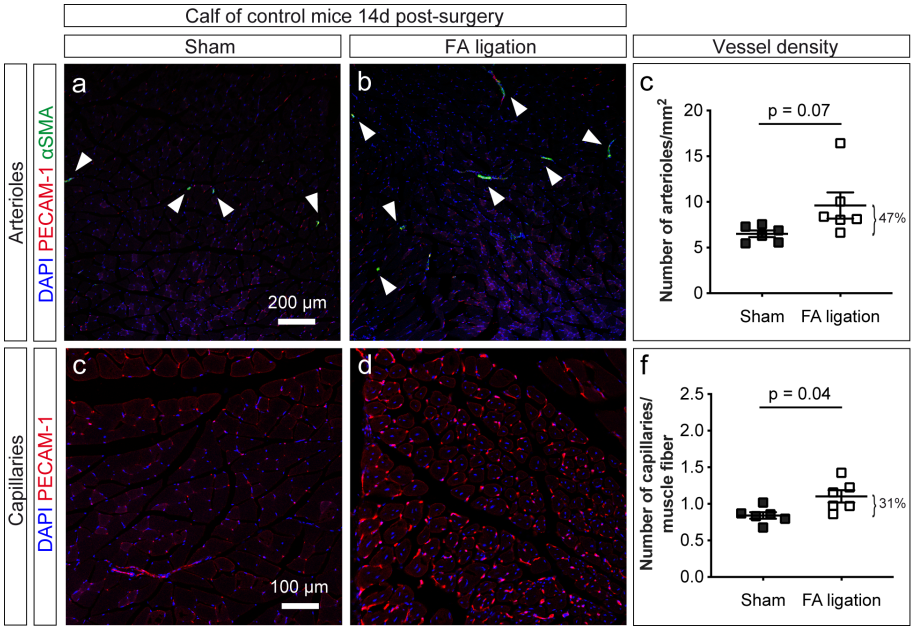

Figure 3.7: HI leads to a significant increase in capillary density and a non-significant increase in arteriole density in the calf of control mice.
Analysis of arteriole and capillary densities in the calves of tamoxifen-treated control mice 14 days following FA ligation. **(a, b)** Representative LSM images of arterioles in the calf muscle after **(a)** sham surgery or **(b)** FA ligation. Arrowheads point to arterioles identified as vessels positive for PECAM-1 and αSMA. Sections were stained for DAPI (cell nuclei, blue), PECAM-1 (ECs, red) and αSMA (smooth muscle cells, green). **(c)** Quantification of arteriole density represented by the number of arterioles per mm^2. **(d, e)** Representative LSM images of capillaries in the calf muscle after **(d)** sham surgery or **(e)** FA ligation. Sections were stained for DAPI (cell nuclei, blue) and PECAM-1 (ECs, red). **(f)** Quantification of capillary density represented by the number of capillaries per muscle fiber. All values are mean ± standard error of the mean (SEM) with n = 6 per condition; statistical significance was determined using paired, two-tailed Student's t-test. Anna Branopolski, Carina Henning and Dominik Schuler performed the presented experiment.

After the analyses of the long-term vascular response to FA ligation in control mice, here represented by changes in arteriole and capillary densities, we investigated whether mice with an endothelium-specific β1 integrin deletion exhibited an analogical response. Importantly, arteriole and capillary densities in the hindlimbs of *Itgb1*^{iECKO} mice were not significantly affected by tamoxifen treatment alone (Henning et al., 2019). As opposed to control mice, in *Itgb1*^{iECKO} mice, no significant increase in arteriole density was observed in the thighs after FA ligation compared to the sham surgery, indicating that HI failed to induce arteriole formation in these mice (Fig. 3.8 a-c). Furthermore, there was no considerable angiogenic response to HI in the thigh as indicated by similar average capillary densities upon FA ligation and sham surgery (Fig. 3.8 d-f).

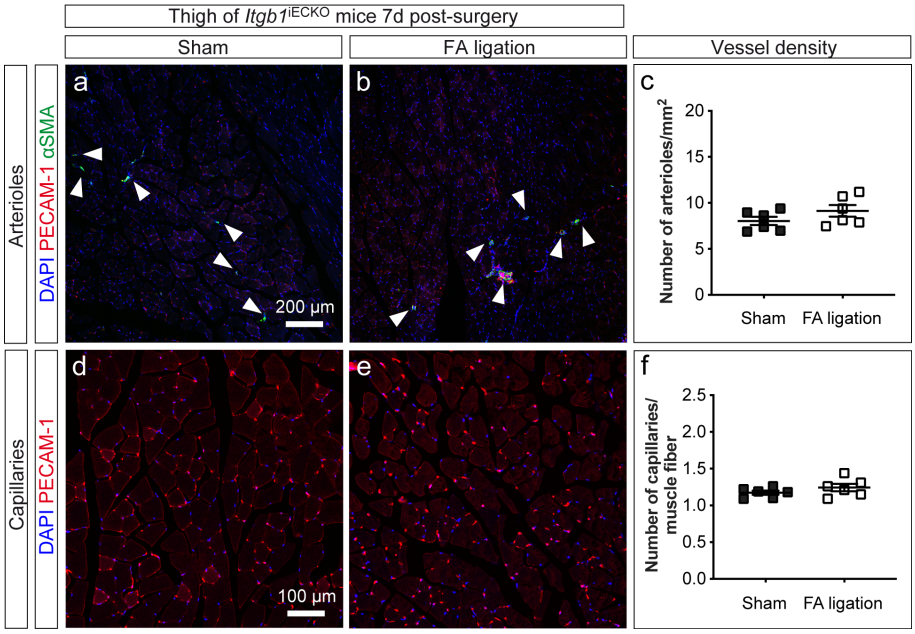

Figure 3.8: HI-induced vascular growth in the thigh is inhibited in mice with EC-specific β1 integrin deletion.
Analysis of arteriole and capillary densities in the thighs of tamoxifen-treated *Itgb1*^{iECKO} mice 7 days following FA ligation. **(a, b)** Representative LSM images of arterioles in the thigh muscle after **(a)** sham surgery or **(b)** FA ligation. Sections were stained for DAPI (cell nuclei, blue), PECAM-1 (ECs, red) and αSMA (smooth muscle cells, green). Arrowheads point to arterioles identified as vessels positive for PECAM-1 and αSMA. **(c)** Quantification of arteriole density represented by the number of arterioles per mm^2. **(d, e)** Representative LSM images of capillaries in the thigh muscle after **(d)** sham surgery or **(e)** FA ligation. Sections were stained for DAPI (cell nuclei, blue) and PECAM-1 (ECs, red). **(f)** Quantification of capillary density represented by the number of capillaries per muscle fiber. All values are mean ± standard error of the mean (SEM) with n = 6 per condition; statistical significance was determined using paired, two-tailed Student's t-test. Anna Branopolski, Carina Henning and Dominik Schuler performed the presented experiment.

Finally, in contrast to control mice, HI did not result in any remarkable changes in both arteriole (Fig. 3.9 a-c) and capillary densities in the calves of *Itgb1*^{iECKO} mice (Fig. 3.9 d-f). Similar results were obtained when applying pharmacological inhibition of β1 integrin (Henning et al., 2019). Furthermore, HI-induced collateral artery enlargement was abolished when β1 integrin blocking antibody was applied (Henning et al., 2019).

In summary, the described results indicate that endothelial β1 integrin is required for HI-induced arteriole formation in both the thigh and the calf, and for angiogenesis that predominantly takes place in the calf.

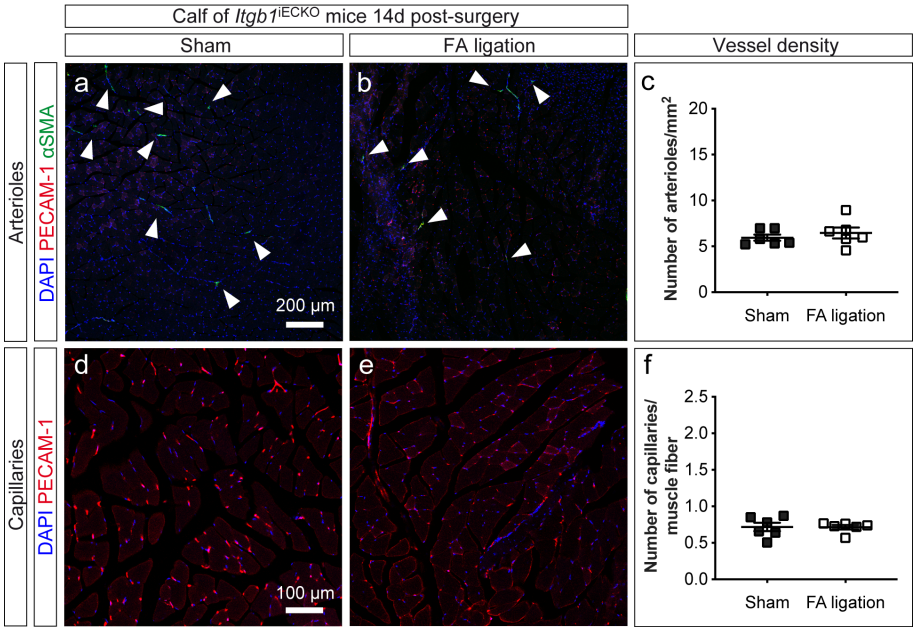

Figure 3.9: HI-induced vascular growth in the calf is inhibited in mice with EC-specific β1 integrin deletion.
Analysis of arteriole and capillary densities in the calves of tamoxifen-treated *Itgb1*^{iECKO} mice 14 days following FA ligation. **(a, b)** Representative LSM images of arterioles in the calf muscle after **(a)** sham surgery or **(b)** FA ligation. Arrowheads point to arterioles identified as vessels positive for PECAM-1 and αSMA. Sections were stained for DAPI (cell nuclei, blue), PECAM-1 (ECs, red) and αSMA (smooth muscle cells, green). **(c)** Quantification of arteriole density represented by the number of arterioles per mm^2. **(d, e)** Representative LSM images of capillaries in the thigh muscle after **(d)** sham surgery or **(e)** FA ligation. Sections were stained for DAPI (cell nuclei, blue) and PECAM-1 (ECs, red). **(f)** Quantification of capillary density represented by the number of capillaries per muscle fiber. All values are mean ± standard error of the mean (SEM) with n = 6 per condition; statistical significance was determined using paired, two-tailed Student's t-test. Anna Branopolski, Carina Henning and Dominik Schuler performed the presented experiment.

3.3 Procedure of RepI/R and its effect on β1 integrin expression

By using the murine model of HI we could show that endothelial β1 integrin is required for peripheral vascular growth in response to FA ligation. This raised the question whether the results can be transferred to the coronary system, where arterial occlusions also result in hemodynamic changes, as demonstrated by studies on hearts of larger animals (Joyce and Gregg, 1967). Since, to our knowledge, no studies on the role of the mechanosensor β1 integrin in adult coronary growth yet exist, we decided to investigate this aspect by using a murine closed-chest model of ischemia/reperfusion (I/R) to induce brief, repeated ischemic events in the left myocardium (RepI/R), as previously described (Lavine et al., 2013). This procedure was shown to trigger microvascular changes in the murine heart and to have cardioprotective properties. Moreover, taking into account that RepI/R presumably reflects the pathological conditions in patients with coronary artery disease

(CAD), it potentially may be used as a clinically relevant model to study the mechanisms of ischemia-induced coronary growth and cardioprotection (Lavine et al., 2013)

To perform RepI/R, an occluder system was installed around the LAD. For this, the heart was exposed via thoracotomy (Fig. 3.10 a). Afterwards, the mice were allowed to recover from surgical trauma for a few days prior to the first ischemic event. Left ventricular (LV) myocardial ischemia was induced by exerting tension on the occluder (Fig. 3.10 b, c) and confirmed by ST segment elevation on the ECG as a characteristic indication of transmural myocardial ischemia (Fig. 3.10 d). When the tension was released again after 15 minutes, the ECG signal returned back to baseline, indicating successful reperfusion. The procedure of ischemia induction was performed every second day. The RepSham surgery included analogous steps except for exerting tension on the occluder. For immunohistochemical analyses, transversal cryosections at the papillary muscle level below the occlusion were used (Fig. 3.10 e). Moreover, we discriminated between the hypoxia-exposed LV myocardium (termed as “ischemic myocardium”) and the remaining, normoxic regions including the septum and the right ventricular (RV) myocardium (termed as “non-ischemic myocardium”), during LAD-occlusions (Fig. 3.10 f), as revealed by a staining of hypoxic regions (Henning et al., 2021).

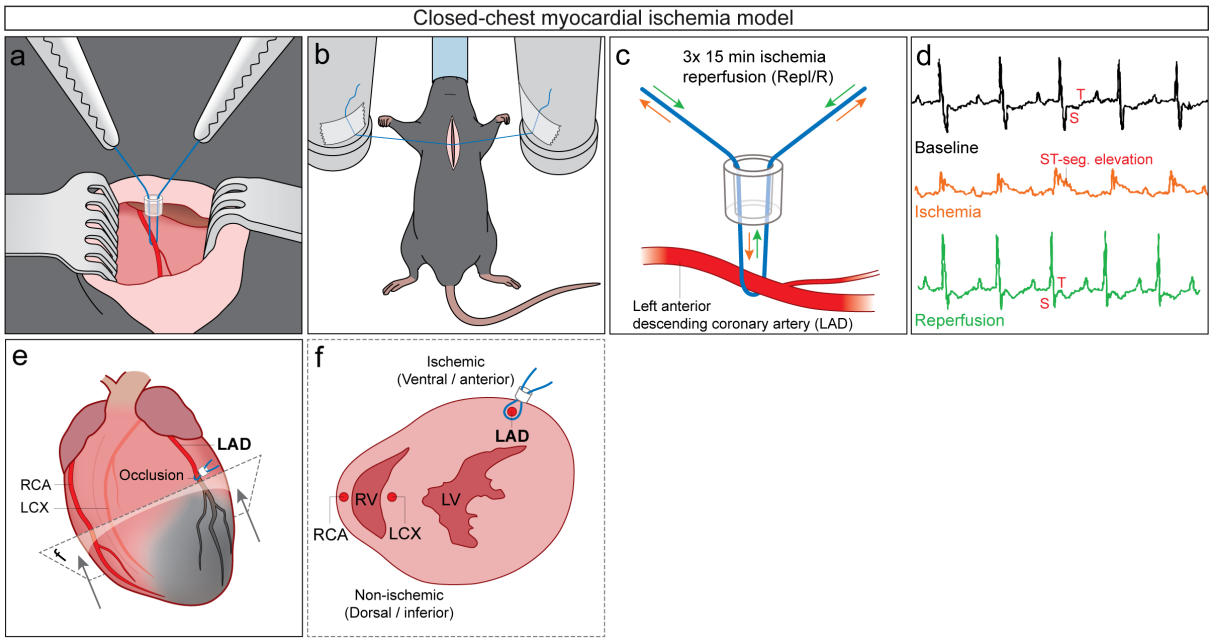

Figure 3.10: Overview of the closed-chest myocardial ischemia/reperfusion model.
(a) Schematic illustration of the occluder system, composed of a prolene suture and a plastic tube and implanted around the LAD. **(b, c)** Induction of 3x 15 minute-myocardial ischemia with subsequent reperfusion (RepI/R) in the closed-chest mouse model by exerting tension on the suture (ischemia, orange arrows) and releasing the tension (reperfusion, green arrows). **(d)** Monitoring of the procedure by ECG recordings before (baseline, black line), during (ischemia, orange line) and after the LAD occlusion (reperfusion, green line). **(e)** Illustration of an adult mouse heart, showing the right coronary artery (RCA), the left circumflex artery (LCX) and the left anterior descending artery (LAD) and indicating the position of the occluder, the ischemic myocardium (gray) during the LAD occlusion and of a cross-section through the mouse heart. **(f)** Schematic illustration of a cross-section through the ischemic and non-ischemic myocardium, showing the left and the right ventricles (LV and RV) and the

coronary arteries (RCA, LCX and LAD). Images were drafted by Carina Henning and Anna Branopolski and illustrated by Yousun Koh.

In our HI-experiments, we found FA ligation to induce β1 integrin expression in the ECs of the hindlimb, especially in the distal regions exhibiting severe hypoxia. In terms of myocardial ischemia, it was previously reported that permanent LAD ligation in rats and mice enhances β1 integrin expression in the myocardium, however, without quantifying its endothelial expression (Krishnamurthy et al., 2006; Sun et al., 2003). We therefore wished to determine whether brief, repeated LAD occlusions have a similar effect, thereby differentiating between total and endothelial expression. For this, wild-type mice underwent either RepSham or RepI/R surgeries, and the obtained cross-sections were analyzed for the mean intensity of β1 integrin immunostaining in total or selectively within the endothelium defined by PECAM-1-positive area (Fig. 3.11 a-d).

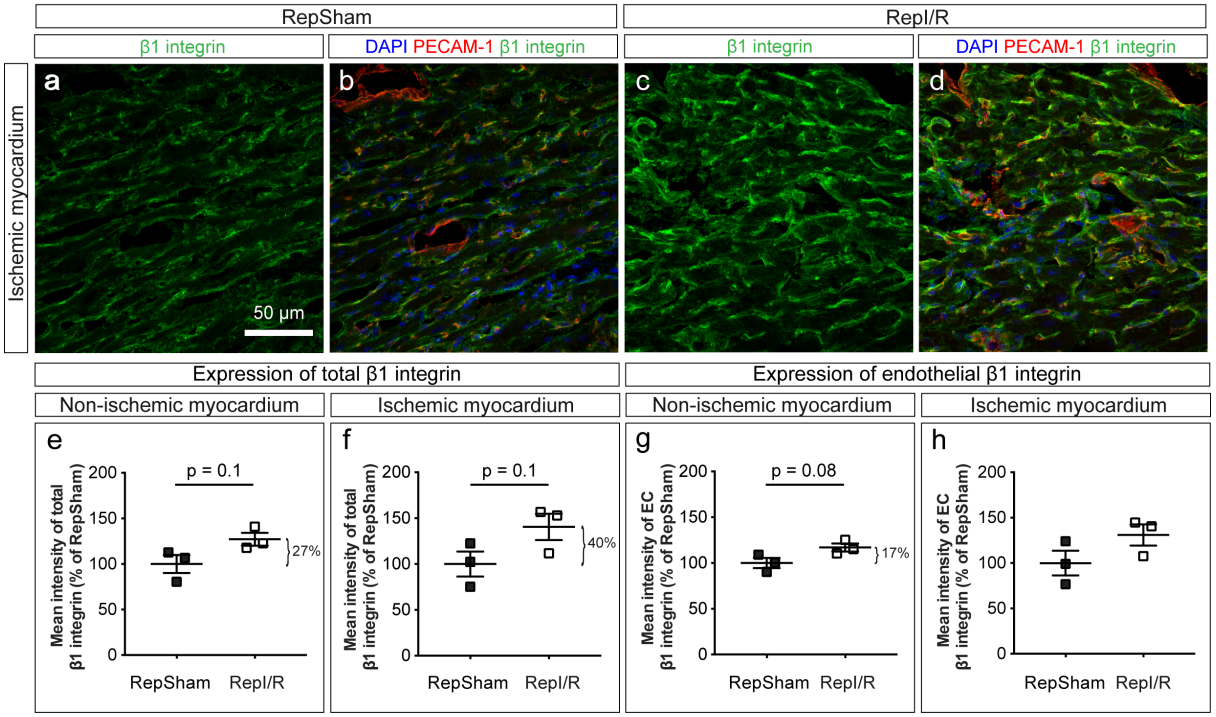

Figure 3.11: RepI/R leads to a non-significant increase in expression of total and endothelial β1 integrin in both the ischemic and the non-ischemic myocardium.
Analysis of total and endothelial β1 integrin expression in the myocardium 7 days after RepI/R. **(a, b, c, d)** Representative LSM images of sections through the ischemic myocardium of wild-type mice after **(a, b)** RepSham or **(c, d)** RepI/R treatment. Sections were stained for DAPI (cell nuclei, blue), PECAM-1 (ECs, red) and β1 integrin (green). **(e-h)** Quantification of **(e, f)** total and **(g, h)** endothelial β1 integrin expression in **(e, g)** non-ischemic and **(f, h)** ischemic myocardium, represented by the mean intensity of β1 integrin staining within PECAM-1 positive areas, shown as percentage of RepSham. All values are mean ± standard error of the mean (SEM) with n = 3 per condition; statistical significance was determined using unpaired, two-tailed Student's t-test. Anna Branopolski and Carina Henning performed the presented experiment.

When comparing the intensities of total β1 integrin in the hearts of mice that underwent RepSham or RepI/R surgeries, the latter were found with increased expression of this integrin subunit by 27% in the non-ischemic region and by 40% in the ischemic region, which was, however, not significant (Fig. 3.11 e, f). This observation is in line with the above-mentioned studies on mouse and rat hearts (Sun, 2003; Krishnamurthy, 2006). Similarly, quantification of the mean intensity exclusively in the endothelium revealed a non-significant enhancement of its expression by 17% in the non-ischemic myocardium and by around 30% in the ischemic myocardium after RepI/R surgery (Fig. 3.11 g, h), consistent with the greater induction of the endothelial β1 integrin expression in the calf than in the less hypoxic thigh.

In summary, although the observed differences were not significant, the results of the expression studies show that brief ischemic events were sufficient to slightly enhance β1 integrin expression not only in the myocardium generally, but specifically in cardiac ECs. The latter points to a possible role of endothelial β1 integrin in the vascular response to RepI/R.

3.4 Impact of pharmacological inhibition of β1 integrin on RepI/R-induced coronary growth and cardioprotection

Addressing the role of β1 integrin in the adult coronary growth, we combined the RepI/R treatment with pharmacological inhibition using an antibody selectively targeting this integrin subunit. We first examined RepI/R for the induction of coronary growth, represented by EC proliferation and arteriole formation, and, in addition, for cardiopotective effects, with respect to β1 integrin function.

3.4.1 RepI/R-mediated induction of EC proliferation is inhibited by pharmacological ablation of β1 integrin function

Since EC proliferation is thought to be an initial and hence critical step of the formation or enlargement of collateral arteries (Cai and Schaper, 2008; Moraes et al., 2014; Seiler et al., 2013), we examined cardiac ECs for the incorporation of 5-bromo-2'-deoxyuridine (BrdU), a thymidine analogue, after RepI/R with regard to β1 integrin function. For this, mice underwent RepSham or RepI/R procedure and received intravenous injections of β1 integrin blocking antibody or an isotype-matched control antibody one day before every ischemic event or sham surgery (Fig. 3.12 a). BrdU-filled osmotic pumps were intraperitoneally implanted at the day of the first ischemic event, and the isolated hearts

were immunohistochemically analyzed for proliferating ECs, identified as cells positive for both PECAM-1 and BrdU and related to the tissue area in mm^2. We thereby differentiated between the ischemic and the non-ischemic territories.

The quantification of BrdU-positive ECs in control antibody-treated mice showed a significant increase of BrdU-positive ECs by 249% in the non-ischemic myocardium (Fig. 3.12 b-f) and by 582% in the ischemic myocardium (Fig. 3.12 g) upon RepI/R treatment as compared to RepSham surgery. These results indicate that repeated LV-myocardial ischemia induced EC proliferation in both analyzed regions. Interestingly, according to the relative values of BrdU-positive ECs, in the ischemic myocardium, the proliferative response seemed to be stronger compared to the non-ischemic myocardium.

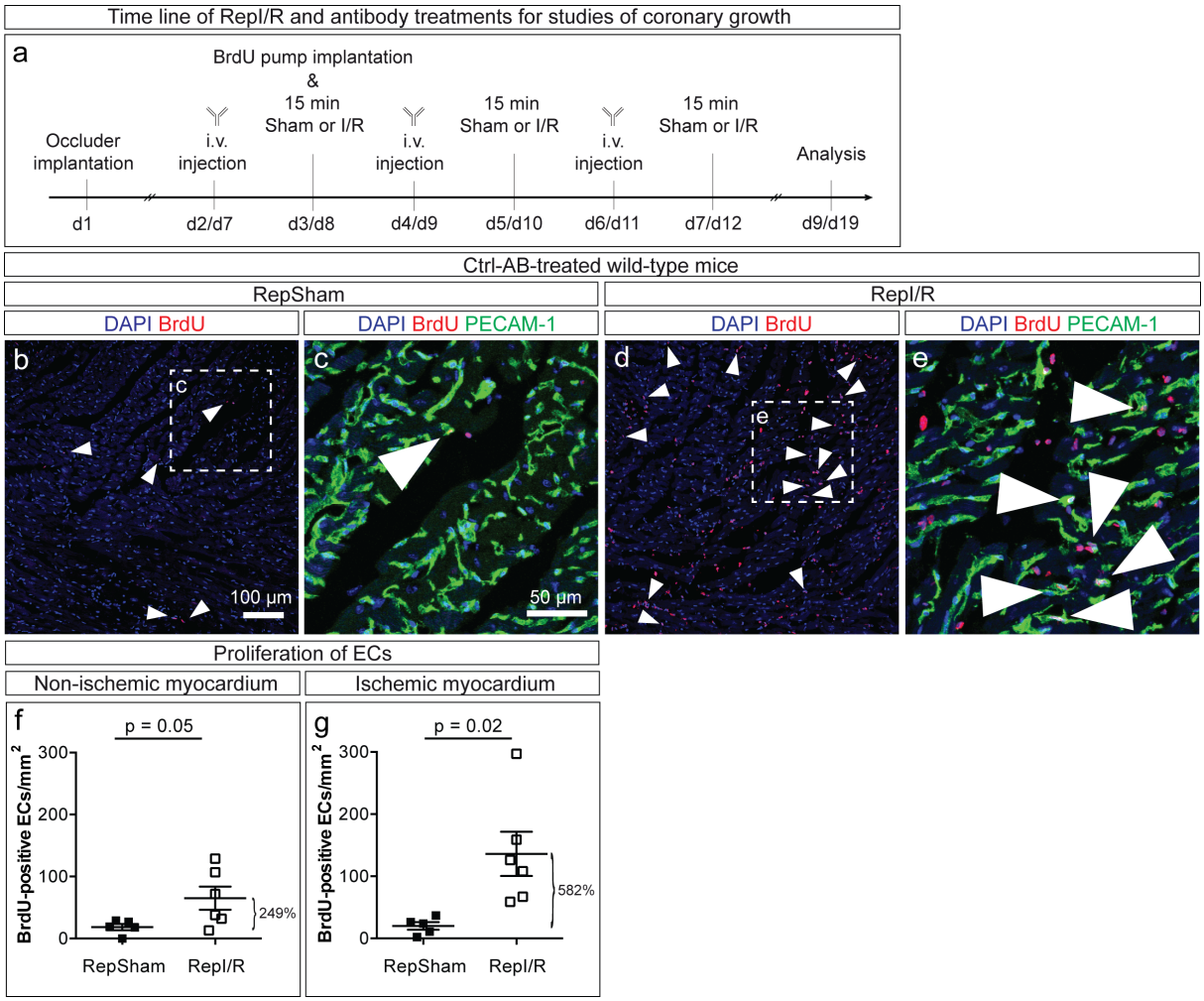

Figure 3.12: RepI/R triggers proliferation of ECs in the ischemic and non-ischemic myocardium of wild-type mice treated with control antibody.
(**a**) Time line of the RepI/R experiments employing pharmacological inhibition of β1 integrin by using specific blocking antibodies (β1-B-AB) and application of an isotype-matched control antibody (ctrl-AB) for studies of coronary growth. (**b-g**) Analysis of EC proliferation in ctrl-AB-treated wild-type mice upon RepI/R by BrdU incorporation. **(b-e)** Representative LSM images of sections through the non-ischemic myocardium after **(b, c)** RepSham or **(d, e)** RepI/R treatment. Sections were stained for BrdU (red), DAPI (blue), PECAM-1 (green). **(f, g)** Quantification of BrdU-positive ECs per mm^2 in **(f)** the non-ischemic and **(g)** the ischemic myocardium. All values are mean ± standard error of the mean

(SEM) with RepSham n = 5 and RepI/R n = 6; statistical significance was determined using unpaired, two-tailed Student's t-test. Carina Henning performed the presented experiment.

Strikingly, the proliferative response of cardiac ECs to RepI/R was abolished in the non-ischemic and ischemic myocardium when β1 integrin function was pharmacologically inhibited, as evidenced by similar numbers of proliferating ECs in the respective region after RepI/R and RepSham treatments (Fig. 3.13).

In summary, the results demonstrate that brief LAD occlusions effectively induce EC proliferation in both the ischemic and the non-ischemic myocardium, and that this induction strictly requires β1 integrin function.

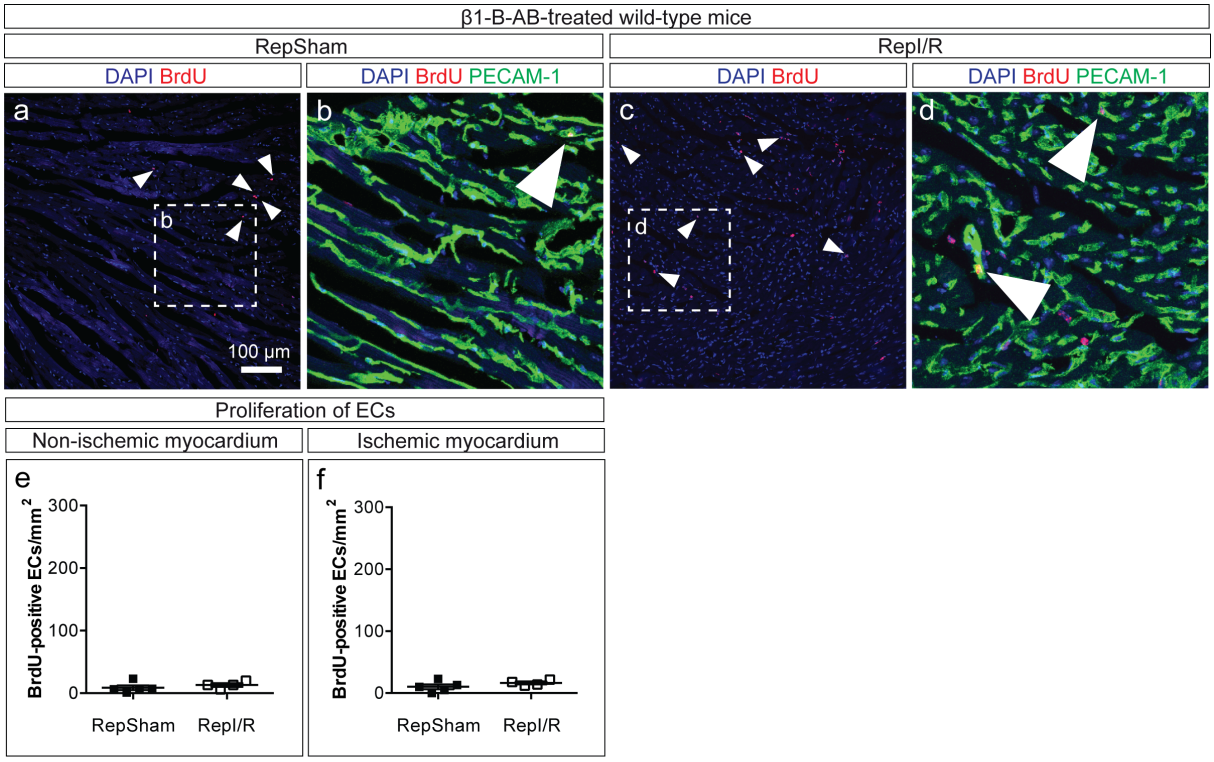

Figure 3.13: RepI/R-triggered proliferation of ECs in the ischemic and non-ischemic myocardium is inhibited by blocking β1 integrin function.
Analysis of EC proliferation in β1-B-AB-treated wild-type mice upon RepI/R by BrdU incorporation. **(a-d)** Representative LSM images of sections through the non-ischemic myocardium after **(a, b)** RepSham or **(c, d)** RepI/R treatment. Sections were stained for BrdU (red), DAPI (blue), PECAM-1 (green). **(e, f)** Quantification of BrdU-positive ECs per mm^2 in **(e)** the non-ischemic and **(f)** the ischemic myocardium. All values are mean ± standard error of the mean (SEM) with RepSham n = 5 and RepI/R n = 6; statistical significance was determined using unpaired, two-tailed Student's t-test. Carina Henning performed the presented experiment.

3.4.2 RepI/R-mediated formation of arterioles is inhibited by pharmacological ablation of β1 integrin function

Considering arterioles as vessels with a potential to develop to large-caliber collateral vessels, we next performed studies focusing on the arteriole formation upon RepI/R with regard to β1 integrin function (Schaper and Scholz, 2003). For this, mice were treated with either control or β1 integrin blocking antibodies and exposed to RepSham or RepI/R, respectively (3.12 a). Afterwards, cardiac cross-sections were immunohistochemically analyzed for arteriole formation using antibodies against αSMA and PECAM-1 to quantify arterioles, as described above for HI experiments.

Similar to the results obtained from the EC proliferation studies, we observed a significant rise in arteriole density by 37% in the non-ischemic myocardium (Fig. 3.14 a-e) and by 34% in the ischemic myocardium (Fig. 3.14 f) after RepI/R treatment when compared to RepSham treatment. These results are in line with published data demonstrating an increase in microvascular density in the ischemic and the border areas after RepI/R, but additionally suggest arteriole formation to occur in the non-ischemic area (Lavine et al., 2013).

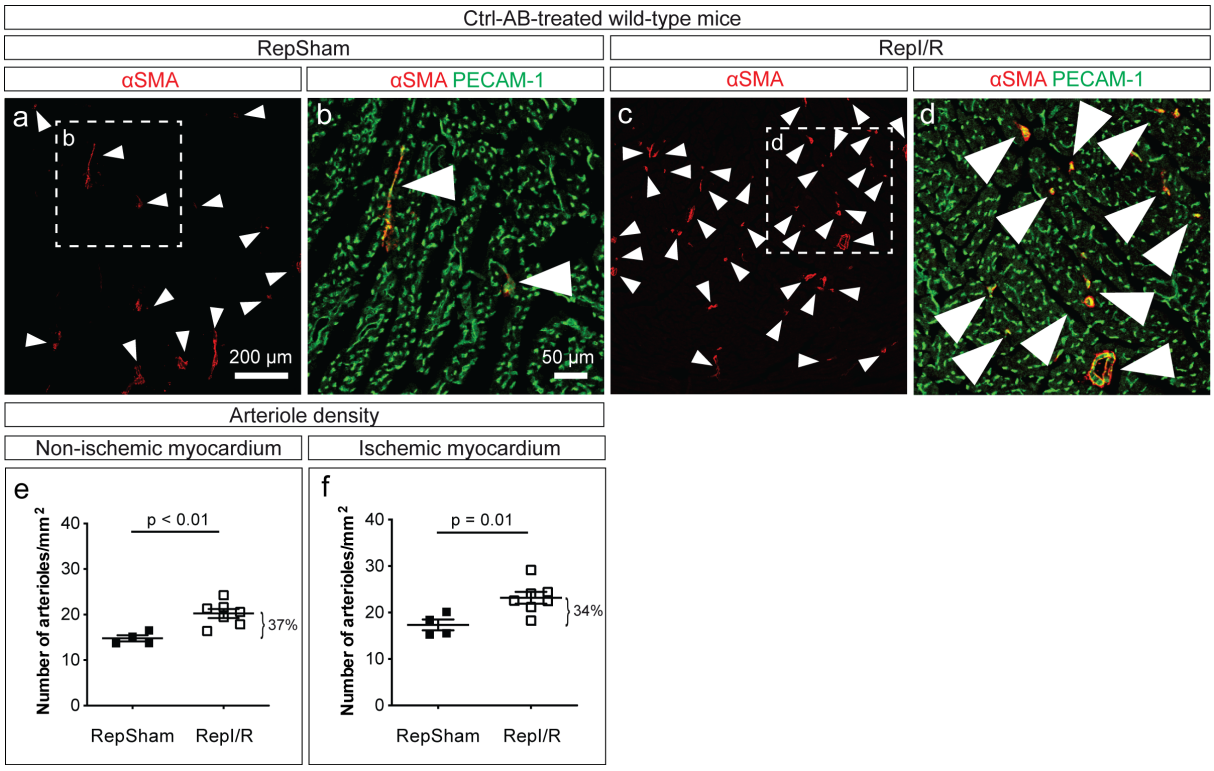

Figure 3.14: RepI/R triggers the formation of arterioles in the ischemic and non-ischemic myocardium of wild-type mice treated with control antibody.
Analysis of arteriole formation in ctrl-AB-treated wild-type mice upon RepI/R. **(a-d)** Representative LSM images of sections through the non-ischemic myocardium after **(a, b)** RepSham or **(c, d)** RepI/R treatment. Sections were stained for α-smooth muscle actin (αSMA, red) and PECAM-1 (green). Arrowheads point to arterioles identified as vessels positive for PECAM-1 and αSMA. **(e, f)** Quantification of arterioles per mm^2 in **(e)** the non-ischemic and **(f)** the ischemic myocardium. All values are mean ± standard error of the mean (SEM) with RepSham n = 4 and RepI/R n = 7;

statistical significance was determined using unpaired, two-tailed Student's t-test. Anna Branopolski and Carina Henning performed the presented experiment.

Strikingly, pharmacological ablation of β1 integrin completely abolished arteriole formation in the non-ischemic area, as indicated by the lack of increase in arteriole density (Fig. 3.15 a-e). Interestingly, as opposed to the non-ischemic area, a slight non-significant increase in arteriole density by 17% was still observed in the ischemic myocardium (Fig. 3.15 f).

Taken together, the results show that RepI/R triggers arteriole formation in the ischemic and non-ischemic myocardium to a similar extent and that β1 integrin function is important for this response, especially in the non-ischemic region.

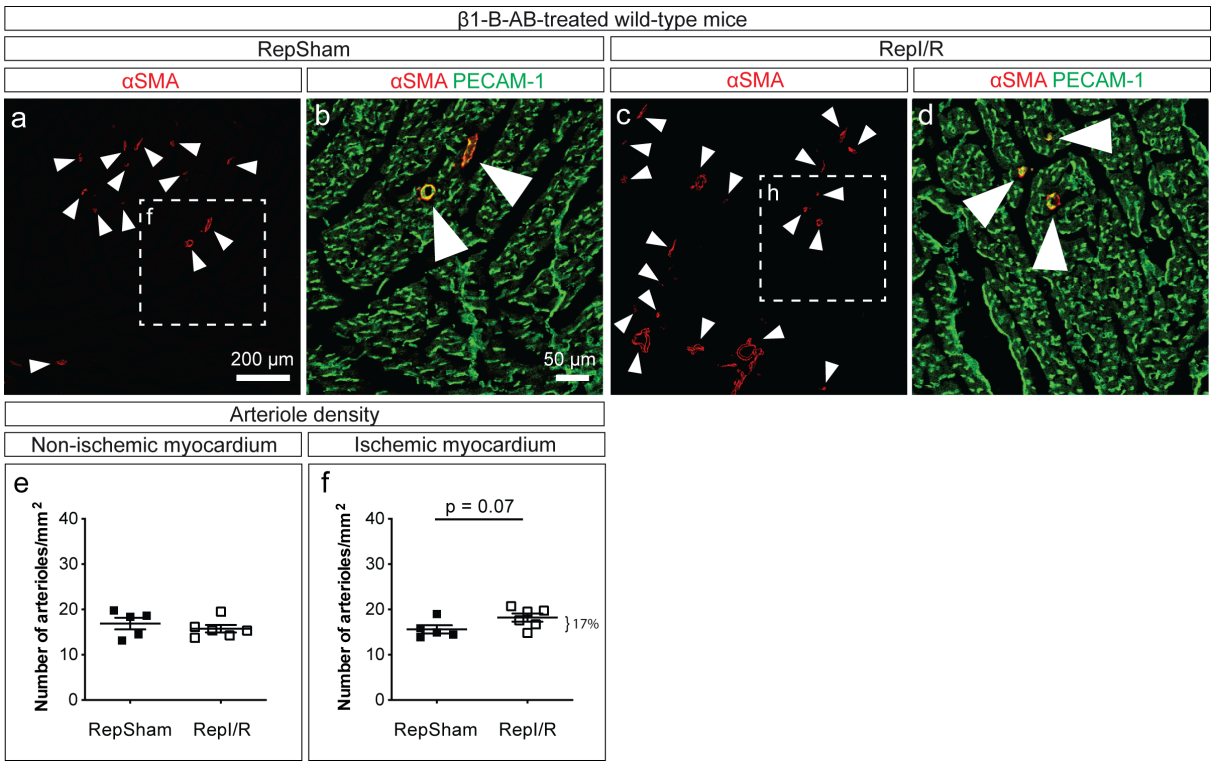

Figure 3.15: RepI/R-triggered arteriole formation in the ischemic and non-ischemic myocardium is inhibited by blocking β1 integrin function.
Analysis of arteriole formation in β1-B-AB-treated wild-type mice upon RepI/R. **(a-d)** Representative LSM images of sections through the non-ischemic myocardium after **(a, b)** RepSham or **(c, d)** RepI/R treatment. Sections were stained for α-smooth muscle actin (αSMA, red) and PECAM-1 (green). Arrowheads point to arterioles identified as vessels positive for PECAM-1 and αSMA. **(e, f)** Quantification of arterioles per mm^2 in **(e)** the non-ischemic and **(f)** the ischemic myocardium. All values are mean ± standard error of the mean (SEM) with RepSham n = 5 and RepI/R n = 6; statistical significance was determined using unpaired, two-tailed Student's t-test. Anna Branopolski and Carina Henning performed the presented experiment.

3.4.3 Cardioprotective effects of RepI/R are sensitive to pharmacological inhibition of β1 integrin

Clinical studies have reported that occurrence of symptoms of myocardial ischemia, i.e. in form of angina pectoris, during a few weeks prior to an MI is associated with better outcomes, represented by decreased infarct size, protection of microvasculature and preservation of cardiac contractile function (Mladenovic et al., 2008; Solomon et al., 2004). Considering RepI/R as a potential experimental model to simulate repeated conditions of ischemia in the human heart affected by CAD, we next examined its cardioprotective effects and analyzed the role of β1 integrin function in this respect. After RepSham or RepI/R surgery, which were combined with the antibody treatments, mice underwent an additional LAD occlusion for 60 minutes, resulting in an MI. To assess the outcome after experimental MI, infarct size and LV ejection fraction as a measure of LV contractile function were determined by MR-based imaging. The LV ejection fraction was measured 1, 7 and 28 days after MI. For detection of infarcted area 1 day after MI, mice received a gadolinium-based contrast agent via intraperitoneal injection immediately prior to the measurement. Once gadolinium has reached the heart, it evenly distributes in the interstitial space of the myocardial tissue via diffusion, without crossing intact cell membranes. Both the disruption of cell membranes and the rupture of cardiac cells, in consequence of prolonged ischemia, lead to a delayed washout of gadolinium, its accumulation and, hence, increased concentration in the infarcted tissue, which is called late gadolinium enhancement (LGE) and is visible as a bright region on the MR-images (Ibanez et al., 2019; Vermes et al., 2012). The infarcted area was identified based on the LGE pattern, and the infarct size was expressed as a percentage of the total LV volume.

We first examined the impact of RepI/R on the outcome after an MI in control antibody-treated wild-type mice. The analysis of the LGE-MR images showed that RepI/R significantly reduced the infarct size by 23% as compared to the RepSham treatment (Fig. 3.16 a-e). This is consistent with the results obtained from the TTC staining, as an alternative technique to determine the infarct size (Henning et al., 2021). Moreover, RepI/R resulted in an improved myocardial LV function 1, 7 and 28 days following MI, as revealed by significantly increased LV ejection fractions at the respective time points compared to the RepSham group (Fig. 3.16 f). Thus, similar to repeated ischemic events during a few weeks prior to an MI in humans, RepI/R improved the outcome after the experimental MI in mice, which is in line with previously published data (Lavine et al., 2013).

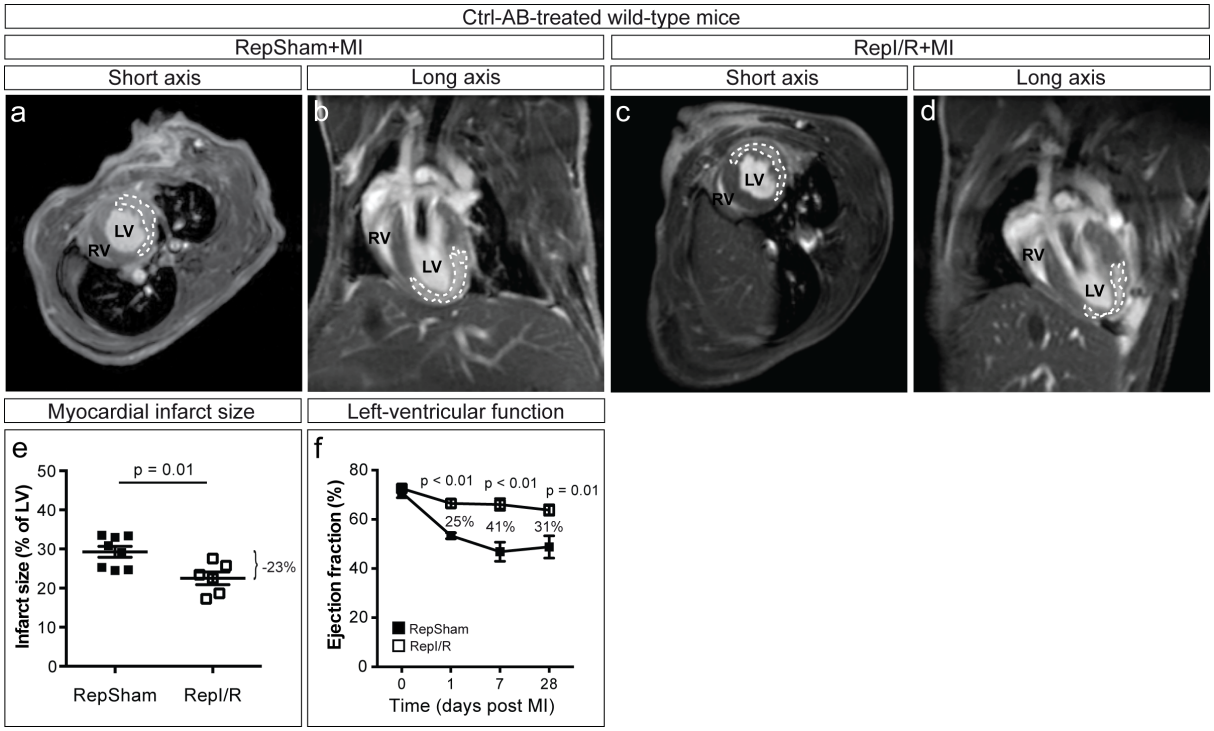

Figure 3.16: RepI/R reduces the infarct size and protects from myocardial dysfunction after MI. Analysis of infarct size and LV ejection fraction in mice treated with ctrl-AB and subjected to RepSham or RepI/R prior to 60 minute-ischemia (MI). **(a-d)** Representative short- and long-axis late gadolinium-enhanced (LGE) MR-images of mouse hearts after **(a, b)** RepSham or **(c, d)** RepI/R treatment followed by MI. LGE areas, indicated by dashed lines, represent the infarcted myocardium. **(e)** Quantification of the infarct size at day 1 post-MI. **(f)** Quantification of the left ventricular (LV) ejection fraction 0, 1, 7 and 28 days after MI. At day 0, wild-type mice without antibody treatment were used. Reported values are means ± SEM with RepSham n = 8 and RepI/R n = 6; statistical significance was determined using unpaired, two-tailed Students t-test. Anna Branopolski and Carina Henning performed the presented experiment.

We then investigated the role of β1 integrin function in RepI/R-induced cardioprotection by pharmacological inhibition of this integrin subunit during RepSham and RepI/R procedures. Notably, when employing β1 integrin blocking antibody, RepI/R resulted only in a slight, non-significant reduction of the infarct size as compared to the RepSham surgery (Fig. 3.17 a-e). Further, in contrast to control antibody-treated mice, RepI/R did not attenuate LV dysfunction after MI, as indicated by largely similar ejection fractions in blocking antibody-treated mice of the RepSham and RepI/R groups (Fig. 3.17 f). Interestingly, pharmacological inhibition of β1 integrin function during RepSham procedure seemed to impair the outcome after MI, as indicated by decreased average ejection fractions in blocking antibody-treated mice compared to control antibody-treated mice. This observation is consistent with a previously published study showing that a global heterozygous deletion of β1 integrin results in an enhanced myocardial dysfunction after a permanent LAD ligation (Krishnamurthy et al., 2006).

All in all, the presented results suggest that β1 integrin function is needed for ischemia-induced cardioprotection, including the reduction of infarct size and prevention of myocardial dysfunction after experimental MI.

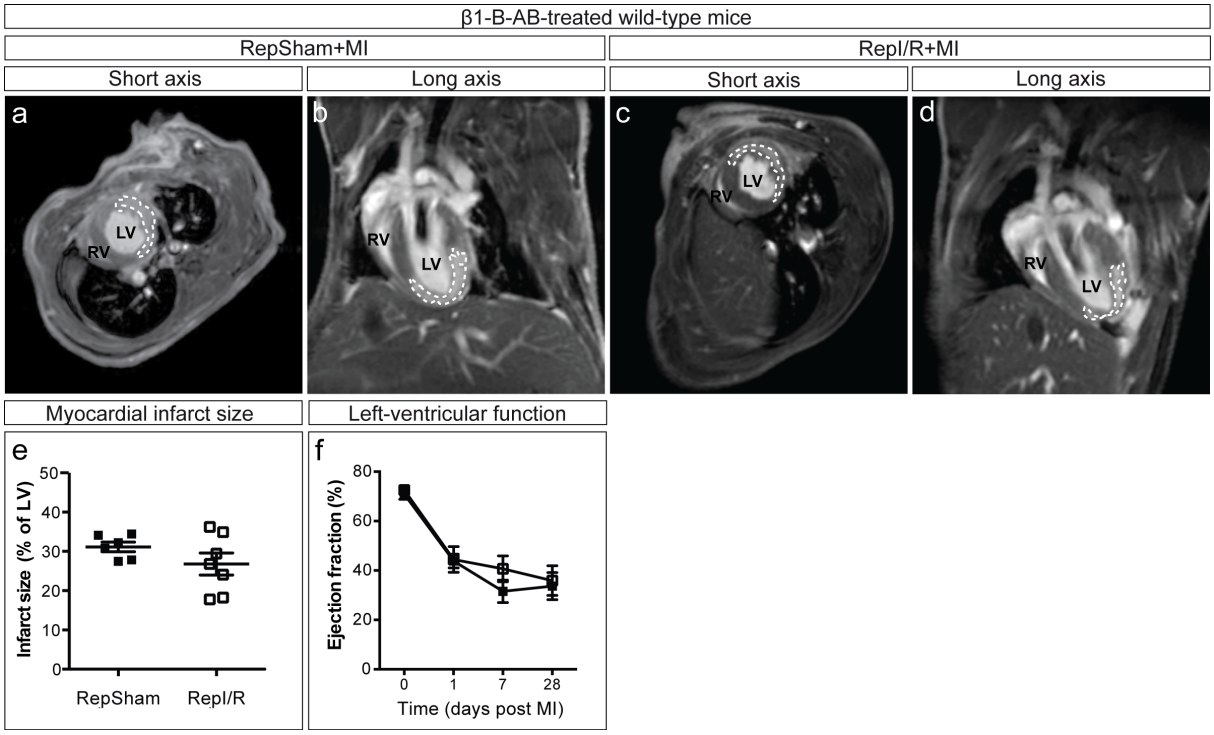

Figure 3.17: RepI/R-mediated reduction of the infarct size and protection from myocardial dysfunction after MI are attenuated by blocking β1 integrin function.
Analysis of infarct size and LV ejection fraction in mice treated with β1-B-AB and subjected to RepSham or RepI/R prior to 60 minute-ischemia (MI). **(a-d)** Representative short- and long-axis LGE-MR images of mouse hearts after **(a, b)** RepSham or **(c, d)** RepI/R treatment followed by MI. LGE areas, indicated by dashed lines, represent the infarcted myocardium. **(e)** Quantification of the infarct size at day 1 post-MI. **(f)** Quantification of the left ventricular (LV) ejection fractions 0, 1, 7 and 28 days after MI. At day 0, wild-type mice without antibody treatment were used as controls. Reported values are means ± SEM with RepSham n = 6 and RepI/R n = 7; statistical significance was determined using unpaired, two-tailed Students t-test. Anna Branopolski and Carina Henning performed the presented experiment.

3.5 Role of endothelial β1 integrin in RepI/R-induced coronary growth and cardioprotection

Experiments employing function-blocking antibodies showed that RepI/R-induced EC proliferation, arteriole formation in the myocardium and cardioprotection are, to different extents, sensitive to pharmacological inhibition of β1 integrin. Since integrins are ubiquitously expressed, a further specification of the involved cell types is necessary for a better understanding of the underlying mechanisms. Based on the finding that endothelial β1 integrin is required for the acute and long-term vascular responses to HI (Henning et al., 2019), we aimed to investigate its role in RepI/R-induced vascular adaptation and protection

from myocardial dysfunction. For this purpose, we first analyzed *Itgb1*^{iECKO} and *Cre* control mice for cardiac EC proliferation and arteriole formation in response to RepI/R. In addition, we assessed the outcomes after an MI in RepI/R-treated control and *Itgb1*^{iECKO} mice.

To ensure a successful deletion of *Itgb1* in cardiac endothelium, cardiac ECs of tamoxifen-treated control and *Itgb1*^{iECKO} mice were MACS-sorted and analyzed by qPCR and Western blotting. The analyses showed a significant reduction of β1 integrin expression in cardiac ECs of *Itgb1*^{iECKO} mice by up to 70% on mRNA and protein levels when compared to control mice, confirming that β1 integrin was efficiently deleted in the cardiac endothelium of *Itgb1*^{iECKO} mice (Henning et al., 2021).

3.5.1 Endothelial β1 integrin is required for RepI/R-induced cardiac EC proliferation

In order to examine the proliferative response of cardiac ECs to RepI/R with regard to the role of endothelial β1 integrin expression, control and *Itgb1*^{iECKO} mice received BrdU-filled osmotic pumps and were subjected to either RepSham or RepI/R treatment, respectively (Fig. 3.18 a). Proliferation of ECs was assessed by immunohistochemistry as described in 3.4.1.

The quantification of BrdU-positive ECs showed that the RepI/R treatment of control mice resulted in a significant increase in proliferating ECs in the non-ischemic myocardium by 98% (Fig. 3.18 b-f) and in the ischemic myocardium by 255% (Fig. 3.18 g) as compared to RepSham controls. Moreover, in the ischemic myocardium, the induction seemed to be stronger. These observations are consistent with the results from our proliferation studies on wild-type mouse hearts (see 3.4.1).

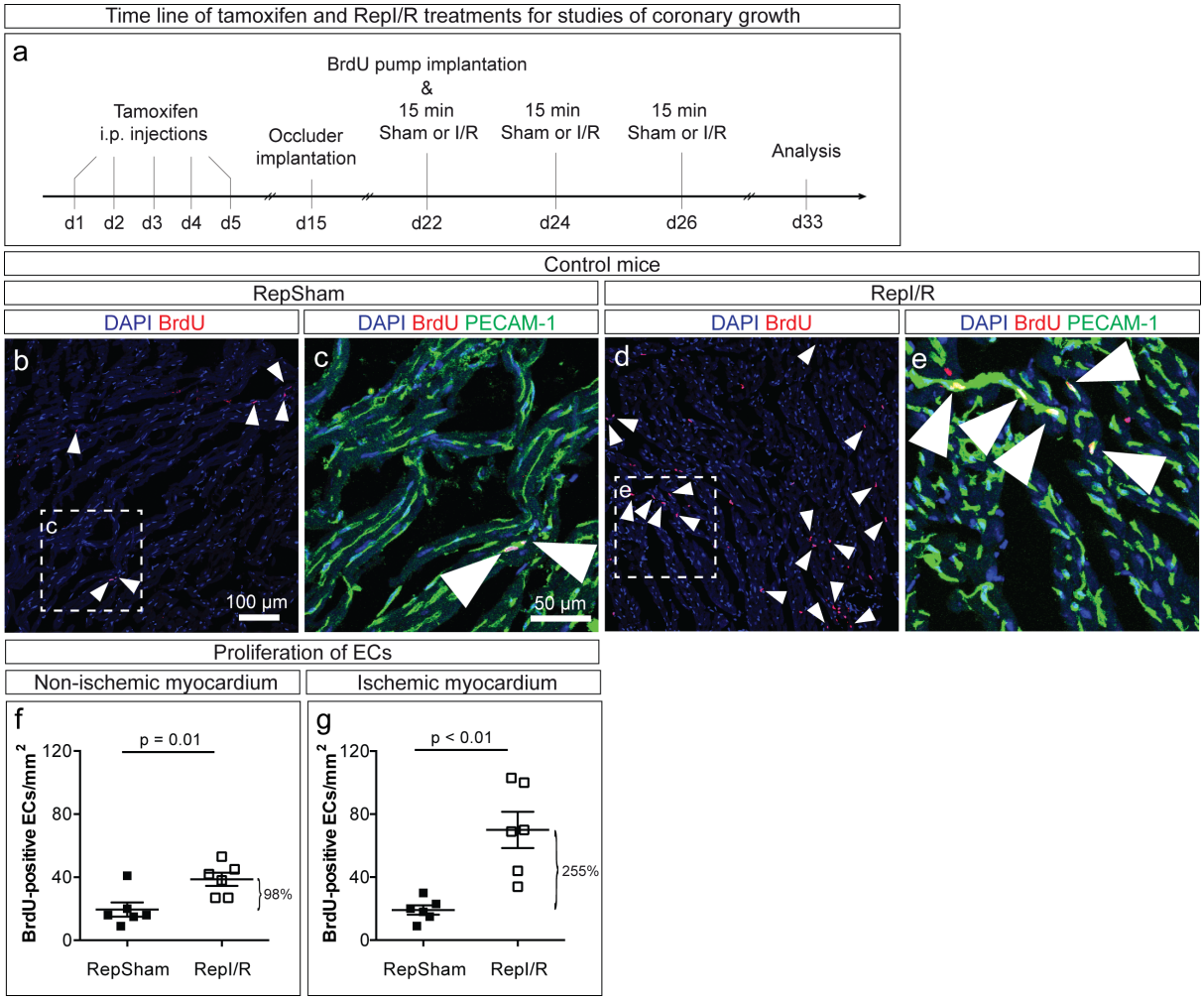

Figure 3.18: RepI/R triggers proliferation of ECs in the ischemic and non-ischemic myocardium of control mice.
(a) Time line of the RepI/R experiments with tamoxifen-inducible genetic deletion of β1 integrin. **(b-g)** Analysis of EC proliferation in tamoxifen-treated control mice upon RepI/R by BrdU incorporation. **(b-e)** Representative LSM images of sections through the non-ischemic myocardium after **(b, c)** RepSham or **(d, e)** RepI/R treatment. Sections were stained for BrdU (red), DAPI (blue), PECAM-1 (green). **(e, f)** Quantification of BrdU-positive ECs per mm^2 in **(e)** the non-ischemic and **(f)** the ischemic myocardium. All values are mean ± standard error of the mean (SEM) with n = 6 per condition; statistical significance was determined using unpaired, two-tailed Student's t-test. Carina Henning performed the presented experiment.

We next examined the proliferative response of cardiac ECs in *Itgb1*^{iECKO} mice to the RepI/R treatment. Strikingly, in contrast to control mice, RepI/R failed to significantly increase the number of proliferating ECs in the non-ischemic (Fig. 3.19 a-e) and in the ischemic (Fig. 3.19 f) myocardium of *Itgb1*^{iECKO} mice when compared to the RepSham controls.

In summary, the results show that EC-specific depletion of the *Itgb1* gene abolished RepI/R-induced proliferation of cardiac ECs, suggesting a key role of endothelial β1 integrin for an adequate proliferative response of the endothelium to transient ischemic events in the adult heart.

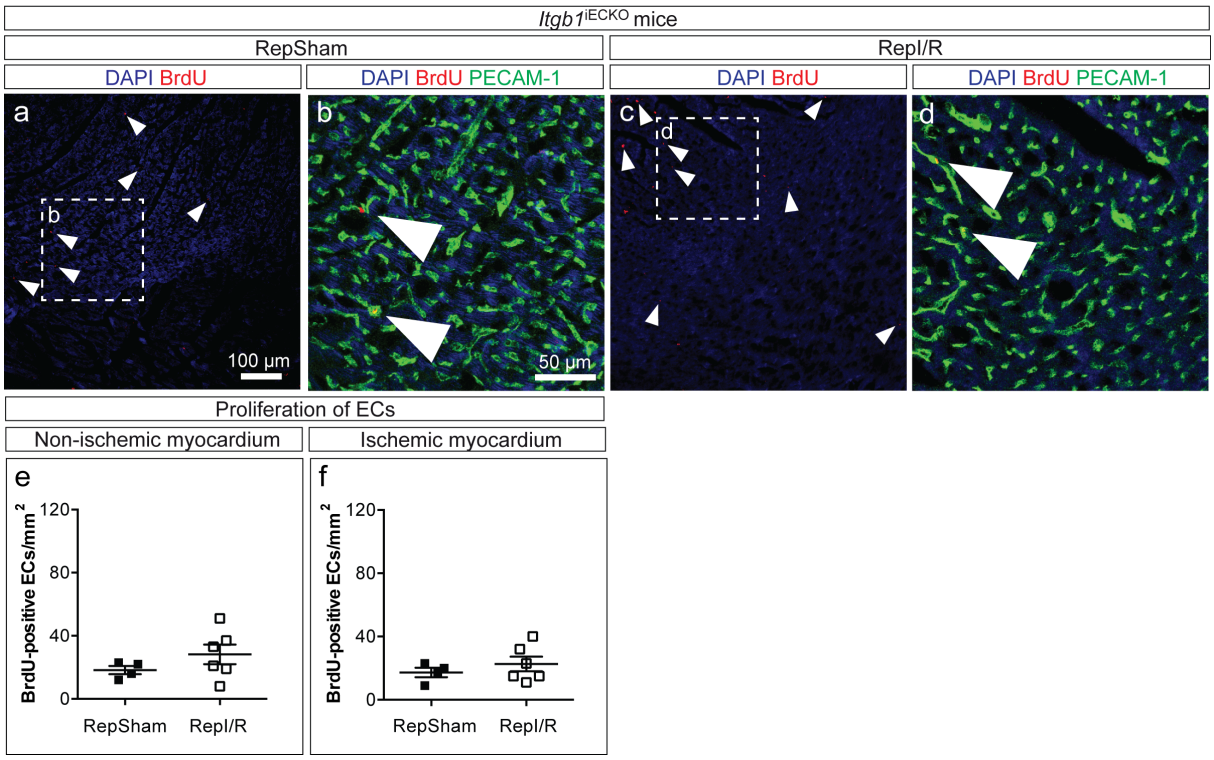

Figure 3.19: RepI/R-triggered proliferation of ECs in the ischemic and non-ischemic myocardium is inhibited in mice with EC-specific β1 integrin deletion.
Analysis of EC proliferation in tamoxifen-treated *Itgb1*^{iECKO} mice upon RepI/R by BrdU incorporation. **(a-d)** Representative LSM images of sections through the non-ischemic myocardium after **(a, b)** RepSham or **(c, d)** RepI/R treatment. Sections were stained for BrdU (red), DAPI (blue), PECAM-1 (green). **(e, f)** Quantification of BrdU-positive ECs per mm^2 in **(e)** the non-ischemic and **(f)** the ischemic myocardium. All values are mean ± standard error of the mean (SEM) with RepSham n = 4 and RepI/R n = 6; statistical significance was determined using unpaired, two-tailed Student's t-test. Carina Henning performed the presented experiment.

3.5.2 Endothelial β1 integrin is required for RepI/R-induced arteriole formation in the non-ischemic myocardium

As a next step, we studied the role of endothelial β1 integrin in the RepI/R-induced formation of arterioles. To this end, control and *Itgb1*^{iECKO} mice were subjected to either RepSham or RepI/R surgery, respectively, and the obtained cardiac cross-sections were analyzed for arteriole density. Consistent with the results of our experiments on coronary growth in wild-type mice (see 3.4.2), treatment of control mice with RepI/R led to an increase in arteriole density in the non-ischemic myocardium by 34% (Fig. 3.20 a-e) and in the ischemic myocardium by 12% (Fig. 3.20 f).

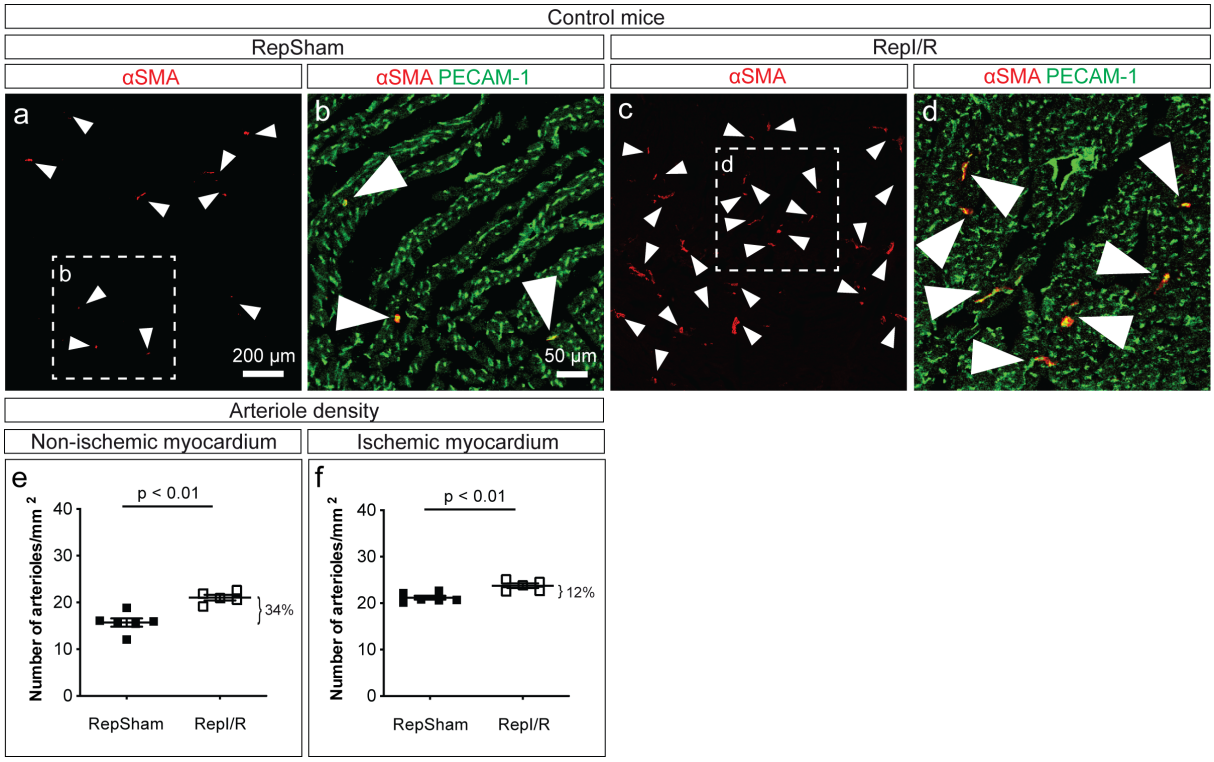

Figure 3.20: RepI/R triggers the formation of arterioles in the ischemic and non-ischemic myocardium in control mice.
Analysis of arteriole formation in tamoxifen-treated control mice upon RepI/R. **(a-d)** Representative LSM images of sections through the non-ischemic myocardium after **(a, b)** RepSham or **(c, d)** RepI/R treatment. Sections were stained for α-smooth muscle actin (αSMA, red) and PECAM-1 (green). Arrowheads point to arterioles identified as vessels positive for PECAM-1 and αSMA. **(e, f)** Quantification of arterioles per mm^2 in **(e)** the non-ischemic and **(f)** the ischemic myocardium. All values are mean ± standard error of the mean (SEM) with RepSham n = 6 and RepI/R n = 5; statistical significance was determined using unpaired, two-tailed Student's t-test. Anna Branopolski and Carina Henning performed the presented experiment.

We then quantified cardiac arteriole density in *Itgb1*^{iECKO} mice and found that RepI/R failed to induce arteriole formation in the non-ischemic myocardium, as indicated by similar arteriole numbers after RepSham as well as RepI/R surgery (Fig. 3.21 a-e). In contrast to the non-ischemic myocardium, we found arteriole density to be significantly increased after RepI/R in the ischemic region of the myocardium of *Itgb1*^{iECKO} mice by 18% compared to the RepSham surgery (Fig. 3.21 f), suggesting that RepI/R was able to trigger arteriole formation in this region despite EC-specific depletion of β1 integrin. Based on these results, we conclude that endothelial β1 integrin expression is required for RepI/R-induced increase in arteriole density in the non-ischemic, but not in the ischemic region, pointing to distinct mechanisms for the induction of arteriole formation in these regions.

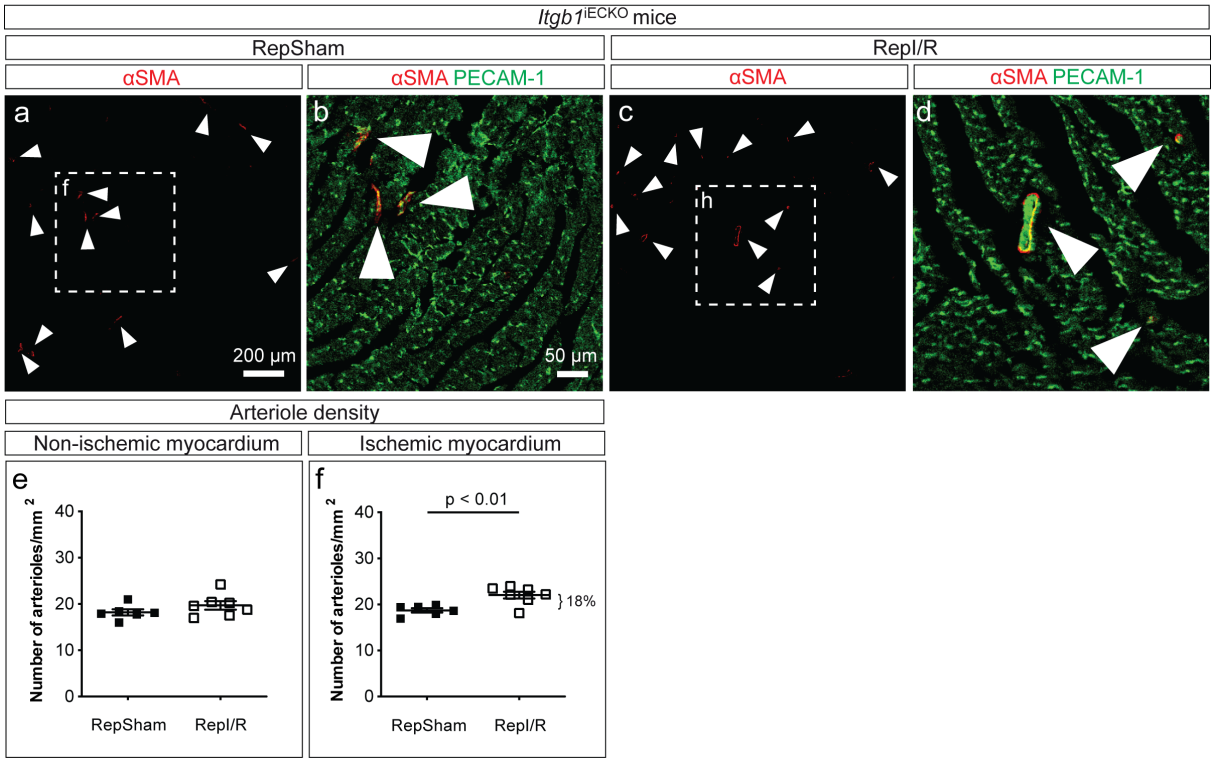

Figure 3.21: Genetic deletion of endothelial β1 integrin inhibits RepI/R-triggered formation of arterioles in the non-ischemic myocardium but not in the ischemic myocardium.
Analysis of arteriole formation in tamoxifen-treated *Itgb1*^{iECKO} mice upon RepI/R. **(a-d)** Representative LSM images of sections through the non-ischemic myocardium after **(a, b)** RepSham or **(c, d)** RepI/R treatment. Sections were stained for α-smooth muscle actin (αSMA, red) and PECAM-1 (green). Arrowheads point to arterioles identified as vessels positive for PECAM-1 and αSMA. **(e, f)** Quantification of arterioles per mm^2 in **(e)** the non-ischemic and **(f)** the ischemic myocardium. All values are mean ± standard error of the mean (SEM) with RepSham n = 6 and RepI/R n = 7; statistical significance was determined using unpaired, two-tailed Student's t-test. Anna Branopolski and Carina Henning performed the presented experiment.

3.5.3 Endothelial β1 integrin contributes to the cardioprotective effects of RepI/R

After we found endothelial β1 integrin to be involved in ischemia-triggered coronary growth, we finally aimed to determine its role in cardioprotective effects of RepI/R. Thus, as a next step, control and *Itgb1*^{iECKO} mice that had received the RepI/R treatment, additionally underwent an MI by occluding the LAD for 60 minutes. Afterwards, these mice were analyzed for infarct size and LV ejection fraction by MR imaging.

The analysis of gadolinium-enhanced areas 1 day after MI revealed a significant increase of the infarct size by 42% in *Itgb1*^{iECKO} mice compared to control mice (Fig. 3.22 a-e). Consistently, *Itgb1*^{iECKO} mice exhibited an impaired contractile function in the acute phase of MI, as indicated by a significantly decreased LV ejection fraction by 10% compared to

control mice 1 day after MI induction. However, no significant differences between the two groups were noted 7 and 28 days after MI (Fig. 3.22 f).

Taking into account our results from studies on wild-type mice, we assume that RepI/R improved the outcome after MI in control mice and, therefore, conclude that its cardioprotective effects were attenuated in *Itgb1*^{iECKO} mice, indicating that β1 integrin in the endothelium contributes to RepI/R-induced cardioprotection.

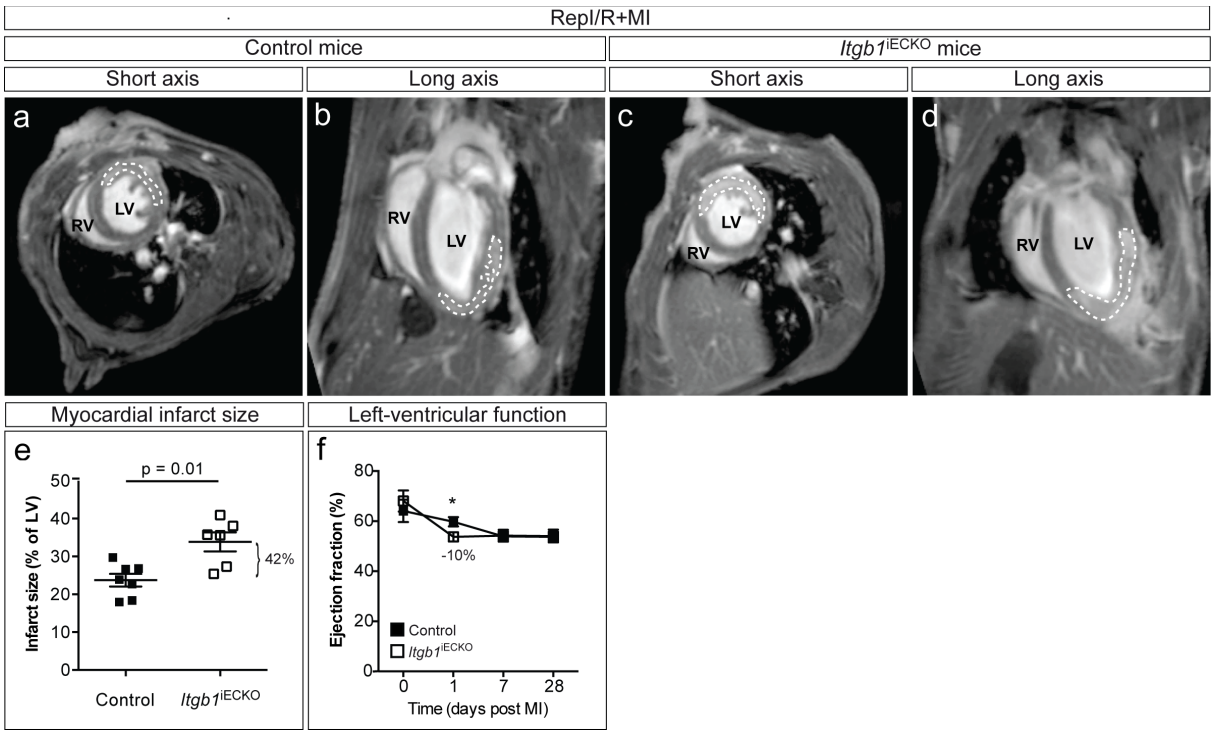

Figure 3.22: Genetic deletion of endothelial β1 integrin results in an increased infarct size and impaired myocardial function on the first day after MI in RepI/R-treated mice.
Analysis of infarct size and LV ejection fraction in tamoxifen-treated control and *Itgb1*^{iECKO} mice subjected to RepI/R treatment prior to 60 minute-ischemia (MI). **(a-d)** Representative short- and long-axis LGE-MR images of **(a, b)** control and **(c, d)** *Itgb1*^{iECKO} mouse hearts after RepI/R treatment and MI. LGE areas, indicated by dashed lines, represent the infarcted myocardium. **(e)** Quantification of the infarct size 1 day post-MI in control and *Itgb1*^{iECKO} mice. **(f)** Quantification of the left ventricular (LV) ejection fraction at days 0, 1, 7, and 28 after MI. Reported values are means ± SEM with control mice n = 7 and *Itgb1*^{iECKO} mice n = 6; statistical significance was determined using unpaired, two-tailed Students t-test. Anna Branopolski and Carina Henning performed the presented experiment.

3.6 *In vitro* studies on primary human cardiac ECs under static conditions

In our *in vivo* studies, we found endothelial β1 integrin to be involved in ischemia-induced vascular growth and protection from MI. We next aimed to explore whether these findings could be principally transferred to the human situation. Therefore, we decided to investigate the function of β1 integrin in primary human cardiac ECs. We first focused on the

question whether β1 integrin plays a role in proliferation of human coronary artery ECs (HCAECs). In addition, we examined whether β1 integrin is involved in regulating the expression of endothelial nitric oxide synthase (eNOS), an important regulator of endothelial function with cardioprotective properties, in these cells (Farah et al., 2017; Heiss et al., 2015). Finally, we analyzed human cardiac microvascular ECs (HCMVECs) for β1 integrin-dependent secretion of cardioprotective factors, using the hepatocyte growth factor (HGF) as representation.

3.6.1 Assessment of *ITGB1* knockdown in HCAECs

To manipulate β1 integrin expression *in vitro*, we established its knockdown in HCAECs by electroporation-mediated transfection with one of three different siRNA constructs specifically targeting the *ITGB1* gene (referred to as β1-siRNA1, β1-siRNA2 and β1-siRNA3). A non-targeting siRNA (referred to as ctrl-siRNA) was used as control. The knockdown efficiency of *ITGB1* was determined on mRNA and protein levels by qPCR and Western blotting (Fig 3.23).

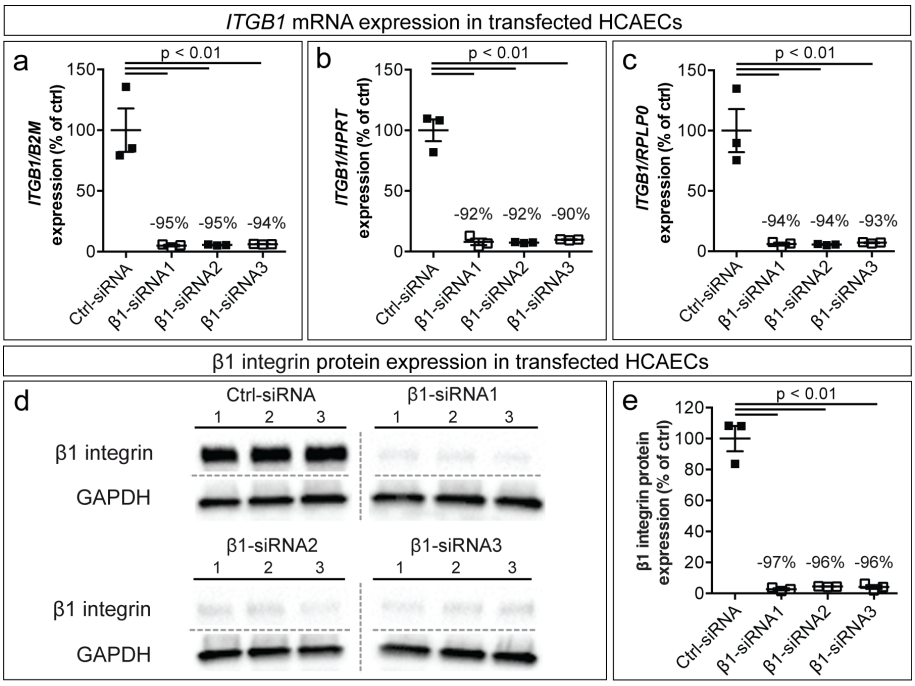

Figure 3.23: β1 integrin is efficiently silenced in HCAECs upon transfection with specific siRNAs.
Analysis of the efficiency of siRNA-mediated *ITGB1* knockdown in human coronary artery endothelial cells (HCAECs) by qPCR and Western blotting. **(a-c)** Quantification of *ITGB1* gene expression after transfection of HCAECs with control siRNA (ctrl-siRNA) or one of three different siRNAs against *ITGB1* (referred to as β1-siRNA1, β1-siRNA2 and β1-siRNA3) by using three housekeeping genes, that is **(a)** *B2M*, **(b)** *HPRT1* and **(c)** *RPLP0*. **(d)** Representative Western blot images of β1 integrin and GAPDH protein expression in HCAECs after transfection with ctrl-siRNA, β1-siRNA1, β1-siRNA2 and β1-siRNA3. **(e)** Semi-quantitative analysis of β1 integrin protein expression related to the expression of GAPDH as a housekeeping protein. Reported values are means ± standard error of the mean (SEM) with n = 3 independent transfections per siRNA. Statistical significance was determined using

one-way ANOVA with Dunnett's multiple comparison test. Anna Branopolski performed the presented experiment.

We normalized the expression of *ITGB1*-mRNA to that of three different housekeeping genes and observed a reduction of more than 90% in *ITGB1* expression for all β1-siRNA constructs when compared to non-targeting siRNA (Fig 3.23 a-c). Consistently, β1 integrin protein expression was significantly reduced by more than 90% in HCAECs transfected with any of the three β1-siRNAs (Fig. 3.23 d, e). Importantly, transfected cells were able to grow to a confluent monolayer and did not exhibit remarkable morphological changes, as evaluated by visual examination. In conclusion, *ITGB1* was efficiently silenced in HCAECs, providing a suitable tool to study the function of human β1 integrin *in vitro*.

3.6.2 Role of β1 integrin in basal proliferation of HCAECs

As our mouse studies showed endothelial β1 integrin expression to be required for the proliferative response of cardiac ECs to transient LAD occlusions, we wished to find out whether β1 integrin has a related function in the human situation. We therefore studied the impact of *ITGB1* silencing on the proliferation of HCAECs. To this end, the cells were transfected with either ctrl-siRNA or one of three β1-siRNAs and examined for proliferation by incorporation of BrdU and immunofluorescence microscopy. Nuclei of proliferating cells were identified by co-localization of DAPI with BrdU and normalized to total cell nuclei number. In addition, we repeated the transfection procedure and analyzed HCAECs for Ki67 expression by immunofluorescence microscopy. While BrdU, as a thymidine analogue, is incorporated into replicating DNA during the S phase, Ki67 is expressed in proliferating cells during all cell cycle phases, but not in resting cells in the G0 phase (Gerdes et al., 1984; Gratzner et al., 1975; Gratzner, 1982). Thus, detection of Ki67 expression served as second approach to evaluate cell proliferation.

Analysis of immunofluorescence images showed that transfection of HCAECs with each β1-siRNA resulted in a significantly reduced number of BrdU-positive cells by around one-quarter when compared to transfection with ctrl-siRNA (Fig. 3.24 a-e). This observation suggests that silencing of *ITGB1* attenuated the proliferation of HCAECs *in vitro*. In line with this, we noted a trend towards a decreased total number of *ITGB1*-silenced HCAECs after two days of incubation compared to control cells (Fig. 3.24 f). Quantification of Ki67-positive HCAECs revealed that transfection with each β1-siRNA significantly reduced the relative number of those cells by around 10% compared to ctrl-siRNA (Fig. 3.24 g), which confirms the results obtained from the BrdU proliferation assay. Moreover, we again observed a trend towards a reduction of the total cell number for β1-siRNA1 and even a significant decrease for β1-siRNA2 and β1-siRNA3 compared to ctrl-siRNA (3.24 h). These results collectively

demonstrate the requirement of β1 integrin expression for full proliferation of HCAECs *in vitro*.

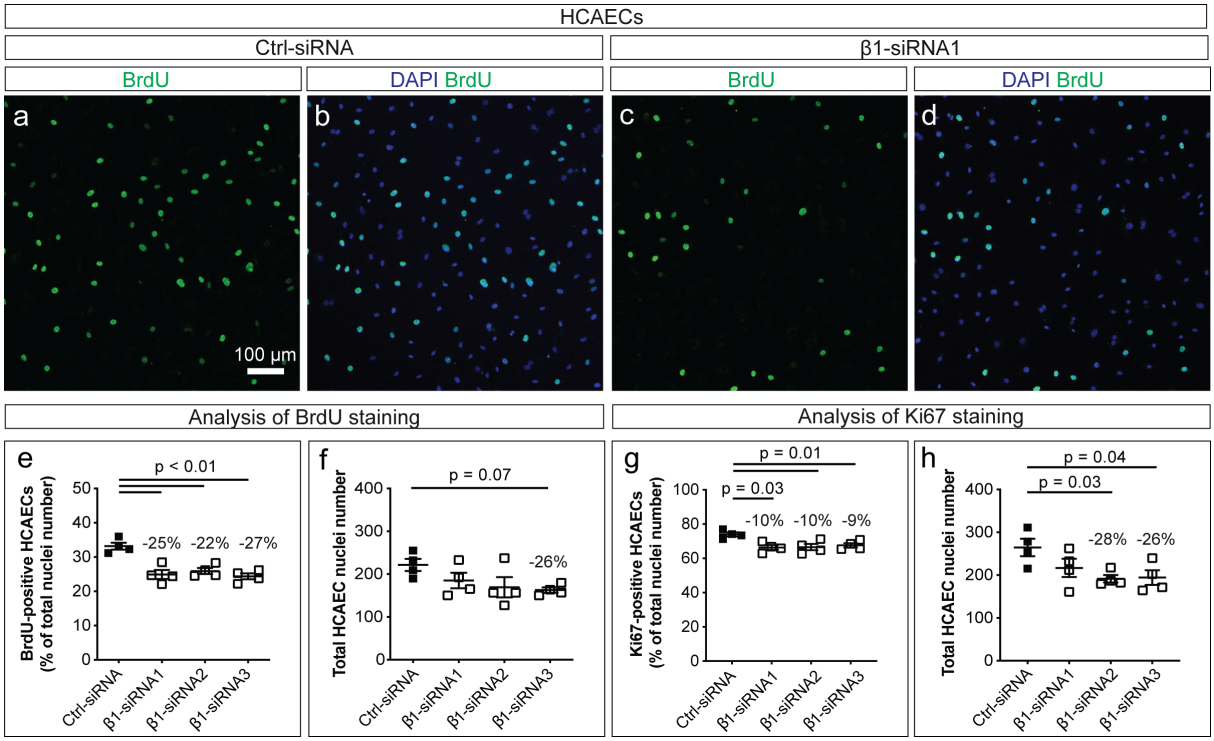

Figure 3.24: Full proliferation of cultured HCAECs requires *ITGB1* gene expression.
Analysis of HCAEC proliferation after transfection with ctrl-siRNA or one of three different siRNAs against *ITGB1* (referred to as β1-siRNA1, β1-siRNA2, β1-siRNA3), by immunofluorescence staining of incoorporated BrdU and Ki67. **(a-d)** Representative LSM images of HCAECs transfected with **(a, b)** ctrl-siRNA or **(c, d)** β1-siRNA1, and stained for BrdU (green) and DAPI (blue). **(e, g)** Quantification of **(e)** BrdU- or **(g)** Ki67-positive HCAEC nuclei, represented as percentage of total cell nuclei number. **(f, h)** Quantification of total number of cell nuclei two days after siRNA transfection. Reported values are means ± standard error of the mean (SEM); n = 4 independent transfections per siRNA. Statistical significance was determined using one-way ANOVA with Dunnett's multiple comparison test. Anna Branopolski performed the presented experiment.

3.6.3 Role of β1 integrin in the regulation of eNOS expression in HCAECs

Nitric oxide (NO) is a central signaling molecule in vascular biology, as it plays an important role in the maintenance of vascular homeostasis. In the vasculature, NO is produced in ECs by eNOS, which has been reported to play an important role in cardioprotection-related processes such as flow-dependent vasodilation as well as vascular growth and remodeling (Dai and Faber, 2010; Heiss et al., 2015). The activity of eNOS is regulated by post-translational modifications including phosphorylation by different kinases, e.g. by AKT (Dimmeler et al., 1999). While it was reported that stimulation of β1 integrin triggers the phosphorylation of AKT in different cell types, only a small number of published studies focused on the question whether β1 integrin and eNOS functionally interact in the context of CVD (Henning et al., 2019; Nho et al., 2005; Velling et al., 2004; Yang and Rizzo,

2013). For instance, it was demonstrated that exposure of human umbilical venous ECs (HUVECs) to shear stress leads to activation of eNOS in a β1 integrin-dependent manner (Yang and Rizzo, 2013). Consistently, the results of FMD measurements in eNOS-deficient mice point to a possible interaction of β1 integrin and eNOS, since function blocking of the integrin did not result in further impairment of the vasodilatory response (Henning et al., 2019). Thus, there is limited knowledge about the link between β1 integrin and eNOS in the context of cardioprotection. We therefore examined the effect of *ITGB1* knockdown on the expression of both total and phosphorylated eNOS at serine 1177 (referred to as P(S1177)-eNOS) as one of the most thoroughly studied activation sites of this enzyme (Qian and Fulton, 2013). To this end, HCAECs were transfected with ctrl-siRNA or β1-siRNA1, incubated for 48 h and analyzed for eNOS and P(S1177)-eNOS expression via Western blotting using GAPDH as an internal reference for normalization (Fig. 3.25 a). Semi-quantitative band density analysis of the obtained immunoblots revealed a significant downregulation of eNOS expression by 73% in *ITGB1* knockdown HCAECs compared to control cells (Fig. 3.25 b). We also observed that P(S1177)-eNOS protein levels were reduced upon silencing of *ITGB1* in HCAECs by 56%, however, not significantly (Fig. 3.25 c).

All in all, the results suggest that β1 integrin is required for full expression of eNOS in HCAECs under static conditions *in vitro*, pointing to a possible role of the integrin in the regulation of NO bioavailability in the coronary system by modulating the expression of eNOS and its modified forms in cardiac ECs.

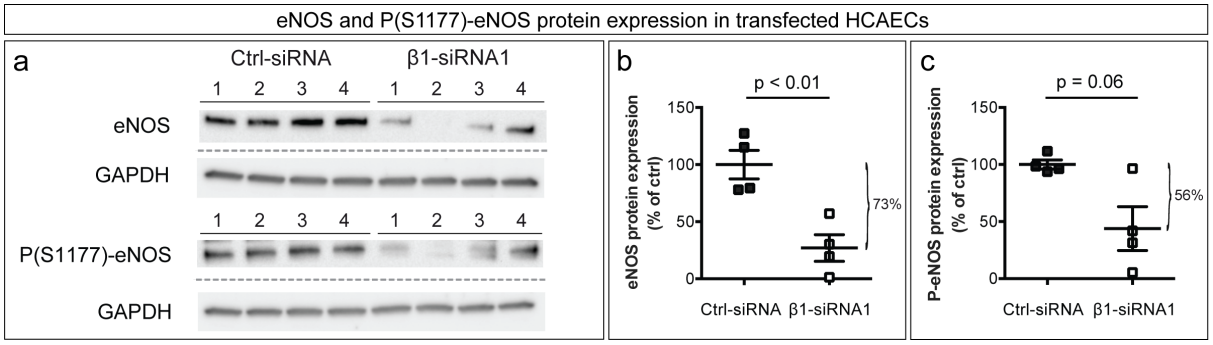

Figure 3.25: Silencing of β1 integrin (*ITGB1*) results in reduced protein expression of eNOS and P(S1177)-eNOS in HCAECs.
Analysis of eNOS and P(S1177)-eNOS protein expression in transfected HCAECs by Western blotting. **(a)** Representative Western blot images of eNOS, P(S1177)-eNOS and GAPDH protein expression in HCAECs after transfection with either ctrl-siRNA or β1-siRNA1. **(b, c)** Semi-quantitative analysis of **(b)** eNOS and **(c)** P(S1177)-eNOS protein expression related to the expression of GAPDH as a housekeeping protein. Reported values are means ± standard error of the mean (SEM) with n = 4 independent transfections per siRNA. Statistical significance was determined using unpaired, two-tailed Students t-test. Anna Branopolski and Carina Henning performed the presented experiment.

3.6.4 Role of β1 integrin in secretion of HGF by HCMVECs

ECs can secrete growth factors such as hepatocyte growth factor (HGF), thereby promoting tissue growth and survival (Lorenz et al., 2018; Rafii et al., 2016). Increased levels of serum HGF have been observed in patients in the early phase of acute MI (Matsumori et al., 1996). Moreover, in a rat model of I/R, HGF was reported to be upregulated in the myocardium after MI and to have a cardioprotective function (Nakamura et al., 2000; Ono et al., 1997). Recently, it was shown that endothelial β1 integrin is required for the production of HGF during liver development (Lorenz et al., 2018). These reports altogether raised the question whether stimulation of β1 integrin signaling affects HGF secretion by primary human cardiac ECs. To address this question, we activated β1 integrin in those ECs using a specific antibody and analyzed the effect of this activation on HGF protein concentration in the supernatant via ELISA (Wayner et al., 1993). When working with the supernatants of HCAECs, we noted that HGF concentrations were under the detection limit in all tested conditions. Moreover, the distribution of HCAECs in the heart and hence their interaction with the surrounding tissue are generally limited to the location of the coronary artery tree. For both reasons, in this experimental series we employed primary human cardiac microvascular ECs (HCMVECs), that secrete detectable amounts of HGF *in vitro* and are found in the entire myocardium, potentially enabling a more comprehensive secretion of cardioprotective factors.

In order to ensure that the used antibody was able to activate β1 integrin in our experimental setup, HCMVECs were treated with either control antibody or β1 integrin activating antibody for 90 minutes and immunostained for the active form of the integrin. Immunofluorescence analysis showed that the mean intensity of the activated β1 integrin was significantly increased after the treatment of HCMVECs with the activating antibody by 91% compared to control antibody (Fig. 3.26 a-e), verifying successful activation of the integrin. We then determined the concentration of HGF in the supernatants of HCMVECs after the respective antibody treatment. Repeating the experiment three times in total, we obtained different results. In particular, the treatment with β1 integrin activating antibody resulted in 1) no increase, 2) a significant increase and 3) a tendency towards an increased HGF concentration as compared to control antibody. The latter results are presented below (Fig. 3.26 f).

Taken together, the results show that the activation of β1 integrin in HCMVECs can, to some extent, induce HGF secretion, thereby pointing to a possible link between endothelial β1 integrin-mediated cardioprotection and HGF secretion.

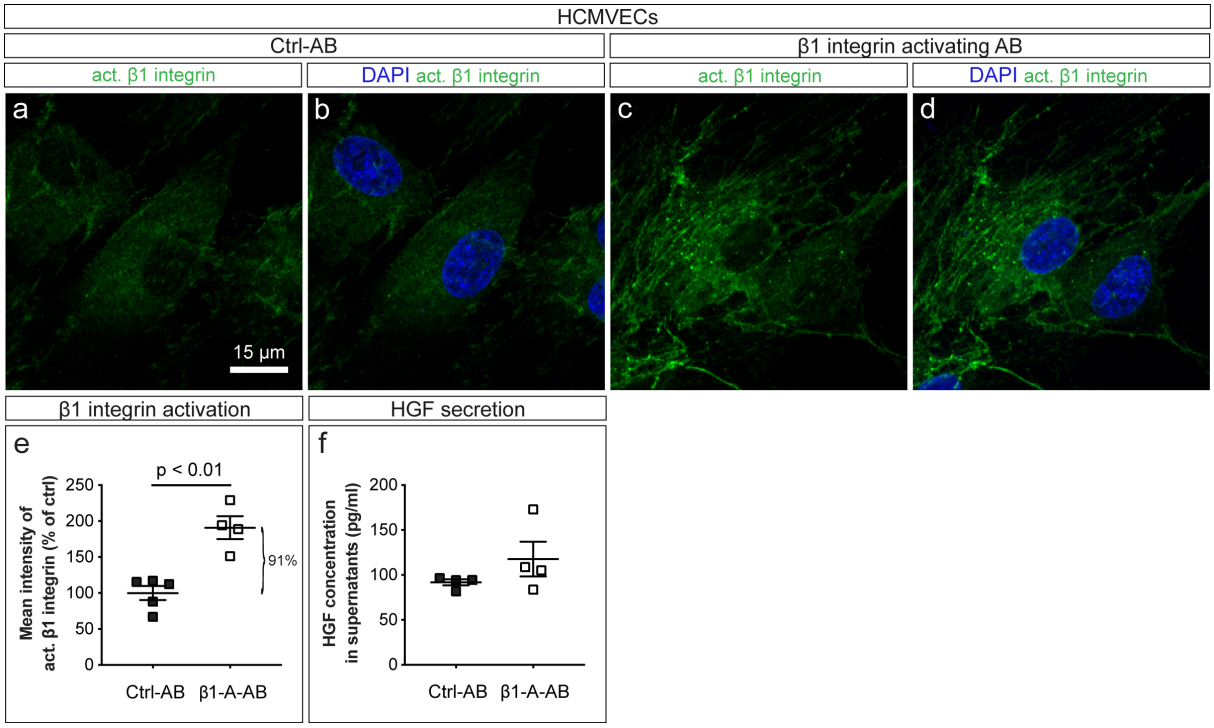

Figure 3.26: Activation of β1 integrin in HCMVECs results in a non-significant increase in HGF concentration in the supernatant.
Analysis of HGF secretion by human cardiac microvascular endothelial cells (HCMVECs) after the treatment with control antibody (ctrl-AB) and β1 integrin activating antibody (β1-A-AB). **(a-d)** Representative LSM images of HCMVECs treated with **(a, b)** ctrl-AB or **(c, d)** β1-A-AB and stained for activated β1 integrin (green) and DAPI (blue). **(e)** Quantification of the mean intensity of activated β1 integrin, shown as percentage of ctrl-AB-treated cells. **(f)** Quantification of HGF concentration (in pg/ml) in the supernatants of HCMVECs after ctrl-AB or β1-A-AB treatment. Reported values are means ± standard error of the mean (SEM); **(e)** β1 integrin activation: ctrl-AB n = 5 and β1-A-AB n = 4; **(f)** HGF secretion: n = 4 per condition. Statistical significance was determined using unpaired, two-tailed Students t-test. Anna Branopolski performed the presented experiment.

3.7 *In vitro* studies with mechanically stimulated HCAECs

While elevated fluid shear stress (FSS) is regarded as the main force in arteriogenesis, circumferential wall stress (CWS), which is enhanced by shear stress-induced vasodilation, was also proposed to be an important player in this context (Demicheva et al., 2008; Ma and Bai, 2020). These two biomechanical forces are tightly linked to each other, making it difficult to distinguish between their respective effects *in vivo*. With the aim to investigate the proliferative response of cardiac ECs to each of the two stimuli, we designed a series of *in vitro* experiments, including a transient exposure of HCAECs to either FSS increase or mechanical stretching. This way, we intended to mimic the transient biomechanical changes presumably occurring in the vasculature during the RepI/R procedure in our mouse studies.

3.7.1 Influence of increased fluid shear stress on proliferation of HCAECs

In order to study the effect of changes in shear stress on proliferation of HCAECs *in vitro*, we used the computer-controlled ibidi® pump system to generate a defined FSS by modulating the flow rate of the culture medium. To this end, HCAECs were plated into the channel of an ibidi® slide and allowed to adhere to the bottom of the channel for about 1 h (Fig. 3.27 a). Subsequently, steady laminar FSS of 10 dyn/cm^2 was applied for 20 h, enabling the cells to adapt to the environment. To simulate the changes in blood flow presumably resulting from the transient LAD occlusions in our mouse studies, the cells were exposed to a 2-fold increased FSS (20 dyn/cm^2) for 30 minutes and further incubated for 90 minutes under 10 dyn/cm^2 (Fig. 3.27 b). For the presented experiment, we decided to apply 10 dyn/cm^2 as baseline FSS since it is considered as the lowest physiological value for coronary arteries (Samady et al., 2011). Due to technical limitation, a value of 20 dyn/cm^2 was chosen for conditions of increased FSS, which is still within the physiological range (Samady et al., 2011). For analysis of proliferation, BrdU was added to the culture medium immediately before increasing the FSS (Fig. 3.27 b). Control ECs were treated equally, but were constantly kept at 10 dyn/cm^2. Finally, proliferating HCAECs under the respective conditions were detected by immunostaining of BrdU and quantified as described in 3.6.2.

The analysis of the BrdU staining revealed similar rates of BrdU-positive HCAECs under conditions of constant (control) and transiently increased FSS (Fig. 3.27 c-g), indicating that the latter had no effect on HCAEC proliferation. Notably, we observed similar results when increasing FSS from 5 to 10 dyn/cm^2 (data not shown). Interestingly, in porcine vein ECs, application of high FSS was even found to suppress BrdU incorporation compared to low FSS (Ji et al., 2019). Furthermore, it was shown that HUVECs respond to an increase in FSS for 0.5 s with an enhanced proliferation, whereas in case of an application of steady laminar FSS for 20 minutes, the proliferation was inhibited (White et al., 2001). However, the researchers used HUVECs under static conditions as controls, which is not directly comparable with our experimental set-up and less representative for the situation *in vivo*.

In sum, the obtained results indicate that a transient increase in FSS had no effect on the rate of proliferating HCAECs, pointing out that changes in blood flow and hence FSS alone may not be sufficient to induce cardiac EC proliferation.

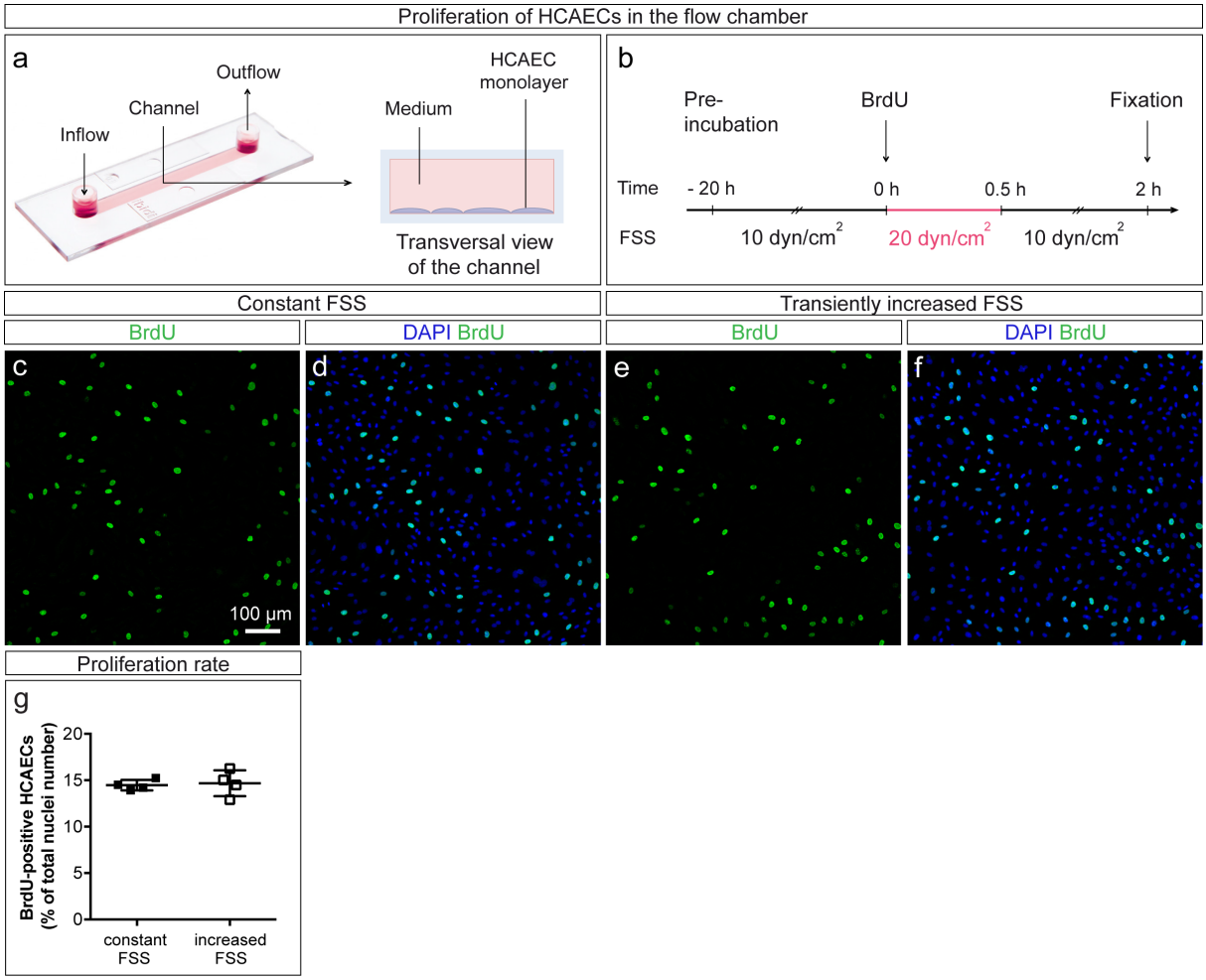

Figure 3.27: Transient increase in shear stress does not induce a proliferative response in cultured HCAECs.
(a) Overview of the ibidi® flow chamber, including the channel and two reservoirs for medium inflow and outflow via a tube system, connected to the ibidi® pump, and a schematic illustration of the channel with the HCAEC monolayer. **(b)** Time line of the experimental procedure: After pre-incubation under a fluid shear stress (FSS) of 10 dyn/cm^2 for 20 h in ibidi® flow chambers, BrdU was added, and HCAECs were immediately exposed to an FSS of 20 dyn/cm^2 for 30 minutes, followed by a return to 10 dyn/cm^2 for 90 minutes. Control cells were treated equally except for the FSS increase. **(c-f)** Representative LSM images of HCAECs **(c, d)** under constant shear stress or **(e, f)** after a transiently increased shear stress. ECs were stained for BrdU (green) and DAPI (blue). **(g)** Quantification of BrdU-positive HCAEC nuclei, represented as percentage of total cell nuclei number. Reported values are means ± standard error of the mean (SEM); n = 4 per condition. Statistical significance was determined using unpaired, two-tailed Students t-test. Anna Branopolski performed the presented experiment. The image of the ibidi® flow chamber was modified from www.ibidi.com.

3.7.2 Influence of mechanical stretching on proliferation of HCAECs

We next examined the influence of mechanical stretching of HCAECs on their proliferation as an *in vitro* method to simulate the effects of vasodilation and hence increased CWS on cardiac ECs. To this end, we used a manual cell stretching system with flexible stretching chambers, composed of polydimethylsiloxane, a silicone elastomer (Fig

3.28 a). HCAECs were allowed to grow on these stretching chambers for 2 days and, afterwards, were subjected to a transient 25% stretching for 30 minutes, followed by an incubation under unstretched conditions for 90 minutes. For detection of proliferating cells, BrdU was added immediately prior to stretching and incubated for 2 h in total (Fig 3.28 b). Control cells were grown on stretching chambers and treated with BrdU for 2 h under unstretched conditions. Proliferating cells were quantified as described in 3.6.2.

The analysis of the BrdU incorporation assay revealed a significant increase in BrdU-positive HCAEC nuclei by 31% after stretching compared to the unstretched control cells (Fig. 3.28 c-g), indicating that transient mechanical stretching induces proliferation of HCAECs. This is consistent with recently published *in vitro* studies reporting that mechanical stretching increases the proliferation rate of lymphatic ECs and bovine aortic ECs (BAECs) as well (Nishimura et al., 2006; Planas-Paz et al., 2012).

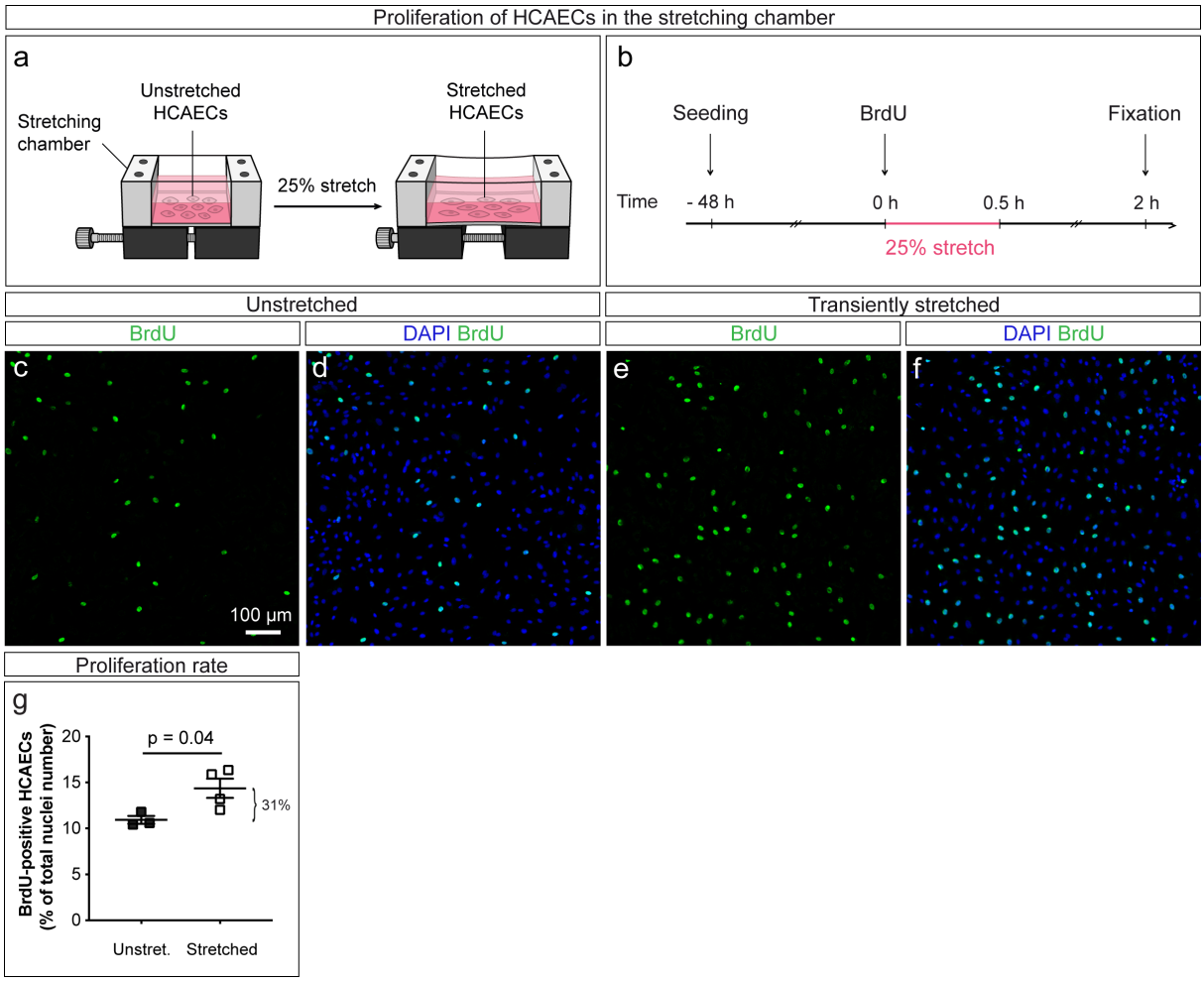

Figure 3.28: Transient mechanical stretching induces proliferation of HCAECs.
(a) Schematic illustration of the manual cell stretching system, showing an unstretched and a stretched chamber containing a HCAEC monolayer. **(b)** Time line of the experimental procedure: 48 h after seeding, BrdU was applied, and HCAECs were immediately exposed to 25% mechanical stretching for 30 minutes, followed by an incubation for further 90 minutes under unstretched conditions. Control cells were treated equally except for the stretching. **(c-f)** Representative LSM images of **(c, d)** unstretched or **(e, f)** transiently stretched HCAECs. ECs were stained for BrdU (green) and DAPI (blue). **(g)** Quantification of BrdU-positive HCAEC nuclei, represented as

percentage of total cell nuclei number. Reported values are means ± standard error of the mean (SEM); n = 3 unstretched ECs and n = 4 stretched ECs. Statistical significance was determined using unpaired, two-tailed Students t-test. Anna Branopolski performed the presented experiment. The illustration of the stretching chamber was modified from Lorenz et al., 2018.

3.7.3 Effect of mechanical stretching on β1 integrin activation and AKT phosphorylation in HCAECs

Our *in vivo* studies showed that the proliferative response of cardiac ECs to transient ischemia was inhibited in mice lacking endothelial β1 integrin. Given the increased proliferation rate of stretched HCAECs *in vitro*, but not of those exposed to an increased FSS, we wished to investigate whether mechanical stretching has an effect on β1 integrin signaling pathway in HCAECs. The kinase AKT has an important function in the regulation of cell proliferation and is a potential interaction partner of integrins in the context of mechanical stimulation. In particular, *ex vivo* experiments on resistance arteries isolated from rats and mice indicated that α1 integrins mediate flow-induced vasodilation via activation of phosphoinositide 3-kinase (PI3K) and AKT (Loufrani et al., 2008). Further, it was shown that exposure of BAECs to shear stress results in a β1 integrin-dependent phosphorylation of AKT at serine 473, one of the most thoroughly studied activation sites of this kinase (Yang and Rizzo, 2013). Thus, we next examined the impact of mechanical stretching of HCAECs on the activation of β1 integrin and phosphorylation of AKT at serine 473, in the following abbreviated as P(S473)-AKT. To this end, HCAECs were stretched for 15 or 30 minutes and immediately fixed for the detection of activated β1 integrin by immunofluorescence staining or lysed for analysis of AKT phosphorylation by Western blotting, respectively. For the latter, we used specific antibodies against total AKT, P(S473)-AKT as well as GAPDH for normalization.

The analysis of immunofluorescence images revealed a significant increase in the mean intensity of the activated form of β1 integrin in stretched HCAECs by 36% compared to unstretched control cells (Fig. 3.29 a-e). This observation indicates that exposure of HCAECs to mechanical stretching leads to β1 integrin activation, which is consistent with studies on lymphatic and hepatic ECs (Lorenz et al., 2018; Planas-Paz et al., 2012). Moreover, mechanical stimulation of HCAECs resulted in the activation of AKT, as indicated by a significant 2.6-fold increase in P(S473)-AKT levels normalized to total AKT levels (Fig. 3.29 f, g). The latter is in line with *in vitro* studies on BAECs and SMCs demonstrating cyclic stretch to induce AKT phosphorylation (Chen et al., 2001; Haga et al., 2003; Nishimura et al., 2006).

Taken together, the results indicate that mechanical stretching of HCAECs activates both β1 integrin and AKT, which points to a possible functional interaction of these proteins in the context of mechanotransduction and stretch-induced proliferation.

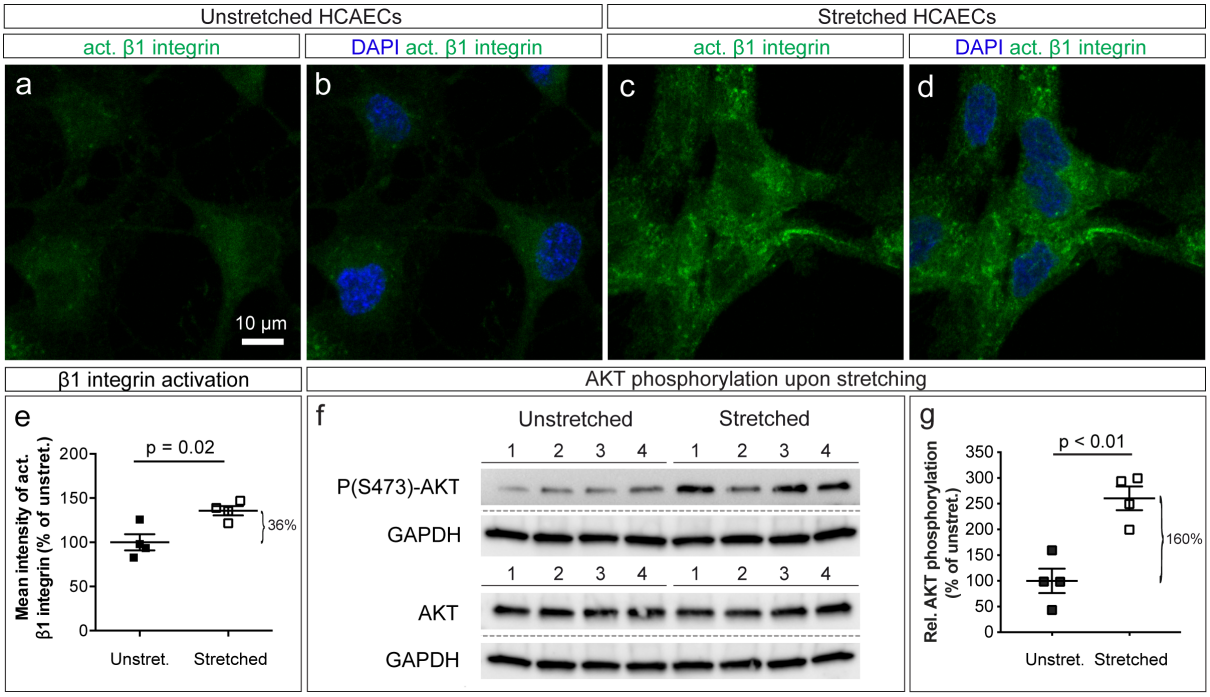

Figure 3.29: Mechanical stretching of HCAECs results in an enhanced β1 integrin activation and AKT phosphorylation.
Analysis of β1 integrin activation and AKT phosphorylation at serine 473 upon stretching of HCAECs. **(a-d)** Representative LSM images of **(a, b)** unstretched or **(c, d)** stretched HCAECs, stained for activated β1 integrin (green) and DAPI (blue). **(e)** Quantification of the mean intensity of activated β1 integrin, shown as percentage of unstretched cells. **(f)** Representative Western blot images of AKT, P(S473)-AKT and GAPDH expression in unstretched and stretched HCAECs. **(g)** Quantification of phosphorylated AKT, related to total AKT expression and shown as percentage of unstretched ECs. GAPDH was used as housekeeping protein for normalization of AKT and P(S473)-AKT. Reported values are means ± standard error of the mean (SEM); n = 4 per condition for β1 integrin activation and n = 4 per condition for AKT phosphorylation. Statistical significance was determined using unpaired, two-tailed Students t-test. Anna Branopolski performed the presented experiment.

3.7.4 Role of β1 integrin in stretch-induced AKT phosphorylation and HCAEC proliferation

Based on our observations that mechanical stretching of HCAECs activates β1 integrin and results in both enhanced AKT phosphorylation and cell proliferation, we wished to determine whether the latter effects are dependent on β1 integrin. In this respect, we next analyzed the impact of siRNA-mediated *ITGB1* gene silencing on stretch-induced AKT phosphorylation in HCAECs and their proliferation. Following 48 h of incubation after transfection with either ctrl-siRNA or β1-siRNA1, HCAECs were stretched and analyzed for

AKT phosphorylation by Western blotting as well as BrdU incorporation by immunofluorescence staining as described in 3.7.3 and 3.6.2.

Semi-quantitative band density analysis of the obtained immunoblots revealed a 5.4-fold increase in phosphorylated AKT in the lysates of ctrl-siRNA-transfected HCAECs after stretching as compared to the unstretched cells (Fig. 3.30 a, b). Thus, although statistically not significant, stretching of ctrl-siRNA-transfected HCAECs seemed to activate the AKT signaling pathway, which is consistent with the results of the above described experiment (see Fig. 3.29 g). In contrast, in case of the transfection with β1-siRNA1, the relative levels of P(S473)-AKT were similar between unstretched and stretched HCAECs (Fig. 3.30 c, d), indicating that silencing of *ITGB1* inhibited AKT phosphorylation in response to mechanical stretching.

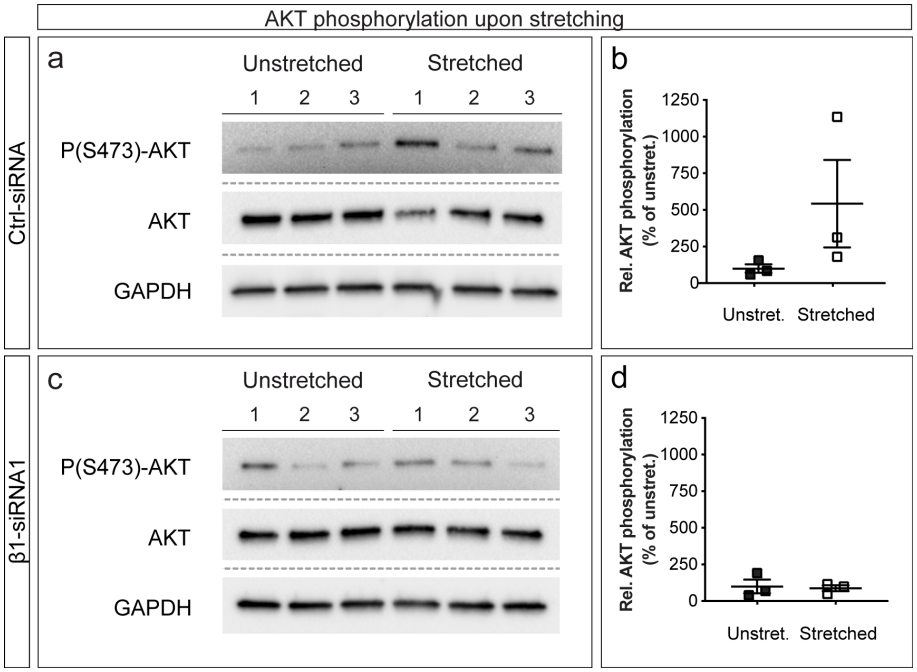

Figure 3.30: The non-significant increase in AKT phosphorylation in response to mechanical stretching is inhibited upon silencing of β1 integrin (*ITGB1*) in HCAECs.
(a-d) Western blotting analysis of AKT phosphorylation at serine 473 upon mechanical stretching of **(a, b)** control and **(c, d)** *ITGB1* knockdown HCAECs. **(a, c)** Representative Western blot images of AKT, P(S473)-AKT and GAPDH expression in unstretched and stretched HCAECs, transfected with either **(a)** ctrl-siRNA or **(b)** β1-siRNA1, respectively. **(b, d)** Semi-quantitative analysis of phosphorylated AKT, related to total AKT expression in unstretched and stretched HCAECs after transfection with **(b)** ctrl-siRNA or **(d)** β1-siRNA1. P(S473)-AKT levels are shown as percentage of unstretched HCAECs. GAPDH was used as housekeeping protein for normalization of AKT and P(S473)-AKT. Reported values are means ± standard error of the mean (SEM) with n = 3 per condition. Statistical significance was determined using unpaired, two-tailed Students t-test. Anna Branopolski performed the presented experiment.

The quantification of BrdU incorporation in ctrl-siRNA-transfected HCAECs showed mechanical stretching to significantly increase the number of BrdU-positive HCAECs by 21% compared to unstretched cells (3.31 a-d, i). This, first, confirms the results obtained from

proliferation studies without transfection (see 3.7.2), and, second, ensures an adequate proliferative response of electroporated cells to stretching. Strikingly, when analyzing β1-siRNA1-transfected HCAECs, we found that mechanical stretching failed to induce proliferation, as indicated by similar numbers of BrdU-positive HCAECs under unstretched and stretched conditions (Fig. 3.31 e-h, j). This is consistent with a previous study, where silencing of β1 integrin was observed to reduce the proliferation rates of stretched lymphatic ECs (Planas-Paz et al., 2012). Moreover, we noticed a reduced number of proliferating HCAECs under unstimulated conditions after transfection with β1-siRNA1 as compared to ctrl-siRNA, and this inhibitory effect seemed to be stronger when using stretching chambers compared to 24-well plates (see Fig. 3.23). Thus, on the one hand, this observation is consistent with the results of our proliferation studies performed under static conditions, presented in 3.6.2. On the other hand, it points to a possible differential influence of the well plate and stretching chamber properties on the inhibitory effect of β1 integrin silencing on proliferation.

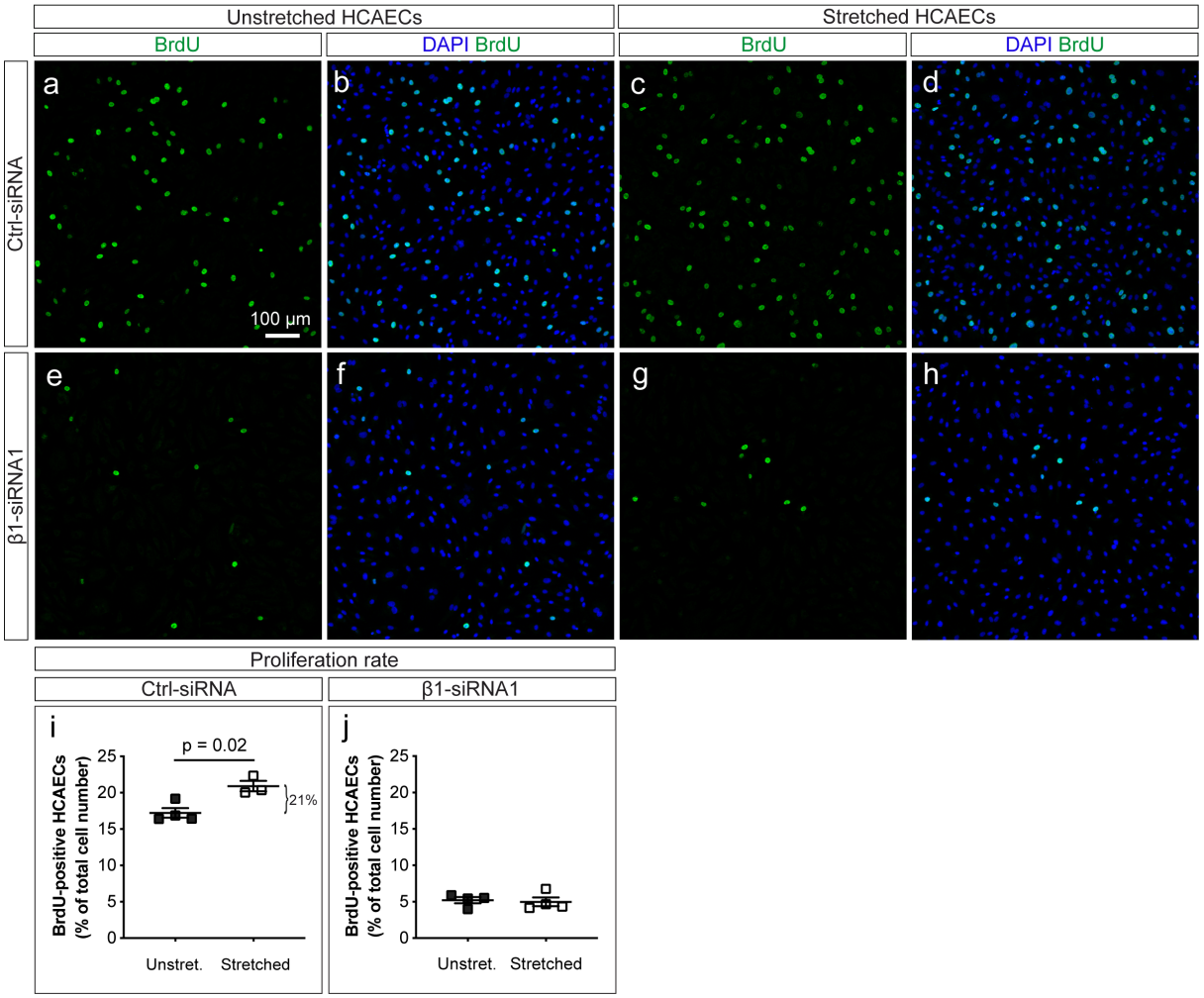

Figure 3.31: Stretch-induced HCAEC proliferation is inhibited upon β1 integrin (*ITGB1*) silencing.
Analysis of control and *ITGB1* knockdown HCAEC proliferation upon transient mechanical stretching. **(a-h)** Representative LSM images of HCAECs transfected with either **(a-d)** ctrl-siRNA or **(e-h)** β1-siRNA1 and **(a, b, e, f)** incubated unstretched or **(c, d, g, h)** exposed to transient stretching. ECs were

stained for BrdU (green) and DAPI (blue). **(I, j)** Quantification of BrdU-positive nuclei of **(i)** ctrl-siRNA- and **(j)** β1-siRNA1-transfected HCAECs, represented as percentage of total cell nuclei number. Reported values are means ± standard error of the mean (SEM); n = 4 ctrl-siRNA-transfected, unstretched, n = 3 ctrl-siRNA-transfected, stretched, n = 4 β1-siRNA1-transfected, unstretched and n = 4 β1-siRNA1-transfected, stretched ECs. Statistical significance was determined using unpaired, two-tailed Students t-test. Anna Branopolski performed the presented experiment.

In conclusion, the obtained results suggest that β1 integrin plays a key role in stretch-induced activation of the AKT signaling pathway in HCAECs as well as in their proliferation, pointing to a possible interaction between β1 integrin and AKT in the context of adaptive vascular growth.

The following chapter contains parts described in our publications Henning et al., 2019 and Henning et al., 2021.

4. Discussion

4.1 Role of endothelial β1 integrin in adult coronary and peripheral vascular growth

Chronic hemodynamic changes in consequence of an arterial occlusion can trigger vascular remodeling processes including vascular growth. This adaptive response is essential to restore sufficient blood supply of ischemic territories and, in turn, relies on an adequate sensation and transmission of mechanical stimuli (Hoefer et al., 2013; Schaper and Scholz, 2003; Schaper, 2009; Zimarino et al., 2014). The main focus of the present study was to investigate the role of endothelial β1 integrin, as a mechanosensory protein, in adult coronary and peripheral vascular growth.

4.1.1 Role of mechanical forces in the proliferation of cardiac ECs

Proliferation of endothelial cells (ECs) is a characteristic feature of biomechanically activated endothelium and is considered as an initial and essential step in adult vascular growth (Cai and Schaper, 2008; Moraes et al., 2014; Seiler et al., 2013). In order to study cardiac EC proliferation *in vivo*, we induced coronary growth in mice by using the model of repetitive myocardial ischemia (RepI/R). This model is supposed to reflect the transient ischemic events occurring in the human heart affected by coronary artery disease (CAD) (Lavine et al., 2013).

We found RepI/R to induce EC proliferation in both the ischemic and the non-ischemic myocardium. In the ischemic myocardium, this effect might be mediated by hypoxia during the occlusion, e.g. via the induction of the well-characterized hypoxia-inducible factor-1α (HIF-1α) pathway or inflammation-associated processes, combined with biomechanical forces in the blood vasculature (Cai and Schaper, 2008; Heil et al., 2006; Henning et al., 2021; Seiler et al., 2013). Since in the non-ischemic myocardium, the observed proliferative response was independent of local hypoxia, changes in biomechanical forces may act as a principal trigger here. This would be consistent with the widely accepted hypothesis of fluid shear stress (FSS)-mediated, hypoxia-independent EC activation in arteriogenesis (Heil et al., 2006; Schaper and Scholz, 2003).

From the hemodynamic point of view, FSS likely increases in the non-LAD circulation during the occlusion and in the LAD circulation after re-opening of the artery due to reactive

hyperemia. Previous studies concerning the effect of high FSS on EC proliferation have provided controversial results, which were highly dependent on the applied conditions (Akimoto et al., 2000; Ji et al., 2019; White et al., 2001). Moreover, none of these studies reflect the transient nature of the increases in FSS related to CAD. This raised the question about the individual contribution of FSS and the associated circumferential wall stress (CWS) to the proliferative response of cardiac ECs to transient arterial occlusions. Therefore, we investigated the effects of transiently applied high laminar FSS and mechanical stretching, as an experimental representative of CWS, on the proliferation of primary human coronary artery ECs (HCAECs) *in vitro*. We observed that mechanical stretching but not elevated FSS increased the proliferation rate of these cells. Of note, the pro-proliferative effect of *in vitro* mechanical stretching has already been described for other cell types including lymphatic and non-cardiac blood vascular ECs as well as for vascular smooth muscle cells (VSMCs) (Li and Sumpio, 2005; Planas-Paz et al., 2012). In contrast, application of steady laminar FSS on cultured vascular ECs was reported to induce cell cycle arrest through an upregulation of p21, a well-characterized regulator of cell cycle progression, thereby inhibiting cell proliferation (Akimoto et al., 2000). Largely consistent with published studies, our *in vitro* findings point out that increased FSS itself may not be the main driving force for the biomechanically induced proliferative response of cardiac ECs to transient arterial occlusions, but rather the consequently increased CWS due to shear stress-induced vasodilation in the affected circulation (Ma and Bai, 2020; Simons and Eichmann, 2015). Additionally, the phenomenon of ischemic or hypoxic vasodilation during the occlusion, which has been previously described for canine coronary arterioles, may contribute to the overall stretch and hence to the proliferative response of ECs in the ischemic myocardium (Nishikawa et al., 2004).

Proliferating ECs seemed to be widely distributed within the sections of RepI/R-treated hearts. In the case of a stretch-dependent mechanism, such a comprehensive proliferative response would imply the ability of coronary microvessels to undergo vasodilation and, hence, the presence of VSMCs and/or pericytes. The latter were reported to regulate the capillary diameter, e.g. in the pancreas and the cerebrovascular system (Almaca et al., 2018; Hall et al., 2014; Hamilton et al., 2010). Although it is known that pericytes cover cardiac capillaries in humans, little is known about their role in the regulation of capillary diameter and blood flow in the heart (Nees et al., 2012; Su et al., 2021). Therefore, it is not clear whether proliferation of cardiac capillary ECs, in principal, would be directly induced by stretch or rather by growth factors released by ECs from surrounding dilated arterioles or arteries. To address this aspect, cardiac vessels that display EC proliferation after RepI/R should be characterized in respect to the coverage by VSMCs and pericytes.

The theory that FSS mediates endothelial activation and the subsequent vascular response indirectly via CWS is supported by further reports of distinct effects of FSS and mechanical stretching on ECs *in vitro*. For instance, stretching of ECs was shown to induce the expression of monocyte chemoattractant protein-1 (MCP-1), a potent arteriogenic factor that is upregulated in the activated endothelium, whereas application of FSS had no significant effect (Demicheva et al., 2008; Okada et al., 1998). Moreover, it was shown that the DNA-binding transcription factor Kruppel-like factor 2 (KLF2) is induced in ECs in response to high FSS but not to mechanical stretching (Dekker et al., 2005; Nakajima and Mochizuki, 2017). Importantly, KLF2 was shown to exhibit anti-proliferative properties, which may contribute to the differential effects of these two biomechanical forces on EC proliferation, as was observed in our and others' studies (Atkins and Jain, 2007). Regarding the *in vivo* situation, the pro-proliferative effects of increased CWS seem to dominate. A further differentiation of the actions of CWS and FSS in the vascular system is interesting to be addressed in future research by using *in vitro* cultured ECs or by *ex vivo* studies on arteries isolated from mice or larger animals. Besides, for a more precise interpretation of the *in vivo* data, it would be also important to prove the presumed biomechanical changes in the murine myocardium during and after LAD occlusions. However, the assessment of hemodynamics in the mouse heart is technically difficult and requires further improvements in ultrasound techniques for the mouse coronary system.

4.1.2 Role of endothelial β1 integrin in the proliferative response of cardiac ECs to coronary occlusions

To date, the molecular mechanisms of biomechanical activation of ECs are poorly understood. To determine whether endothelial β1 integrin is involved in RepI/R-induced EC proliferation as a mechanosensory protein, we employed a pharmacological inhibition of this integrin as well as an endothelium-specific deletion of the *Itgb1* gene (*Itgb1*^{iECKO}). Both the pharmacological and genetic manipulations were found to inhibit the proliferative response of ECs to RepI/R in the ischemic and the non-ischemic myocardium, suggesting a critical role of endothelial β1-integrin in this context.

When focusing on the non-ischemic myocardium, where the increased EC proliferation is likely a result of biomechanical stimulation, we observed a trend towards an increased expression of both total and endothelial β1 integrin upon RepI/R. This is in line with a previous *in vitro* study, showing a time-dependent regulation of α5β1 integrin expression by FSS in human umbilical vein ECs (HUVECs) (Urbich et al., 2000). The same heterodimer was also revealed to be upregulated in the vascular wall of collateral vessels after increases in FSS due to femoral artery (FA) ligation in rabbits (Cai et al., 2009). Consistent with its mechanosensory function, we found that mechanical stretching of

HCAECs activates β1 integrin *in vitro*. Moreover, the relevance of endothelial β1 integrin in sensation of changes in biomechanical forces and their transduction into an adequate vascular response was indicated by *in vivo* studies of FA hemodynamics, revealing an attenuated flow-mediated dilation (FMD) response in *Itgb1*^{iECKO} mice compared to control mice (Henning et al., 2019). Therefore, critically impaired endothelial mechanotransduction is the likely reason for the inhibited proliferative response of cardiac ECs to RepI/R in the non-ischemic myocardium of *Itgb1*^{iECKO} mice. This is supported by our *in vitro* studies showing that, in *ITGB1*-silenced HCAECs, stretch induced neither proliferation nor the activating phosphorylation of AKT at S473, as opposed to control cells, i.e. cells transfected with a non-targeting siRNA. Noteworthy, despite the considerable difference in relative AKT phosphorylation in stimulated versus non-stimulated control cells, no statistical difference was indicated, probably due to the high standard deviation. The AKT kinase is involved in various cellular processes including cell proliferation, survival and migration (Manning and Toker, 2017). According to previous studies, AKT can be activated in response to both FSS and stretch, and is capable of regulating the activity of eNOS (Dimmeler et al., 1999; Hu et al., 2013; Lee et al., 2014; Loufrani et al., 2008; Shiojima and Walsh, 2002). Moreover, this kinase was identified as a downstream effector of integrins in vascular cells (Dimmeler et al., 1998; Loufrani et al., 2008; Shiojima and Walsh, 2002; Yang and Rizzo, 2013; Zhang et al., 2005). For instance, α1 integrins were reported to mediate the FMD response in isolated mesenteric resistance arteries via activation of phosphoinositide 3-kinase (PI3K) and AKT (Loufrani et al., 2008). Furthermore, a study on cultured bovine aortic ECs (BAECs) demonstrated that β1 integrin function is critical for FSS-induced phosphorylation of AKT and eNOS (Yang and Rizzo, 2013). Finally, in eNOS knockout mice, which displayed an impaired FMD response, blocking of β1 integrin function had no further negative effect, supporting the relevance of the β1 integrin/AKT/eNOS axis in the acute vascular response to hemodynamic changes (Henning et al., 2019). Based on our and others' findings, endothelial β1 integrin appears to regulate two critical steps implied in the biomechanically induced proliferative response of ECs to arterial occlusions. First, β1 integrin signaling promotes FSS-dependent dilation as an acute response, possibly through AKT and eNOS, resulting in circumferential stretch of ECs as the likely trigger of proliferation. Second, this integrin mediates the proliferative response of ECs to stretch as an essential component of vascular growth. Whether this proliferative response depends on AKT function should be explored in further studies.

While circumferential stretch likely affects the apical and basal surfaces of ECs to a similar extent, fluid flow primarily acts on the apical endothelium. Yet initially, the flow sensing function of integrins was mainly attributed to those located at the basal surface of ECs (Muller et al., 1997; Tzima et al., 2001). More recent studies have provided evidence that apically expressed integrins can also sense and respond to flow (Xanthis et al., 2019;

Yang and Rizzo, 2013). Our immunohistochemical analysis showed that β1 integrin is expressed at the apical and basal sides of the endothelium in the arteries of the murine thigh muscle, pointing that both sides can theoretically contribute to mechanosensation of the murine endothelium. Apical integrins are harbored within the endothelial glycocalyx layer, which coats the luminal surface of the blood vessels and contains other glycoproteins as well as proteoglycans, glycosaminoglycans and plasma proteins (Reitsma et al., 2007; Urner et al., 2018). Interestingly, some of the components of this macromolecular network were shown to be involved in FSS-induced NO production *in vitro* and *in vivo* (Bartosch et al., 2017; Mochizuki et al., 2003; Pahakis et al., 2007; Yen et al., 2015). Moreover, according to a simulation study, the glycocalyx may be an important regulator of integrin function, since simulated variations in its properties were found to modulate the process of integrin clustering (Paszek et al., 2009). Thus, it would be of great interest to explore whether and how physical and molecular properties of the endothelial glycocalyx influence β1 integrin-mediated mechanotransduction. In face of the distinct molecular as well as biomechanical environments at the apical and basal surfaces of ECs, it would be also interesting to investigate the role of β1 integrin in the cellular response to mechanical stretch in regard to its subcellular localization.

As discussed above, it is likely that biomechanical forces contribute to RepI/R-induced EC proliferation in the ischemic myocardium. Also conditions of hypoxia, considered as a modulator of EC proliferation, are probably involved in this response, especially given the apparently stronger induction in the ischemic region compared to the non-ischemic region (Pugh and Ratcliffe, 2003). In a previous *in vitro* study, expression of a constitutively stable form of HIF-1α resulted in an increased proliferation rate of primary human ECs (Yamakawa et al., 2003). Thus, HIF-1α could be a possible candidate mediating hypoxia-dependent induction of EC proliferation by RepI/R. Of note, HIF-1α was shown to induce β1 integrin expression in cultured fibroblasts (Keely et al., 2009). In line with this, the expression of total β1 integrin was found to be increased in the rat and the mouse heart under conditions of chronic myocardial ischemia (Krishnamurthy et al., 2006; Sun et al., 2003). Moreover, the data from our HI experiments revealed an increase in endothelial β1 integrin expression upon FA ligation, which was significant in the hypoxic calf but non-significant in the less hypoxic thigh, underlining the link between hypoxia and the expression of this integrin subunit. Following RepI/R, the expression of both total and endothelial β1 integrin was also increased in the ischemic myocardium, however, this increase was not significant, probably due to the short duration of each ischemic episode. Indeed, previous studies could show that β1 integrin is involved in hypoxia-induced proliferation of mouse cerebral ECs and embryonic stem cells (Lee et al., 2011; Li et al., 2012a).

Another way how ischemia induces EC proliferation could be via inflammation-associated processes. In this regard, immune cells recruited to the hypoxic myocardium

could secrete growth factors and pro-proliferative cytokines, both stimulating ECs to proliferate (Holzinger et al., 1993; Koch et al., 1992; Loganadane et al., 1997; Peet et al., 2020; Presta et al., 1992). Given that integrins play an important role in growth factor-induced cell proliferation, it is possible that secreted pro-proliferative factors fail to induce proliferation in case of abrogated β1 integrin signaling in ECs (Eliceiri, 2001; Schwartz and Assoian, 2001). This possible explanation is in line with our *in vitro* data showing that *ITGB1* silencing reduced HCAEC proliferation under static conditions, where EC proliferation was mainly stimulated by growth factors present in the culture medium. Whether endothelial β1 integrin deletion affects ischemia-induced immune response itself, e.g. with regard to the quantity and composition of inflammatory cells, should be addressed in further studies.

It is known that, apart from arterial occlusions, exercise training can generate acute increases in FSS and vessel diameter and, depending on its intensity, even result in hypoxia (Brocherie and Millet, 2020; Goto et al., 2007; Katz et al., 1996; Tinken et al., 2010). Previous studies in animals and humans suggest that exercise promotes luminal expansion and numerical increases of blood vessels as well as improves the collateral circulation in humans (Huonker et al., 2003; Kojda and Hambrecht, 2005; Mobius-Winkler et al., 2016; Prior et al., 2004; Stebbings et al., 2013; Zbinden et al., 2004; Zbinden et al., 2007). It would be interesting to examine whether these exercise-induced vascular effects comprise β1 integrin-dependent proliferative responses of ECs to mechanical stimuli or hypoxia.

4.1.3 Role of endothelial β1 integrin in adult arteriole and capillary formation

We could show *in vivo* that initial, ischemia-induced cardiac EC proliferation strictly depends on endothelial β1 integrin, and this was strongly supported by our *in vitro* data. We also investigated whether this integrin is required for the consequent vascular remodeling and growth, here represented by capillary and arteriole formation. For this purpose, we used the mouse models of RepI/R and hindlimb ischemia (HI) for coronary and peripheral vascular growth, respectively (Lavine et al., 2013; Limbourg et al., 2009).

We characterized the arteriole formation in response to ischemia in the heart and the hindlimb. Consistent with our proliferation studies and the literature, we found RepI/R to induce arteriole formation in the ischemic and non-ischemic myocardium (Lavine et al., 2013). We could not detect large-caliber collateral vessels after RepI/R, which is also in agreement with other studies involving myocardial I/R (He et al., 2017; Lavine et al., 2013; Miquerol et al., 2015). Probably, the formation of such vessels in the murine heart requires more prolonged biomechanical and/or hypoxic stimulation, as provided by e.g. a permanent LAD ligation (Das et al., 2019; Henning et al., 2021; Zhang and Faber, 2015). Since large-caliber collateral vessels are known to develop from arterioles, the formation of the latter may

generally facilitate collateral growth and is, therefore, of clinical relevance (Faber et al., 2014; Meier et al., 2013). Further, we found that permanent FA ligation induces arteriole formation in the thigh and, not significantly however, in the calf. In addition, the induction of capillary formation, representing the angiogenic response to HI, was found significant in the calf and non-significant in the thigh. It is noteworthy that, upon FA ligation, the perfusion in the calf was reduced for a longer period of time compared to the thigh muscle (Henning et al., 2019). Together, the findings from our coronary and peripheral vascular growth studies indicate that capillary formation is mainly driven by hypoxia-related mechanisms, whereas arteriole formation does not necessarily require hypoxic conditions, which is overall consistent with the literature (Lavine et al., 2013; Limbourg et al., 2009; Persson and Buschmann, 2011).

One possibility to explain how arterioles may develop in the adult heart and hindlimb is via capillary arterialization, a process that was previously identified in the spinotrapezius muscle of adult mice after an arteriolar ligation. Capillary arterialization is required for the recovery of blood perfusion to ischemic territories and, according to the proposed mechanism, involves the expansion of capillary diameter as well as the investment of mural cells (Mac Gabhann and Peirce, 2010; Simons and Eichmann, 2015). Regarding our experiments, it would be interesting to characterize the morphology of the newly formed arterioles in the heart and the hindlimb as well as to investigate whether or not these arterioles are indeed functional.

When we investigated the role of endothelial β1 integrin in coronary vascular growth, we found that this integrin is required for ischemia-induced arteriole formation in the non-ischemic myocardium, but not in the ischemic myocardium. This is in contrast to our proliferation studies and suggests that, in the ischemic myocardium, new arterioles were formed despite inhibited EC proliferation. Interestingly, in the case of pharmacological inhibition of β1 integrin function, RepI/R failed to significantly induce arteriole formation in both regions. This observation might be due to the broad spectrum of cell types affected by the blocking antibody, for instance, inflammatory cells. In particular, integrins in inflammatory cells are essential for their adhesion to ECs and may hence be important in ischemia-related inflammation, which in turn is known to promote vascular growth (Evans et al., 2009; Jin et al., 2006; Mezu-Ndubuisi and Maheshwari, 2020; Schaper and Scholz, 2003). As opposed to the myocardium, we did not detect such regional differences in the hindlimb experiments. In particular, we found endothelial β1 integrin to be required for the induction of arteriole formation in the thigh and the non-significant increase in arteriole density in the calf.

Genetic deletion of β1 integrin in ECs has been associated with vascular abnormalities in embryonic development as well as impairments of adult vascular remodeling in response to hemodynamic changes (Lei et al., 2008; Yamamoto et al., 2015; Zovein et al., 2010). Therefore, even though we detected arteriole formation in the ischemic myocardium

of *Itgb1*^{iECKO} mice, the impact of endothelial β1 integrin deficiency on the morphology of new arterioles cannot be excluded and should be addressed in further studies. While it is unclear how new arterioles form in the absence of EC proliferation, the underlying mechanism appears to involve aspects of capillary arterialization, in particular, the acquirement of a medial layer. The latter may be mediated by either a recruitment of VSMCs or expression of smooth muscle markers by preexistent cells such as pericytes (Mac Gabhann and Peirce, 2010). Further, EC migration may be another important part of EC proliferation-independent formation of arterioles. Specifically, EC migration is a key event in artery reassembly, a process underlying the collateral formation in the neonatal murine heart (Das et al., 2019). In the retinas of neonatal mice, it has been shown that ECs can migrate from an angiogenic front towards arteries to mediate their growth (Pitulescu et al., 2017).

Stimulation of angiogenesis is regarded as a promising strategy for treating peripheral artery disease (PAD), as it can improve the local blood supply of ischemic territories. This strategy may be of particular importance for those patients with PAD who exhibit reduced capillary densities (Annex, 2013; Duscha et al., 2011; Iyer and Annex, 2017; Jones et al., 2007). Previous studies have already revealed a link between integrins and angiogenesis. For instance, tumor angiogenesis is impaired in mice lacking the subunit α1 (Bloch et al., 1997). Moreover, β1 subunit containing integrins were shown to be involved in growth factor-induced skin angiogenesis as well as in tumor angiogenesis (Pozzi et al., 2000; Senger et al., 1997). Particularly endothelial β1 integrin was found to be essential for aspects of developmental angiogenesis including the adhesion, migration and survival of ECs (Carlson et al., 2008). Finally, we identified its critical role in ischemia-induced EC proliferation, which is a crucial process in angiogenesis. Our analyses of peripheral capillary densities revealed that endothelium-specific deletion of β1 integrin inhibits the angiogenic response to HI. Importantly, we did not observe increased rates of apoptotic ECs in *Itgb1*^{iECKO} mice compared to control mice, indicating that this inhibitory effect is not a result of altered EC viability. Consistent with the literature and our findings, the here presented HI experiments revealed that ischemia-induced peripheral capillary formation strictly requires endothelial β1 integrin expression.

As downstream targets of β1 integrin in the context of biomechanical stimulation, both AKT and eNOS may be important in mediating β1 integrin-dependent vascular remodeling in response to ischemia. For instance, studies employing the model of HI demonstrated a reduced arteriogenic response and impaired blood flow recovery after ischemia in mice lacking AKT in ECs, suggesting an important role for endothelial AKT signaling in arteriogenesis (Lee et al., 2018). Moreover, eNOS has been reported to be involved in vascular growth, as indicated by impaired angiogenic and arteriogenic responses to HI in eNOS knockout mice (Dai and Faber, 2010; Murohara et al., 1998; Park et al., 2010; Yu et al., 2005). Conversely, overexpression of eNOS resulted even in an improved

collateralization and perfusion in the ischemic rat hindlimb (Brevetti et al., 2003). Of note, we observed a reduced eNOS expression in cultured HCAECs upon silencing β1 integrin expression. *Vice versa*, immunohistochemical analyses of cardiac sections revealed an increased expression of endothelial β1 integrin in eNOS knockout mice compared to corresponding control mice, pointing to a possible compensatory mechanism (Henning et al., 2021). Furthermore, a recent study showed that shear stress-induced expression of eNOS was inhibited in HUVECs treated with a β1 integrin-blocking antibody (Xanthis et al., 2019). Combined, our and others' data point out that β1 integrin-mediated vascular growth involves AKT and eNOS as functional interaction partners.

4.2 Role of β1 integrin in cardioprotection

To date, only a few studies have addressed the role of β1 integrin in cardioprotection. For instance, it was demonstrated that a global heterozygous deletion of β1 integrin results in an impaired outcome after a permanent LAD ligation (Krishnamurthy et al., 2006). In addition, a deletion of this integrin specifically in cardiomyocytes was associated with impaired mechanical and signaling responses of the myocardium as well as cardiac fibrosis and failure (Li et al., 2012b; Shai et al., 2002). Moreover, a recent study focused on the role of endothelial β1 integrin in lipopolysaccharide-induced vascular leakage (Hakanpaa et al., 2018). To our knowledge, the function of endothelial β1 integrin in the context of myocardial infarction (MI) has not been investigated yet. Therefore, we aimed to determine its role in ischemia-induced cardioprotection.

First, in line with previously published data, we could demonstrate the cardioprotective effects of RepI/R in that it reduced the infarct size and improved the cardiac function after MI (Lavine et al., 2013). On the one hand, these effects may be mediated by an improved myocardial perfusion due to the observed vascular growth. On the other hand, further aspects such as altered gene expression or secretion profiles might contribute to the cardioprotective effects of the RepI/R. For instance, it was reported that various genes related to inflammation, ECM structure, cell adhesion and vascular development were down- or upregulated in the myocardium upon RepI/R (Lavine et al., 2013).

Consistent with the studies employing a permanent LAD ligation, the three-time application of β1 integrin function blocking antibodies in the RepSham group alone seemed to impair the LV contractile function after the MI, indicating that this subunit is, in general, important for myocardial recovery after an I/R injury (Henning et al., 2021; Krishnamurthy et al., 2006). Strikingly, β1 integrin function-blocking attenuated the cardioprotective effects of RepI/R, suggesting that it is specifically relevant in RepI/R-induced protection from MI.

Further, endothelium-specific β1 integrin deficiency in RepI/R-treated mice was found to increase the infarct size and to impair the cardiac function at the first day after MI when compared to the corresponding control mice. The fact that the effects obtained in the pharmacological approach seemed stronger is likely due to targeting β1 integrin in cardiomyocytes themselves as well as in other cell types involved in tissue repair, e.g. mural cells, inflammatory cells and fibroblasts (Li et al., 2012b; Mezu-Ndubuisi and Maheshwari, 2020; Prabhu and Frangogiannis, 2016; Shai et al., 2002). The here presented data specify that β1 integrin in ECs contributes to ischemia-induced cardioprotection.

Apart from its role in coronary growth, endothelial β1 integrin may contribute to RepI/R-induced cardioprotection through mechanisms involving cytoprotection. For instance, the secretion of cytoprotective angiocrine factors, such as the hepatocyte growth factor (HGF), might influence the acute and the healing phases in the infarcted heart. Particularly in the setting of myocardial I/R injury in mice, exogenous HGF has been demonstrated to protect cardiac cells from apoptosis via the AKT pathway and to promote angiogenesis (Wang et al., 2004). In addition, HGF has been shown to inhibit fibrosis in the context of ischemic cardiomyopathy as well as MI, and to modulate the immune response in experimental myocarditis (Azuma et al., 2006; Chen et al., 2007; Futamatsu et al., 2005; Wang et al., 2004). A recently published study demonstrated, among others, that normal HGF production during mouse liver development requires endothelial β1 integrin and that mechanical stretching leads to increased HGF concentration in the supernatant of cultured human hepatic ECs (Lorenz et al., 2018). In line with this, we observed that HGF release by human cardiac microvascular ECs was increased by trend upon β1 integrin activation. Thus, biomechanical activation of endothelial β1 integrin in consequence of brief I/R episodes might repetitively induce HGF production and/or secretion by cardiac ECs and modulate the molecular environment in the myocardium, thereby reducing cardiac cell death after prolonged ischemia. In addition, HGF might act in an autocrine manner on ECs themselves or influence other blood vascular cells to promote coronary growth.

Another potent aspect in RepI/R-induced cardioprotection could be the long-term enhancement of nitric oxide (NO) bioavailability through a β1 integrin-dependent, FSS-induced modulation of eNOS expression in the ECs of RepI/R-treated hearts (Davis et al., 2001; Xanthis et al., 2019). On the one hand, NO-mediated signaling has been associated with mobilization of endothelial progenitor cells important for vascular repair and neovascularization (Aicher et al., 2003). On the other hand, endothelium-derived NO can diffuse to adjacent cardiomyocytes (Davidson and Yellon, 2018; Kelm, 1999). In the latter, NO was reported to be involved in the reduction of oxidative stress and promotion of mitochondrial biogenesis, both of which are important in the context of MI (Bartz et al., 2015; Li et al., 2017a). Interestingly, previous studies in animals and humans suggest that regular exercise training leads to an increased expression and activation of eNOS and improves the

endothelial function (Beck et al., 2013; Green et al., 2004; Hambrecht et al., 2003; Kojda et al., 2001; Sessa et al., 1994). Based on our and others' findings, it is possible that endothelial β1 integrin contributes to the beneficial effects of the exercise training on the cardiovascular system by mediating the upregulation of eNOS in the blood vascular ECs.

While the discussed aspects provide possible scenarios of how endothelial β1 integrin could mediate the cardioprotective effects of transient ischemic events and cardioprotection in general, the precise mechanistic details remain to be specified.

4.3 Translational implications and complications of targeting β1 integrin in prevention and treatment of acute ischemic events

As a promising approach in prevention and treatment of CVDs, stimulation of vascular growth and enhancement of collateralization have been addressed in several human studies, which involved application of growth factors but, however, did not show significant protective effects in the long term (Lederman et al., 2002; van Royen et al., 2009; Ziegler et al., 2010; Zimarino et al., 2014). Yet an effective stimulation of vascular growth could be beneficial especially with regard to individuals with insufficient collateralization. Aside from genetic predisposition, diabetes has been associated with impaired collateralization (Abaci et al., 1999; Shen et al., 2018). Interestingly, the vascular extracellular matrix (ECM) of patients with diabetes displays compositional alterations compared to non-diabetic individuals (Goldin et al., 2006). These alterations lead to an increased arterial stiffness, possibly implicating a disturbed integrin-mediated interaction between ECs and the ECM, which may, at least in part, explain the impaired collateralization in individuals with diabetes. Similarly, arterial stiffness along with disturbed EC-ECM interactions have been observed in humans with advanced age (De Luca, 2019; Robert, 1998; Sun, 2015). Of note, studies on mice of different age demonstrated that ageing is associated with collateral rarefaction as well as impaired angiogenesis and collateral remodeling in the hindlimb and the cerebrum, which was accompanied by a dysfunctional eNOS signaling (Faber et al., 2011). Furthermore, both ageing and diabetes have been linked to deteriorated glycocalyx, which likely impairs the mechanosensory function of the endothelium at the luminal surface of blood vessels (Machin et al., 2019). Collectively, previous reports and our findings highlight the relevance of targeting endothelial β1 integrin signaling to promote vascular growth, especially in patients with advanced age and/or diabetes.

To date, a number of integrin agonists have been discovered or designed and applied in experimental *in vivo* and *in vitro* studies (Lorenz et al., 2018; Schwartz et al., 2008;

Tolomelli et al., 2017; Wayner et al., 1993). Because β1 integrin, as one of the most widely expressed integrin subunits, is crucial for normal physiological functions, it would be important to restrict its stimulation to the endothelium in preclinical and clinical trials, thereby reducing severe systemic side effects (Schwartz et al., 2008). Since growing evidence exists that β1 integrins at the apical surface of ECs act as mechanotransducers, application of intraluminal agents may be sufficient to initiate vascular growth. Importantly, endothelial β1 subunit containing integrins have been linked to tumor angiogenesis (Boudreau and Varner, 2004; Lugano et al., 2018; Pozzi et al., 2000). Therefore, a repetitive local application of an agonist with a short half-life, combined with a careful screening of tumor biomarkers, would minimize the tumor-promoting potential of β1 integrin activation. Noteworthy, integrins also respond to disturbed flow patterns and are implicated in atherosclerosis (Budatha et al., 2018; Demos et al., 2020; Sun et al., 2016; Yurdagul et al., 2014; Zhang et al., 2020). Thus, in face of the ambivalent nature of integrin signaling, it is important to further specify the molecular mechanisms underlying β1 integrin-mediated vascular growth, thereby providing more specific targets for clinical implication in the future.

4.4 Conclusions

The most important finding presented in this thesis is the essential role of endothelial β1 integrin in ischemia-induced peripheral and coronary vascular growth (Fig. 4.1). In particular, using the mouse model of HI, we could show that the expression of this integrin is required for peripheral capillary and arteriole formation as an adaptive vascular response to ischemia. Employing the mouse model of RepI/R, which presumably reflects the transient ischemic events in the human heart affected by CAD, we found endothelial β1 integrin to be needed for full vascular response to myocardial ischemia, including EC proliferation in the ischemic and non-ischemic myocardium as well as arteriole formation in the latter. Moreover, data obtained from the pharmacological approach reveal the critical role of β1 integrin in ischemia-induced cardioprotection, while genetic experiments indicate a contributing role for endothelial β1 integrin in this respect. Our *in vitro* data underline that stretching and hence changes in CWS rather than in FSS are responsible for hypoxia-independent EC proliferation in the setting of transient arterial occlusions. As another major finding, we found β1 integrin expression to be required for stretch-induced proliferation of human cardiac ECs, which hints to a corresponding role for this integrin in the human situation. Finally, our results point to AKT, eNOS and HGF as possible candidates contributing to β1 integrin-mediated vascular growth and cardioprotection. In summary, our studies identify β1 integrin signaling as a potential therapeutic target to stimulate blood vessel growth as part of prevention and treatment of acute ischemic events in humans with CVD.

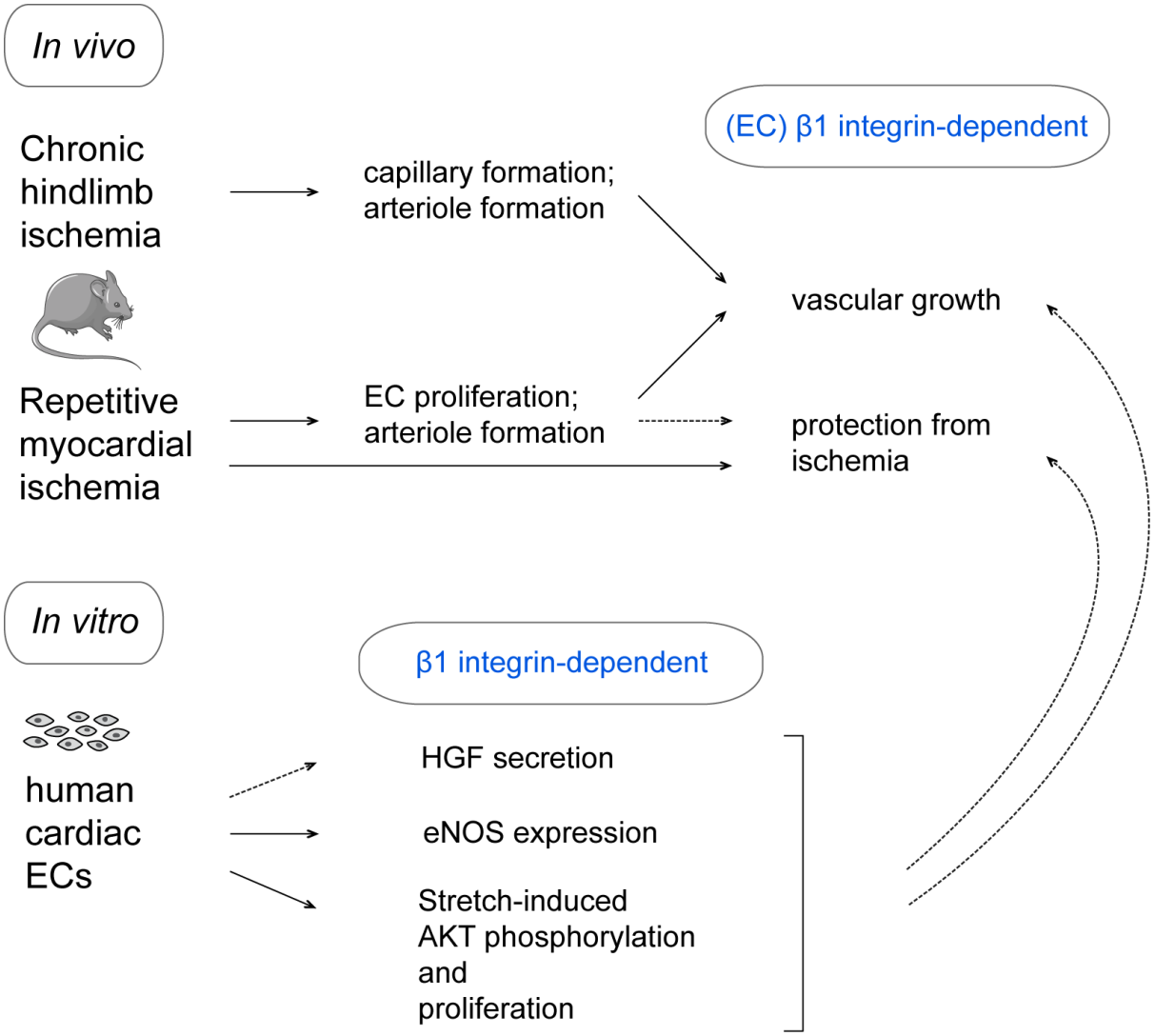

Figure 4.1: Schematic overview of the main findings.
In vivo experiments: HI- and RepI/R-induced blood vascular growth requires endothelial β1 integrin; RepI/R induces protection from ischemia in a β1 integrin-dependent manner. *In vitro* experiments on primary human cardiac ECs: β1 integrin is possibly involved in HGF secretion and is required for full basal eNOS expression as well as stretch-induced AKT phosphorylation and proliferation. Thus, HGF, eNOS and AKT are possible candidates contributing to β1 integrin-mediated vascular growth and cardioprotection. EC and mouse illustrations were modified from Lorenz et al., 2018 and Servier Medical ART (section: "Animals"), respectively.

Publications

This dissertation contains parts described in our publications Henning et al., 2019 and Henning et al., 2021:

Henning C*, Branopolski A*, Schuler D*, Dimitroulis D, Hülsemann P, Nicolaus C, Sansone R, Ludolf Postma J, Eberhard D, Le Noble F, Kelm M, Lammert E*, Heiss C*:
Requirement of β1 integrin for endothelium-dependent vasodilation and collateral formation in hindlimb ischemia.
Nature Scientific Reports, 2019
* equal contribution

Henning C*, Branopolski A*, Follert P, Lewandowska O, Ayhan A, Benkhoff M, Flögel U, Kelm M, Heiss C*, Lammert E*:
Endothelial β1 Integrin-Mediated Adaptation to Myocardial Ischemia.
Thrombosis and Haemostasis, 2021
* equal contribution

Other publications:

Urner S, Planas-Paz L, Hilger LS, Henning C, Branopolski A, Kelly-Goss M, Stanczuk L, Pitter B, Montanez E, Peirce SM, Makinen T, Lammert, E**:**
Identification of ILK as a critical regulator of VEGFR3 signalling and lymphatic vascular growth.
EMBO Journal, 2019

Toth C, Funke S, Nitsche V, Liverts A, Zlachevska V, Gasis M, Wiek C, Hanenberg H, Mahotka C, Schirmacher P, Heikaus, S.
The role of apoptosis repressor with a CARD domain (ARC) in the therapeutic resistance of renal cell carcinoma (RCC): the crucial role of ARC in the inhibition of extrinsic and intrinsic apoptotic signalling.
Cell Communication and Signaling, 2017

List of abbreviations

AKT	Protein kinase B
BAECs	Bovine aortic endothelial cells
BCA	Bicinchoninic acid
bp	Base pair
BrdU	5-Bromo-2'-deoxyuridine
BSA	Bovine serum albumin
CAD	Coronary artery disease
Cdh5	Cadherin 5 gene
ctrl-AB	Control antibody
CVD	Cardiovascular disease
CWS	Circumferential wall stress
DAPI	4',6-diamidino-2-phenylindole
ECs	Endothelial cells
ECG	Electrocardiography
ECM	Extracellular matrix
EDTA	Ethylenediaminetetraacetic acid
EF	Ejection fraction
ELISA	Enzyme-linked immunosorbent assay
eNOS	Endothelial nitric oxide synthase
FA	Femoral artery
FGF	Fibroblast growth factor
FISP	Fast gradient echo cine sequence with steady state precession
FMD	Flow-mediated dilation
FSS	Fluid shear stress
GAPDH	Glyceraldehyde 3-phosphate dehydrogenase
h	Hours
HCAECs	Human coronary artery endothelial cells
HDL	High-density lipoprotein
HGF	Hepatocyte growth factor
HI	Hindlimb ischemia
HIF-1α	Hypoxia-inducible factor-1α
HCMVECs	Human cardiac microvascular endothelial cells
HPRT1	Hypoxanthine phosphoribosyltransferase 1 gene
HRP	Horseradish peroxidase

HUVECs	Human umbilical vein endothelial cells
ILK	Integrin-linked protein kinase
I/R	Ischemia/reperfusion
Itgb1 or *ITGB1*	Mouse or human β1 integrin gene
Itgb1^{iECKO}	*Cdh5*-Cre^{ERT2}; homozygous *Itgb1*-knochout mice
KLF2	Kruppel-like factor 2
LAD	Left anterior descending artery
LCA	Left coronary artery
LCX	Left circumflex artery
LDL	Low-density lipoprotein
LGE	Late gadolinium enhancement
LV	Left ventricle
MACS	Magnetic-activated cell sorting
MCP-1	Monocyte chemotactic protein-1
MI	Myocardial infarction
min	Minute(s)
MRI	Magnetic resonance imaging
NO	Nitric oxide
O.C.T	Optimum cutting temperature
PAD	Peripheral artery disease
PBS	Phosphate buffered saline
PBS$^{Ca2+, Mg2+}$	Phosphate buffered saline with Ca^{2+} and Mg^{2+}
PCR	Polymerase chain reaction
PDGF	Platelet derived growth factor
PE	Polyethylene
PECAM-1	Platelet endothelial cell adhesion molecule
PFA	Paraformaldehyde
PI3K	Phosphoinositide 3-kinase
PVDF	Polyvinylidene fluoride
P(S1177) or P(S473)	Phosphorylated at serine 1177 or 473
qPCR	Quantitative polymerase chain reaction
RCA	Right coronary artery
RepI/R	Repetitive ischemia/reperfusion
RepSham	Repetitive sham
RIPA	Radioimmunoprecipitation assay
ROI	Region-of-interest
ROS	Reactive oxygen species
RPLP0	Ribosomal protein lateral stalk subunit P0

rpm	Revolutions per minute
RT	Room temperature
RV	Right ventricle
s	Seconds
SDS-PAGE	Sodium dodecyl sulfate-polyacrylamide gel electrophoresis
SEM	Standard error of the mean
siRNA	Small interfering RNA
TTC	Triphenyl tetrazolium chloride
VEGF	Vascular endothelial growth factor
VEGFR3	Vascular endothelial growth factor receptor 3
VSMCs	Vascular smooth muscle cells
α-SMA	α-smooth muscle actin
β1-B-AB	β1 integrin blocking antibody
β1-siRNA1/2/3	Small interfering RNA targeting β1 integrin gene
β2M	β2-microglobulin gene

References

Abaci, A., et al., 1999. Effect of diabetes mellitus on formation of coronary collateral vessels. Circulation. 99, 2239-2242.

Aicher, A., et al., 2003. Essential role of endothelial nitric oxide synthase for mobilization of stem and progenitor cells. Nat Med. 9, 1370-6.

Akimoto, S., et al., 2000. Laminar shear stress inhibits vascular endothelial cell proliferation by inducing cyclin-dependent kinase inhibitor p21(Sdi1/Cip1/Waf1). Circ Res. 86, 185-90.

Almaca, J., et al., 2018. The Pericyte of the Pancreatic Islet Regulates Capillary Diameter and Local Blood Flow. Cell Metab. 27, 630-644 e4.

Anderson, L.R., Owens, T.W., Naylor, M.J., 2014. Structural and mechanical functions of integrins. Biophysical Reviews. 6, 203-213.

Annex, B.H., 2013. Therapeutic angiogenesis for critical limb ischaemia. Nat Rev Cardiol. 10, 387-96.

Atkins, G.B., Jain, M.K., 2007. Role of Kruppel-like transcription factors in endothelial biology. Circ Res. 100, 1686-95.

Axnick, J., 2016. β1 integrin-dependent mechanotransduction induces angiocrine signaling required to promote liver growth and survival. Institute of Metabolic Physiology (Heinrich-Heine-University Duesseldorf).

Azuma, J., et al., 2006. Angiogenic and antifibrotic actions of hepatocyte growth factor improve cardiac dysfunction in porcine ischemic cardiomyopathy. Gene Ther. 13, 1206-13.

Baeyens, N., et al., 2016. Endothelial fluid shear stress sensing in vasculr health and disease. J Clin Invest. 126, 821-828.

Baeyens, N., Schwartz, M.A., 2016. Biomechanics of vascular mechanosensation and remodeling. Molecular Biology of the Cell. 27, 7-11.

Balaguru, U.M., et al., 2016. Disturbed flow mediated modulation of shear forces on endothelial plane: A proposed model for studying endothelium around atherosclerotic plaques. Sci Rep. 6.

Balligand, J.L., Feron, O., Dessy, C., 2009. eNOS Activation by Physical Forces: From Short-Term Regulation of Contraction to Chronic Remodeling of Cardiovascular Tissues. Physiol Rev. 89, 481-534.

Baroldi, G., Mantero, O., Scomazzoni, G., 1956. The Collaterals of the Coronary Arteries in Normal and Pathologic Hearts. Circ Res. 4, 223-229.

Bartosch, A.M.W., Mathews, R., Tarbell, J.M., 2017. Endothelial Glycocalyx-Mediated Nitric Oxide Production in Response to Selective AFM Pulling. Biophys J. 113, 101-108.

Bartz, R.R., Suliman, H.B., Piantadosi, C.A., 2015. Redox mechanisms of cardiomyocyte mitochondrial protection. Front Physiol. 6, 291.

Bauters, C., et al., 1994. Physiological Assessment of Augmented Vascularity Induced by Vegf in Ischemic Rabbit Hindlimb. Am J Physiol-Heart Circul Physiol. 267, H1263-H1271.

Bazigou, E., Makinen, T., 2013. Flow control in our vessels: vascular valves make sure there is no way back. Cellular and Molecular Life Sciences. 70, 1055-1066.

Beck, D.T., et al., 2013. Exercise training improves endothelial function in young prehypertensives. Exp Biol Med (Maywood). 238, 433-41.

Benedito, R., et al., 2009. The notch ligands Dll4 and Jagged1 have opposing effects on angiogenesis. Cell. 137, 1124-35.

Bentzon, J.F., et al., 2014. Mechanisms of plaque formation and rupture. Circ Res. 114, 1852-66.

Bloch, W., et al., 1997. beta 1 integrin is essential for teratoma growth and angiogenesis. Journal of Cell Biology. 139, 265-278.

Bondareva, O., Sheikh, B.N., 2020. Vascular Homeostasis and Inflammation in Health and Disease-Lessons from Single Cell Technologies. Int J Mol Sci. 21, 4688.

Bonner, F., et al., 2014. Multifunctional MR monitoring of the healing process after myocardial infarction. Basic Res Cardiol. 109, 430.
Bosch-Marce, M., et al., 2007. Effects of aging and hypoxia-inducible factor-1 activity on angiogenic cell mobilization and recovery of perfusion after limb ischemia. Circ Res. 101, 1310-1318.
Boudreau, N.J., Varner, J.A., 2004. The homeobox transcription factor Hox D3 promotes integrin alpha5beta1 expression and function during angiogenesis. J Biol Chem. 279, 4862-8.
Brakenhielm, E., Richard, V., 2019. Therapeutic vascular growth in the heart. Vasc Biol. 1, H9-H15.
Brevetti, L.S., et al., 2003. Overexpression of endothelial nitric oxide synthase increases skeletal muscle blood flow and oxygenation in severe rat hind limb ischemia. J Vasc Surg. 38, 820-6.
Britannica, 2021. Circulatory System. https://www.britannica.com/science/blood-vessel. Encyclopaedia Britannica.
Brocherie, F., Millet, G.P., 2020. Hypoxic exercise as an effective nonpharmacological therapeutic intervention. Exp Mol Med. 52, 529-530.
Budatha, M., et al., 2018. Inhibiting Integrin alpha5 Cytoplasmic Domain Signaling Reduces Atherosclerosis and Promotes Arteriogenesis. J Am Heart Assoc. 7.
Cai, W., Schaper, W., 2008. Mechanisms of arteriogenesis. Acta Biochim Biophys Sin (Shanghai). 40, 681-92.
Cai, W.J., et al., 2009. Activation of the integrins alpha 5 beta 1 and alpha v beta 3 and focal adhesion kinase (FAK) during arteriogenesis. Mol Cell Biochem. 322, 161-169.
Carlson, T.R., et al., 2008. Cell-autonomous requirement for beta 1 integrin in endothelial cell adhesion, migration and survival during angiogenesis in mice. Development. 135, 2193-2202.
Celermajer, D.S., et al., 1992. Noninvasive Detection of Endothelial Dysfunction in Children and Adults at Risk of Atherosclerosis. Lancet. 340, 1111-1115.
Chen, A.H., et al., 2001. Cyclic strain activates the pro-survival Akt protein kinase in bovine aortic smooth muscle cells. Surgery. 130, 378-81.
Chen, X.H., et al., 2007. In vivo hepatocyte growth factor gene transfer reduces myocardial ischemia-reperfusion injury through its multiple actions. J Card Fail. 13, 874-83.
Cheng, C., et al., 2006. Atherosclerotic lesion size and vulnerability are determined by patterns of fluid shear stress. Circulation. 113, 2744-2753.
Chittenden, T.W., et al., 2006. Transcriptional profiling in coronary artery disease - Indications for novel markers of coronary collateralization. Circulation. 114, 1811-1820.
Chiu, J.J., Chien, S., 2011. Effects of Disturbed Flow on Vascular Endothelium: Pathophysiological Basis and Clinical Perspectives. Physiol Rev. 91, 327-387.
Cinthio, M., et al., 2006. Longitudinal movements and resulting shear strain of the arterial wall. Am J Physiol Heart Circ Physiol. 291, H394-402.
Couffinhal, T., et al., 1998. Mouse model of angiogenesis. Am J Pathol. 152, 1667-1679.
Dai, X., Faber, J.E., 2010. Endothelial nitric oxide synthase deficiency causes collateral vessel rarefaction and impairs activation of a cell cycle gene network during arteriogenesis. Circ Res. 106, 1870-81.
Das, S., et al., 2019. A Unique Collateral Artery Development Program Promotes Neonatal Heart Regeneration. Cell. 176, 1128-1142.
Davidson, S.M., Yellon, D.M., 2018. Cardioprotection - is no the answer? A renewed look at nitric oxide signalling in cardiomyocytes. Cardiovasc Res. 114, 773-775.
Davis, M.E., et al., 2001. Shear stress regulates endothelial nitric oxide synthase expression through c-Src by divergent signaling pathways. Circ Res. 89, 1073-80.
De Luca, M., 2019. The role of the cell-matrix interface in aging and its interaction with the renin-angiotensin system in the aged vasculature. Mech Ageing Dev. 177, 66-73.
Dekker, R.J., et al., 2005. Endothelial KLF2 links local arterial shear stress levels to the expression of vascular tone-regulating genes. Am J Pathol. 167, 609-18.

Demicheva, E., Hecker, M., Korff, T., 2008. Stretch-Induced Activation of the Transcription Factor Activator Protein-1 Controls Monocyte Chemoattractant Protein-1 Expression During Arteriogenesis. Circ Res. 103, 477-484.
Demos, C., Williams, D., Jo, H., 2020. Disturbed Flow Induces Atherosclerosis by Annexin A2-Mediated Integrin Activation. Circ Res. 127, 1091-1093.
Dewald, O., et al., 2004. A murine model of ischemic cardiomyopathy induced by repetitive ischemia and reperfusion. Thorac Cardiovasc Surg. 52, 305-11.
Di Angelantonio, E., et al., 2019. World Health Organization cardiovascular disease risk charts: revised models to estimate risk in 21 global regions. Lancet Global Health. 7, E1332-E1345.
Dimmeler, S., et al., 1998. Fluid shear stress stimulates phosphorylation of Akt in human endothelial cells: involvement in suppression of apoptosis. Circ Res. 83, 334-41.
Dimmeler, S., et al., 1999. Activation of nitric oxide synthase in endothelial cells by Akt-dependent phosphorylation. Nature. 399, 601-5.
Duscha, B.D., et al., 2011. Angiogenesis in skeletal muscle precede improvements in peak oxygen uptake in peripheral artery disease patients. Arterioscler Thromb Vasc Biol. 31, 2742-8.
Elias, J., et al., 2017. Impact of Collateral Circulation on Survival in ST-Segment Elevation Myocardial Infarction Patients Undergoing Primary Percutaneous Coronary Intervention With a Concomitant Chronic Total Occlusion. JACC-Cardiovasc Interv. 10, 906-914.
Eliceiri, B.P., 2001. Integrin and growth factor receptor crosstalk. Circ Res. 89, 1104-10.
Elsman, P., et al., 2004. Role of collateral circulation in the acute phase of ST-segment-elevation myocardial infarction treated with primary coronary intervention. Eur Heart J. 25, 854-858.
Evans, R., et al., 2009. Integrins in immunity. J Cell Sci. 122, 215-25.
Faber, J.E., et al., 2011. Aging causes collateral rarefaction and increased severity of ischemic injury in multiple tissues. Arterioscler Thromb Vasc Biol. 31, 1748-56.
Faber, J.E., et al., 2014. A Brief Etymology of the Collateral Circulation. Arterioscler Thromb Vasc Biol. 34, 1854-1859.
Farah, C., et al., 2017. Key role of endothelium in the eNOS-dependent cardioprotection with exercise training. J Mol Cell Cardiol. 102, 26-30.
Fassler, R., Meyer, M., 1995. Consequences of Lack of Beta-1 Integrin Gene-Expression in Mice. Genes & Development. 9, 1896-1908.
Feletou, M., Vanhoutte, P.M., 1996. Endothelium-derived hyperpolarizing factor. Clinical and Experimental Pharmacology and Physiology. 23, 1082-1090.
Friebel, M., et al., 1995. Flow-Dependent Regulation of Arteriolar Diameter in Rat Skeletal-Muscle in-Situ - Role of Endothelium-Derived Relaxing Factor and Prostanoids. Journal of Physiology-London. 483, 715-726.
Fujita, M., et al., 1987. Importance of Angina for Development of Collateral Circulation. British Heart Journal. 57, 139-143.
Fulton, W.F., 1963. Arterial Anastomoses in the Coronary Circulation. Ii. Distribution, Enumeration and Measurement of Coronary Arterial Anastomoses in Health and Disease. Scott Med J. 8, 466-74.
Futamatsu, H., et al., 2005. Hepatocyte growth factor ameliorates the progression of experimental autoimmune myocarditis: a potential role for induction of T helper 2 cytokines. Circ Res. 96, 823-30.
Gaenzer, H., et al., 2001. Flow-mediated vasodilation of the femoral and brachial artery induced by exercise in healthy nonsmoking and smoking men. J Am Coll Cardiol. 38, 1313-9.
Gerdes, J., et al., 1984. Cell cycle analysis of a cell proliferation-associated human nuclear antigen defined by the monoclonal antibody Ki-67. J Immunol. 133, 1710-5.
Gimbrone, M.A., Jr., Garcia-Cardena, G., 2016. Endothelial Cell Dysfunction and the Pathobiology of Atherosclerosis. Circ Res. 118, 620-36.
Gloekler, S., Seiler, C., 2007. Cardiology patient page. Natural bypasses can save lives. Circulation. 116, e340-1.

Goldin, A., et al., 2006. Advanced glycation end products: sparking the development of diabetic vascular injury. Circulation. 114, 597-605.
Goto, C., et al., 2007. Acute moderate-intensity exercise induces vasodilation through oxide bioavailiability an increase in nitric in humans. American Journal of Hypertension. 20, 825-830.
Gratzner, H.G., et al., 1975. The use of antibody specific for bromodeoxyuridine for the immunofluorescent determination of DNA replication in single cells and chromosomes. Exp Cell Res. 95, 88-94.
Gratzner, H.G., 1982. Monoclonal antibody to 5-bromo- and 5-iododeoxyuridine: A new reagent for detection of DNA replication. Science. 218, 474-5.
Green, D.J., et al., 2004. Effect of exercise training on endothelium-derived nitric oxide function in humans. J Physiol. 561, 1-25.
Green, D.J., et al., 2014. Is Flow-Mediated Dilation Nitric Oxide Mediated? A Meta-Analysis. Hypertension. 63, 376-382.
Haberkorn, S.M., et al., 2017. Cardiovascular Magnetic Resonance Relaxometry Predicts Regional Functional Outcome After Experimental Myocardial Infarction. Circ Cardiovasc Imaging. 10.
Habib, G.B., et al., 1991. Influence of Coronary Collateral Vessels on Myocardial Infarct Size in Humans - Results of Phase-I Thrombolysis in Myocardial-Infarction (Timi) Trial. Circulation. 83, 739-746.
Haga, M., et al., 2003. Oscillatory shear stress increases smooth muscle cell proliferation and Akt phosphorylation. J Vasc Surg. 37, 1277-84.
Hahn, C., Schwartz, M.A., 2009. Mechanotransduction in vascular physiology and atherogenesis. Nat Rev Mol Cell Bio. 10, 53-62.
Hakanpaa, L., et al., 2018. Targeting beta1-integrin inhibits vascular leakage in endotoxemia. Proc Natl Acad Sci U S A. 115, E6467-E6476.
Hall, C.N., et al., 2014. Capillary pericytes regulate cerebral blood flow in health and disease. Nature. 508, 55-60.
Hambrecht, R., et al., 2003. Regular physical activity improves endothelial function in patients with coronary artery disease by increasing phosphorylation of endothelial nitric oxide synthase. Circulation. 107, 3152-8.
Hamilton, N.B., Attwell, D., Hall, C.N., 2010. Pericyte-mediated regulation of capillary diameter: a component of neurovascular coupling in health and disease. Front Neuroenergetics. 2.
Harding, I.C., et al., 2018. Pro-atherosclerotic disturbed flow disrupts caveolin-1 expression, localization, and function via glycocalyx degradation. Journal of Translational Medicine. 16.
Hatada, K., et al., 2001. Clinical significance of coronary flow to the infarct zone before successful primary percutaneous transluminal coronary angioplasty in acute myocardial infarction. Chest. 120, 1959-1963.
He, L.J., et al., 2017. Preexisting endothelial cells mediate cardiac neovascularization after injury. J Clin Invest. 127, 2968-2981.
Heil, M., Schaper, W., 2004. Influence of mechanical, cellular, and molecular factors on collateral artery growth (arteriogenesis). Circ Res. 95, 449-458.
Heil, M., et al., 2006. Arteriogenesis versus angiogenesis: similarities and differences. J Cell Mol Med. 10, 45-55.
Heiss, C., et al., 2005. Acute consumption of flavanol-rich cocoa and the reversal of endothelial dysfunction in smokers. J Am Coll Cardiol. 46, 1276-83.
Heiss, C., Rodriguez-Mateos, A., Kelm, M., 2015. Central Role of eNOS in the Maintenance of Endothelial Homeostasis. Antioxidants & Redox Signaling. 22, 1230-1242.
Henning, C., et al., 2019. Requirement of beta 1 integrin for endothelium-dependent vasodilation and collateral formation in hindlimb ischemia. Sci Rep. 9, 16931.
Henning, C., et al., 2021. Endothelial beta1 Integrin-Mediated Adaptation to Myocardial Ischemia. Thromb Haemost. 121, 741-754
Henry, T.D., et al., 2003. Vascular endothelial growth factor in ischemia for vascular angiogenesis. Circulation. 107, 1359-1365.

Heo, K.S., Fujiwara, K., Abe, J., 2011. Disturbed-Flow-Mediated Vascular Reactive Oxygen Species Induce Endothelial Dysfunction. Circulation Journal. 75, 2722-2730.
Herrick, J.B., 1983. Landmark article (JAMA 1912). Clinical features of sudden obstruction of the coronary arteries. By James B. Herrick. JAMA. 250, 1757-65.
Hoefer, I.E., van Royen, N., Jost, M.M., 2006. Experimental models of arteriogenesis: differences and implications. Lab Animal. 35, 36-44.
Hoefer, I.E., den Adel, B., Daemen, M.J.A.P., 2013. Biomechanical factors as triggers of vascular growth. Cardiovasc Res. 99, 276-283.
Holzinger, C., et al., 1993. Effects of Interleukin-1, Interleukin-2, Interleukin-4, Interleukin-6, Interferon-Gamma and Granulocyte-Macrophage Colony-Stimulating Factor on Human Vascular Endothelial-Cells. Immunology Letters. 35, 109-118.
Hong, F.F., et al., 2019. Roles of eNOS in atherosclerosis treatment. Inflamm Res. 68, 429-441.
Hu, Z., et al., 2013. Acute mechanical stretch promotes eNOS activation in venous endothelial cells mainly via PKA and Akt pathways. PLoS One. 8, e71359.
Huonker, M., et al., 2003. Size and blood flow of central and peripheral arteries in highly trained able-bodied and disabled athletes. J Appl Physiol (1985). 95, 685-91.
Hynes, R.O., 2002. Integrins: Bidirectional, allosteric signaling machines. Cell. 110, 673-687.
Ibanez, B., et al., 2019. Cardiac MRI Endpoints in Myocardial Infarction Experimental and Clinical Trials: JACC Scientific Expert Panel. J Am Coll Cardiol. 74, 238-256.
Ingber, D., 1991. Integrins as mechanochemical transducers. Current Opinion in Cell Biology. 3, 841-848.
Insull, W., 2009. The Pathology of Atherosclerosis: Plaque Development and Plaque Responses to Medical Treatment. American Journal of Medicine. 122, S3-S14.
Ito, W.D., et al., 1997. Angiogenesis but not collateral growth is associated with ischemia after femoral artery occlusion. Am J Physiol-Heart Circul Physiol. 273, H1255-H1265.
Iyer, S.R., Annex, B.H., 2017. Therapeutic Angiogenesis for Peripheral Artery Disease: Lessons Learned in Translational Science. JACC Basic Transl Sci. 2, 503-512.
Jackson, Z.S., Gotlieb, A.I., Langille, B.L., 2002. Wall tissue remodeling regulates longitudinal tension in arteries. Circ Res. 90, 918-925.
Jalali, S., et al., 2001. Integrin-mediated mechanotransduction requires its dynamic interaction with specific extracellular matrix (ECM) ligands. Proc Natl Acad Sci U S A. 98, 1042-6.
Ji, Q., et al., 2019. High shear stress suppresses proliferation and migration but promotes apoptosis of endothelial cells co-cultured with vascular smooth muscle cells via down-regulating MAPK pathway. J Cardiothorac Surg. 14, 216.
Jin, H., et al., 2006. Integrin alpha4beta1 promotes monocyte trafficking and angiogenesis in tumors. Cancer Res. 66, 2146-52.
Jones, W.S., et al., 2007. Gender impacts capillary density and skeletal muscle composition in patients with peripheral arterial disease. Circulation. 116, 748-748.
Joyce, E.E., Gregg, D.E., 1967. Coronary artery occlusion in the intact unanesthetized dog: intercoronary reflexes. Am J Physiol. 213, 64-70.
Kamiya, A., Togawa, T., 1980. Adaptive Regulation of Wall Shear-Stress to Flow Change in the Canine Carotid-Artery. Am J Physiol. 239, H14-H21.
Katsumi, A., et al., 2004. Integrins in mechanotransduction. J Biol Chem. 279, 12001-4.
Katz, S.D., et al., 1996. Exercise-induced vasodilation in forearm circulation of normal subjects and patients with congestive heart failure: role of endothelium-derived nitric oxide. J Am Coll Cardiol. 28, 585-90.
Kechagia, J.Z., Ivaska, J., Roca-Cusachs, P., 2019. Integrins as biomechanical sensors of the microenvironment. Nat Rev Mol Cell Bio. 20, 457-473.
Keely, S., et al., 2009. Selective induction of integrin beta1 by hypoxia-inducible factor: implications for wound healing. FASEB J. 23, 1338-46.
Kelm, M., 1999. Nitric oxide metabolism and breakdown. Biochim Biophys Acta. 1411, 273-89.
Kim, S.C., et al., 2012. A Murine Closed-chest Model of Myocardial Ischemia and Reperfusion. Jove-Journal of Visualized Experiments. e3896.

Koch, A.E., et al., 1992. Interleukin-8 as a Macrophage-Derived Mediator of Angiogenesis. Science. 258, 1798-1801.
Kojda, G., et al., 2001. Dysfunctional regulation of endothelial nitric oxide synthase (eNOS) expression in response to exercise in mice lacking one eNOS gene. Circulation. 103, 2839-44.
Kojda, G., Hambrecht, R., 2005. Molecular mechanisms of vascular adaptations to exercise. Physical activity as an effective antioxidant therapy? Cardiovasc Res. 67, 187-97.
Kooijman, M., et al., 2008. Flow-mediated dilatation in the superficial femoral artery is nitric oxide mediated in humans. Journal of Physiology-London. 586, 1137-1145.
Krishnamurthy, P., et al., 2006. Deficiency of beta1 integrins results in increased myocardial dysfunction after myocardial infarction. Heart. 92, 1309-15.
Kwak, B.R., et al., 2014. Biomechanical factors in atherosclerosis: mechanisms and clinical implications. Eur Heart J. 35, 3013-20.
Lammert, E., Axnick, J., 2012. Vascular lumen formation. Cold Spring Harb Perspect Med. 2, a006619.
Lammert, E., Zeeb, M., 2014. Metabolism of Human Diseases, Vol. 1, Springer.
Lavine, K.J., et al., 2013. Repetitive Myocardial Ischemia Promotes Coronary Growth in the Adult Mammalian Heart. J Am Heart Assoc. 2, e000343.
Lederman, R.J., et al., 2002. Therapeutic angiogenesis with recombinant fibroblast growth factor-2 for intermittent claudication (the TRAFFIC study): a randomised trial. Lancet. 359, 2053-8.
Lee, M.Y., et al., 2014. Endothelial Akt1 mediates angiogenesis by phosphorylating multiple angiogenic substrates. Proc Natl Acad Sci U S A. 111, 12865-70.
Lee, M.Y., et al., 2018. Endothelial Cell Autonomous Role of Akt1: Regulation of Vascular Tone and Ischemia-Induced Arteriogenesis. Arterioscler Thromb Vasc Biol. 38, 870-879.
Lee, S.H., Lee, Y.J., Han, H.J., 2011. Role of hypoxia-induced fibronectin-integrin beta1 expression in embryonic stem cell proliferation and migration: Involvement of PI3K/Akt and FAK. J Cell Physiol. 226, 484-93.
Legate, K.R., Fassler, R., 2009. Mechanisms that regulate adaptor binding to beta-integrin cytoplasmic tails. Journal of Cell Science. 122, 187-198.
Lei, L., et al., 2008. Endothelial Expression of Beta-1 Integrin Is Required for Embryonic Vascular Patterning and Postnatal Vascular Remodeling. Faseb Journal. 22.
Lelovas, P.P., Kostomitsopoulos, N.G., Xanthos, T.T., 2014. A comparative anatomic and physiologic overview of the porcine heart. J Am Assoc Lab Anim Sci. 53, 432-8.
Li, F., et al., 2017a. Orientin Reduces Myocardial Infarction Size via eNOS/NO Signaling and Thus Mitigates Adverse Cardiac Remodeling. Front Pharmacol. 8, 926.
Li, J., Springer, T.A., 2017. Integrin extension enables ultrasensitive regulation by cytoskeletal force. Proc Natl Acad Sci U S A. 114, 4685-4690.
Li, J., et al., 2017b. Conformational equilibria and intrinsic affinities define integrin activation. Embo Journal. 36, 629-645.
Li, L., et al., 2012a. An angiogenic role for the alpha5beta1 integrin in promoting endothelial cell proliferation during cerebral hypoxia. Exp Neurol. 237, 46-54.
Li, R., et al., 2012b. beta1 integrin gene excision in the adult murine cardiac myocyte causes defective mechanical and signaling responses. Am J Pathol. 180, 952-962.
Li, W., Sumpio, B.E., 2005. Strain-induced vascular endothelial cell proliferation requires PI3K-dependent mTOR-4E-BP1 signal pathway. Am J Physiol Heart Circ Physiol. 288, H1591-7.
Liebeskind, D.S., 2003. Collateral circulation. Stroke. 34, 2279-2284.
Liebeskind, D.S., et al., 2011. Collaterals Dramatically Alter Stroke Risk in Intracranial Atherosclerosis. Annals of Neurology. 69, 963-974.
Limbourg, A., et al., 2009. Evaluation of postnatal arteriogenesis and angiogenesis in a mouse model of hind-limb ischemia. Nature Protocols. 4, 1737-1748.
Lindsey, M.L., et al., 2018. Guidelines for experimental models of myocardial ischemia and infarction. Am J Physiol-Heart Circul Physiol. 314, H812-H838.
Linton, M.R.F., et al., 2000. The Role of Lipids and Lipoproteins in Atherosclerosis. In: Endotext. Vol., K.R. Feingold, B. Anawalt, A. Boyce, G. Chrousos, W.W. de Herder,

K. Dungan, A. Grossman, J.M. Hershman, J. Hofland, G. Kaltsas, C. Koch, P. Kopp, M. Korbonits, R. McLachlan, J.E. Morley, M. New, J. Purnell, F. Singer, C.A. Stratakis, D.L. Trence, D.P. Wilson. South Dartmouth (MA).
Livak, K.J., Schmittgen, T.D., 2001. Analysis of relative gene expression data using real-time quantitative PCR and the 2(-Delta Delta C(T)) Method. Methods. 25, 402-8.
Loganadane, L.D., et al., 1997. Endothelial cell proliferation regulated by cytokines modulates thrombospondin-1 secretion into the subendothelium. Cytokine. 9, 740-6.
Lorenz, L., et al., 2018. Mechanosensing by beta 1 integrin induces angiocrine signals for liver growth and survival. Nature. 562, 128-132.
Loufrani, L., et al., 2008. Key role of alpha(1)beta(1)-integrin in the activation of PI3-kinase-Akt by flow (shear stress) in resistance arteries. Am J Physiol Heart Circ Physiol. 294, H1906-13.
Lower, R., 1669. Tractatus de corde : item de motu & colore sanguinis, et chyli in eum transitu, Vol., Apud Danielem Elzevirium, Amstelodami.
Lu, D.S., Kassab, G.S., 2011. Role of shear stress and stretch in vascular mechanobiology. Journal of the Royal Society Interface. 8, 1379-1385.
Lugano, R., et al., 2018. CD93 promotes beta1 integrin activation and fibronectin fibrillogenesis during tumor angiogenesis. J Clin Invest. 128, 3280-3297.
Ma, T., Bai, Y.P., 2020. The hydromechanics in arteriogenesis. Aging Med (Milton). 3, 169-177.
Mac Gabhann, F., Peirce, S.M., 2010. Collateral Capillary Arterialization following Arteriolar Ligation in Murine Skeletal Muscle. Microcirculation. 17, 333-347.
Machin, D.R., Phuong, T.T., Donato, A.J., 2019. The role of the endothelial glycocalyx in advanced age and cardiovascular disease. Curr Opin Pharmacol. 45, 66-71.
Manning, B.D., Toker, A., 2017. AKT/PKB Signaling: Navigating the Network. Cell. 169, 381-405.
Matsumori, A., et al., 1996. Increased circulating hepatocyte growth factor in the early stage of acute myocardial infarction. Biochem Biophys Res Commun. 221, 391-5.
McMillan, D., Harris, R., 2018. An Atlas of Comparative Vertebrate Histology, Vol. 1, Elsevier.
Mees, B., et al., 2007. Endothelial nitric oxide synthase activity is essential for vasodilation during blood flow recovery but not for arteriogenesis. Arterioscler Thromb Vasc Biol. 27, 1926-1933.
Meier, P., et al., 2013. The collateral circulation of the heart. BMC Med. 11, 143.
Meisner, J.K., et al., 2013. Trans-illuminated laser speckle imaging of collateral artery blood flow in ischemic mouse hindlimb. Journal of Biomedical Optics. 18, 096011.
Mensah, G.A., et al., 2017. Decline in Cardiovascular Mortality Possible Causes and Implications. Circ Res. 120, 366-380.
Mezu-Ndubuisi, O.J., Maheshwari, A., 2020. The role of integrins in inflammation and angiogenesis. Pediatric Research.
Michael, L.H., et al., 1995. Myocardial ischemia and reperfusion: A murine model. Am J Physiol-Heart Circul Physiol. 269, H2147-H2154.
Milnor, W.R., 1990. Cardiovascular Physiology, Vol., Oxford University Press.
Miquerol, L., et al., 2015. Endothelial Plasticity Drives Arterial Remodeling Within the Endocardium After Myocardial Infarction. Circ Res. 116, 1765-71.
Mitsos, S., et al., 2009. A critical appraisal of open- and closed-chest models of experimental myocardial ischemia. Lab Animal. 38, 167-177.
Mladenovic, Z.T., et al., 2008. The cardioprotective role of preinfarction angina as shown in outcomes of patients after first myocardial infarction. Tex Heart Inst J. 35, 413-8.
Mobius-Winkler, S., et al., 2016. Coronary Collateral Growth Induced by Physical Exercise: Results of the Impact of Intensive Exercise Training on Coronary Collateral Circulation in Patients With Stable Coronary Artery Disease (EXCITE) Trial. Circulation. 133, 1438-48.
Mochizuki, S., et al., 2003. Role of hyaluronic acid glycosaminoglycans in shear-induced endothelium-derived nitric oxide release. Am J Physiol Heart Circ Physiol. 285, H722-6.

Moraes, F.P., et al., 2014. Endothelial cell-dependent regulation of arteriogenesis: the cell type-specific effects of synectin signaling. Angiogenesis. 17, 315-316.
Muller, J.M., Chilian, W.M., Davis, M.J., 1997. Integrin signaling transduces shear stress--dependent vasodilation of coronary arterioles. Circ Res. 80, 320-6.
Mundi, S., et al., 2018. Endothelial permeability, LDL deposition, and cardiovascular risk factors-a review. Cardiovasc Res. 114, 35-52.
Murohara, T., et al., 1998. Nitric oxide synthase modulates angiogenesis in response to tissue ischemia. J Clin Invest. 101, 2567-78.
Nakajima, H., Mochizuki, N., 2017. Flow pattern-dependent endothelial cell responses through transcriptional regulation. Cell Cycle. 16, 1893-1901.
Nakamura, T., et al., 2000. Myocardial protection from ischemia/reperfusion injury by endogenous and exogenous HGF. J Clin Invest. 106, 1511-9.
Nam, D., et al., 2009. Partial carotid ligation is a model of acutely induced disturbed flow, leading to rapid endothelial dysfunction and atherosclerosis. Am J Physiol-Heart Circul Physiol. 297, H1535-H1543.
Nees, S., et al., 2012. Isolation, bulk cultivation, and characterization of coronary microvascular pericytes: the second most frequent myocardial cell type in vitro. Am J Physiol Heart Circ Physiol. 302, H69-84.
Nho, R.S., et al., 2005. Role of integrin-linked kinase in regulating phosphorylation of Akt and fibroblast survival in type I collagen matrices through a beta1 integrin viability signaling pathway. J Biol Chem. 280, 26630-9.
Nishikawa, Y., et al., 2004. In vivo role of heme oxygenase in ischemic coronary vasodilation. Am J Physiol Heart Circ Physiol. 286, H2296-304.
Nishimura, K., et al., 2006. Role of AKT in cyclic strain-induced endothelial cell proliferation and survival. Am J Physiol Cell Physiol. 290, C812-21.
Nossuli, T.O., et al., 2000. A chronic mouse model of myocardial ischemia-reperfusion: essential in cytokine studies. Am J Physiol-Heart Circul Physiol. 278, H1049-H1055.
Okada, M., et al., 1998. Cyclic stretch upregulates production of interleukin-8 and monocyte chemotactic and activating factor/monocyte chemoattractant protein-1 in human endothelial cells. Arterioscler Thromb Vasc Biol. 18, 894-901.
Ono, K., et al., 1997. Enhanced expression of hepatocyte growth factor/c-Met by myocardial ischemia and reperfusion in a rat model. Circulation. 95, 2552-8.
Pahakis, M.Y., et al., 2007. The role of endothelial glycocalyx components in mechanotransduction of fluid shear stress. Biochem Biophys Res Commun. 355, 228-33.
Pan, S., 2009. Molecular Mechanisms Responsible for the Atheroprotective Effects of Laminar Shear Stress. Antioxid Redox Signal. 11, 1669-1682.
Park, B., et al., 2010. Endothelial nitric oxide synthase affects both early and late collateral arterial adaptation and blood flow recovery after induction of hind limb ischemia in mice. Journal of Vascular Surgery. 51, 165-173.
Paszek, M.J., et al., 2009. Integrin clustering is driven by mechanical resistance from the glycocalyx and the substrate. PLoS Comput Biol. 5, e1000604.
Peet, C., et al., 2020. Cardiac monocytes and macrophages after myocardial infarction. Cardiovasc Res. 116, 1101-1112.
Persson, A.B., Buschmann, I.R., 2011. Vascular growth in health and disease. Front Mol Neurosci. 4, 14.
Pitulescu, M.E., et al., 2017. Dll4 and Notch signalling couples sprouting angiogenesis and artery formation. Nat Cell Biol. 19, 915-927.
Planas-Paz, L., et al., 2012. Mechanoinduction of lymph vessel expansion. Embo Journal. 31, 788-804.
Pohl, T., et al., 2001. Frequency distribution of collateral flow and factors influencing collateral channel development - Functional collateral channel measurement in 450 patients with coronary artery disease. J Am Coll Cardiol. 38, 1872-1878.
Pohl, U., et al., 1986. Crucial Role of Endothelium in the Vasodilator Response to Increased Flow Invivo. Hypertension. 8, 37-44.

Potocnik, A.J., Brakebusch, C., Fassler, R., 2000. Fetal and adult hematopoietic stem cells require beta1 integrin function for colonizing fetal liver, spleen, and bone marrow. Immunity. 12, 653-63.
Pozzi, A., et al., 2000. Elevated matrix metalloprotease and angiostatin levels in integrin alpha 1 knockout mice cause reduced tumor vascularization. Proc Natl Acad Sci U S A. 97, 2202-7.
Prabhu, S.D., Frangogiannis, N.G., 2016. The Biological Basis for Cardiac Repair After Myocardial Infarction: From Inflammation to Fibrosis. Circ Res. 119, 91-112.
Presta, M., et al., 1992. Basic fibroblast growth factor bound to cell substrate promotes cell adhesion, proliferation, and protease production in cultured endothelial cells. EXS. 61, 205-9.
Prior, B.M., Yang, H.T., Terjung, R.L., 2004. What makes vessels grow with exercise training? Journal of Applied Physiology. 97, 1119-1128.
Pu, L.Q., et al., 1993. Enhanced Revascularization of the Ischemic Limb by Angiogenic Therapy. Circulation. 88, 208-215.
Pugh, C.W., Ratcliffe, P.J., 2003. Regulation of angiogenesis by hypoxia: role of the HIF system. Nat Med. 9, 677-84.
Qian, J., Fulton, D., 2013. Post-translational regulation of endothelial nitric oxide synthase in vascular endothelium. Front Physiol. 4, 347.
Rafii, S., Butler, J.M., Ding, B.S., 2016. Angiocrine functions of organ-specific endothelial cells. Nature. 529, 316-25.
Reitsma, S., et al., 2007. The endothelial glycocalyx: composition, functions, and visualization. Pflugers Arch. 454, 345-59.
Robert, L., 1998. Mechanisms of aging of the extracellular matrix: role of the elastin-laminin receptor. Gerontology. 44, 307-17.
Rosenthal, S.L., Guyton, A.C., 1968. Hemodynamics of collateral vasodilatation following femoral artery occlusion in anesthetized dogs. Circ Res. 23, 239-48.
Ross, T.D., et al., 2013. Integrins in mechanotransduction. Current Opinion in Cell Biology. 25, 613-618.
Rubanyi, G.M., Romero, J.C., Vanhoutte, P.M., 1986. Flow-Induced Release of Endothelium-Derived Relaxing Factor. Am J Physiol. 250, 1145-1149.
Sabia, P.J., et al., 1992. An Association between Collateral Blood-Flow and Myocardial Viability in Patients with Recent Myocardial-Infarction. New England Journal of Medicine. 327, 1825-1831.
Samady, H., et al., 2011. Coronary artery wall shear stress is associated with progression and transformation of atherosclerotic plaque and arterial remodeling in patients with coronary artery disease. Circulation. 124, 779-88.
Santini, L., et al., 2020. Modelling genetic diseases for drug development: Hypertrophic cardiomyopathy. Pharmacol Res. 160, 105176.
Schaper, W., et al., 1976. Quantification of Collateral Resistance in Acute and Chronic Experimental Coronary-Occlusion in Dog. Circ Res. 39, 371-377.
Schaper, W., Scholz, D., 2003. Factors regulating arteriogenesis. Arterioscler Thromb Vasc Biol. 23, 1143-51.
Schaper, W., 2009. Collateral circulation Past and present. Basic Research in Cardiology. 104, 5-21.
Schmidt, R.F., Lang, F., Heckmann, M., 2011. Physiologie des Menschen: mit Pathophysiologie, Vol. 31, Springer.
Schretzenmayr, A., 1933. Über kreislaufregulatorische Vorgänge an den großen Arterien bei der Muskelarbeit. Pflüger's Archiv für die gesamte Physiologie des Menschen und der Tiere. 232, 743-748.
Schuler, D., et al., 2014. Measurement of Endothelium-Dependent Vasodilation in Mice-Brief Report. Arterioscl Throm Vasc Biol. 34, 2651-7.
Schwartz, M.A., Assoian, R.K., 2001. Integrins and cell proliferation: regulation of cyclin-dependent kinases via cytoplasmic signaling pathways. J Cell Sci. 114, 2553-60.
Schwartz, M.A., et al., 2008. Integrin Agonists as Adjuvants in Chemotherapy for Melanoma. Clinical Cancer Research. 14, 6193-6197.
Secomb, T.W., 2016. Hemodynamics. Comprehensive Physiology. 6, 975-1003.

Seiler, C., 2003. The human coronary collateral circulation. Heart. 89, 1352-1357.
Seiler, C., et al., 2013. The human coronary collateral circulation: development and clinical importance. Eur Heart J. 34, 2674-82.
Seiler, C., Meier, P., 2014. Historical aspects and relevance of the human coronary collateral circulation. Curr Cardiol Rev. 10, 2-16.
Senger, D.R., et al., 1997. Angiogenesis promoted by vascular endothelial growth factor: regulation through alpha1beta1 and alpha2beta1 integrins. Proc Natl Acad Sci U S A. 94, 13612-7.
Servier, 2021. „Cardiovascular System“ and „Animals“. https://smart.servier.com/. Servier Medical ART.
Sessa, W.C., et al., 1994. Chronic exercise in dogs increases coronary vascular nitric oxide production and endothelial cell nitric oxide synthase gene expression. Circ Res. 74, 349-53.
Shai, S.Y., et al., 2002. Cardiac myocyte-specific excision of the beta1 integrin gene results in myocardial fibrosis and cardiac failure. Circ Res. 90, 458-64.
Shattil, S.J., Kim, C., Ginsberg, M.H., 2010. The final steps of integrin activation: the end game. Nat Rev Mol Cell Bio. 11, 288-300.
Shen, Y., et al., 2018. Reduced coronary collateralization in type 2 diabetic patients with chronic total occlusion. Cardiovascular Diabetology. 17, 26.
Shiojima, I., Walsh, K., 2002. Role of Akt signaling in vascular homeostasis and angiogenesis. Circ Res. 90, 1243-50.
Silva, R., et al., 2008. Integrins - The keys to unlocking angiogenesis. Arterioscler Thromb Vasc Biol. 28, 1703-1713.
Simons, M., Eichmann, A., 2015. Molecular Controls of Arterial Morphogenesis. Circ Res. 116, 1712-1724.
Solomon, S.D., et al., 2004. Angina pectoris prior to myocardial infarction protects against subsequent left ventricular remodeling. J Am Coll Cardiol. 43, 1511-4.
Stebbings, G.K., et al., 2013. Resting arterial diameter and blood flow changes with resistance training and detraining in healthy young individuals. J Athl Train. 48, 209-19.
Steinman, D.A., 2002. Image-based computational fluid dynamics modeling in realistic arterial geometries. Annals of Biomedical Engineering. 30, 483-497.
Stephens, L.E., et al., 1995. Deletion of Beta-1 Integrins in Mice Results in Inner Cell Mass Failure and Periimplantation Lethality. Genes & Development. 9, 1883-1895.
Su, H., et al., 2021. Emerging Role of Pericytes and Their Secretome in the Heart. Cells. 10, 548.
Sun, M., et al., 2003. Temporal response and localization of integrins beta1 and beta3 in the heart after myocardial infarction: regulation by cytokines. Circulation. 107, 1046-52.
Sun, X., et al., 2016. Activation of integrin alpha5 mediated by flow requires its translocation to membrane lipid rafts in vascular endothelial cells. Proc Natl Acad Sci U S A. 113, 769-74.
Sun, Z., 2015. Aging, arterial stiffness, and hypertension. Hypertension. 65, 252-6.
Sun, Z.Q., Costell, M., Fassler, R., 2019. Integrin activation by talin, kindlin and mechanical forces. Nature Cell Biology. 21, 25-31.
Tanjore, H., et al., 2008. beta 1 integrin expression on endothelial cells is required for angiogenesis but not for vasculogenesis. Developmental Dynamics. 237, 75-82.
Thondapu, V., et al., 2017. Biomechanical stress in coronary atherosclerosis: emerging insights from computational modelling. Eur Heart J. 38, 81-92c.
Timmis, A., et al., 2020. European Society of Cardiology: Cardiovascular Disease Statistics 2019 (Executive Summary). Eur Heart J-Quality of Care and Clinical Outcomes. 6, 7-9.
Tinken, T.M., et al., 2010. Shear stress mediates endothelial adaptations to exercise training in humans. Hypertension. 55, 312-8.
Tolomelli, A., et al., 2017. Can Integrin Agonists Have Cards to Play against Cancer? A Literature Survey of Small Molecules Integrin Activators. Cancers. 9, 78.
Traub, O., Berk, B.C., 1998. Laminar shear stress - Mechanisms by which endothelial cells transduce an atheroprotective force. Arterioscler Thromb Vasc Biol. 18, 677-685.

Tulis, D.A., Unthank, J.L., Prewitt, R.L., 1998. Flow-induced arterial remodeling in rat mesenteric vasculature. Am J Physiol-Heart Circul Physiol. 274, H874-H882.
Tyrrell, D.J., Goldstein, D.R., 2020. Ageing and atherosclerosis: vascular intrinsic and extrinsic factors and potential role of IL-6. Nat Rev Cardiol. 58-68.
Tzima, E., et al., 2001. Activation of integrins in endothelial cells by fluid shear stress mediates Rho-dependent cytoskeletal alignment. Embo Journal. 20, 4639-4647.
Unthank, J.L., et al., 1996. Wall remodeling during luminal expansion of mesenteric arterial collaterals in the rat. Circ Res. 79, 1015-1023.
Urbich, C., et al., 2000. Laminar shear stress upregulates integrin expression: role in endothelial cell adhesion and apoptosis. Circ Res. 87, 683-9.
Urner, S., et al., 2018. Mechanotransduction in Blood and Lymphatic Vascular Development and Disease. Adv Pharmacol. 81, 155-208.
Urner, S., et al., 2019. Identification of ILK as a critical regulator of VEGFR3 signalling and lymphatic vascular growth. Embo Journal. 38, e99322.
van Royen, N., et al., 2009. A critical review of clinical arteriogenesis research. J Am Coll Cardiol. 55, 17-25.
van Thiel, B.S., et al., 2017. Structure and Cell Biology of the Vessel Wall, Vol. 1.
Velling, T., et al., 2004. beta1-Integrins induce phosphorylation of Akt on serine 473 independently of focal adhesion kinase and Src family kinases. EMBO Rep. 5, 901-5.
Vermes, E., et al., 2012. Patterns of myocardial late enhancement: typical and atypical features. Arch Cardiovasc Dis. 105, 300-8.
Wang, J.C., Bennett, M., 2012. Aging and Atherosclerosis Mechanisms, Functional Consequences, and Potential Therapeutics for Cellular Senescence. Circ Res. 111, 245-259.
Wang, Y., et al., 2004. Hepatocyte growth factor prevents ventricular remodeling and dysfunction in mice via Akt pathway and angiogenesis. J Mol Cell Cardiol. 37, 1041-52.
Wang, Y., et al., 2010. Ephrin-B2 controls VEGF-induced angiogenesis and lymphangiogenesis. Nature. 465, 483-6.
Wayner, E.A., et al., 1993. Epiligrin, a component of epithelial basement membranes, is an adhesive ligand for alpha 3 beta 1 positive T lymphocytes. J Cell Biol. 121, 1141-52.
White, C.R., et al., 2001. Temporal gradients in shear, but not spatial gradients, stimulate endothelial cell proliferation. Circulation. 103, 2508-13.
Willerson, J.T., et al., 2007. Cardiovascular Medicine, Vol. 3, Springer.
Won, D., et al., 2007. Relative reduction of endothelial nitric-oxide synthase expression and transcription in atherosclerosis-prone regions of the mouse aorta and in an in Vitro model of disturbed flow. Am J Pathol. 171, 1691-1704.
Wustmann, K., et al., 2003. Is there functional collateral flow during vascular occlusion in angiographically normal coronary arteries? Circulation. 107, 2213-2220.
Xanthis, I., et al., 2019. beta1 integrin is a sensor of blood flow direction. J Cell Sci. 132, jcs229542.
Yamakawa, M., et al., 2003. Hypoxia-inducible factor-1 mediates activation of cultured vascular endothelial cells by inducing multiple angiogenic factors. Circ Res. 93, 664-73.
Yamamoto, H., et al., 2015. Integrin beta 1 controls VE-cadherin localization and blood vessel stability. Nat Commun. 6, 6429.
Yang, B., Rizzo, V., 2013. Shear Stress Activates eNOS at the Endothelial Apical Surface Through beta1 Containing Integrins and Caveolae. Cell Mol Bioeng. 6, 346-354.
Yen, W., et al., 2015. Endothelial surface glycocalyx can regulate flow-induced nitric oxide production in microvessels in vivo. PLoS One. 10, e0117133.
Yoon, S.J., et al., 2009. Impact of coronary artery collaterals on infarct size assessed by serial cardiac magnetic resonance imaging after primary percutaneous coronary intervention in patients with acute myocardial infarction. Coronary Artery Disease. 20, 440-445.
Yu, J., et al., 2005. Endothelial nitric oxide synthase is critical for ischemic remodeling, mural cell recruitment, and blood flow reserve. Proc Natl Acad Sci U S A. 102, 10999-11004.

Yurdagul, A., Jr., et al., 2014. alpha5beta1 integrin signaling mediates oxidized low-density lipoprotein-induced inflammation and early atherosclerosis. Arterioscler Thromb Vasc Biol. 34, 1362-73.
Zaromitidou, M., et al., 2016. Chapter 2 - Atherosclerosis and Coronary Artery Disease: From Basics to Genetics, Vol. 1, Academic Press, Boston.
Zbinden, R., et al., 2004. Direct demonstration of coronary collateral growth by physical endurance exercise in a healthy marathon runner. Heart. 90, 1350-1351.
Zbinden, R., et al., 2007. Coronary collateral flow in response to endurance exercise training. Eur J Cardiovasc Prev Rehabil. 14, 250-7.
Zhang, C., et al., 2020. Coupling of Integrin alpha5 to Annexin A2 by Flow Drives Endothelial Activation. Circ Res. 127, 1074-1090.
Zhang, H., Faber, J.E., 2015. De-novo collateral formation following acute myocardial infarction: Dependence on CCR2(+) bone marrow cells. J Mol Cell Cardiol. 87, 4-16.
Zhang, X., Groopman, J.E., Wang, J.F., 2005. Extracellular matrix regulates endothelial functions through interaction of VEGFR-3 and integrin alpha5beta1. J Cell Physiol. 202, 205-14.
Zhao, H.N., Chappell, J.C., 2019. Microvascular bioengineering: a focus on pericytes. Journal of Biological Engineering. 13.
Ziegler, M.A., et al., 2010. Marvels, Mysteries, and Misconceptions of Vascular Compensation to Peripheral Artery Occlusion. Microcirculation. 17, 3-20.
Zimarino, M., et al., 2014. The dynamics of the coronary collateral circulation. Nat Rev Cardiol. 11, 191-197.
Zovein, A.C., et al., 2010. beta 1 Integrin Establishes Endothelial Cell Polarity and Arteriolar Lumen Formation via a Par3-Dependent Mechanism. Dev Cell. 18, 39-51.

Supplementary information

Uncropped Western blot membrane images used for the figures in this thesis:

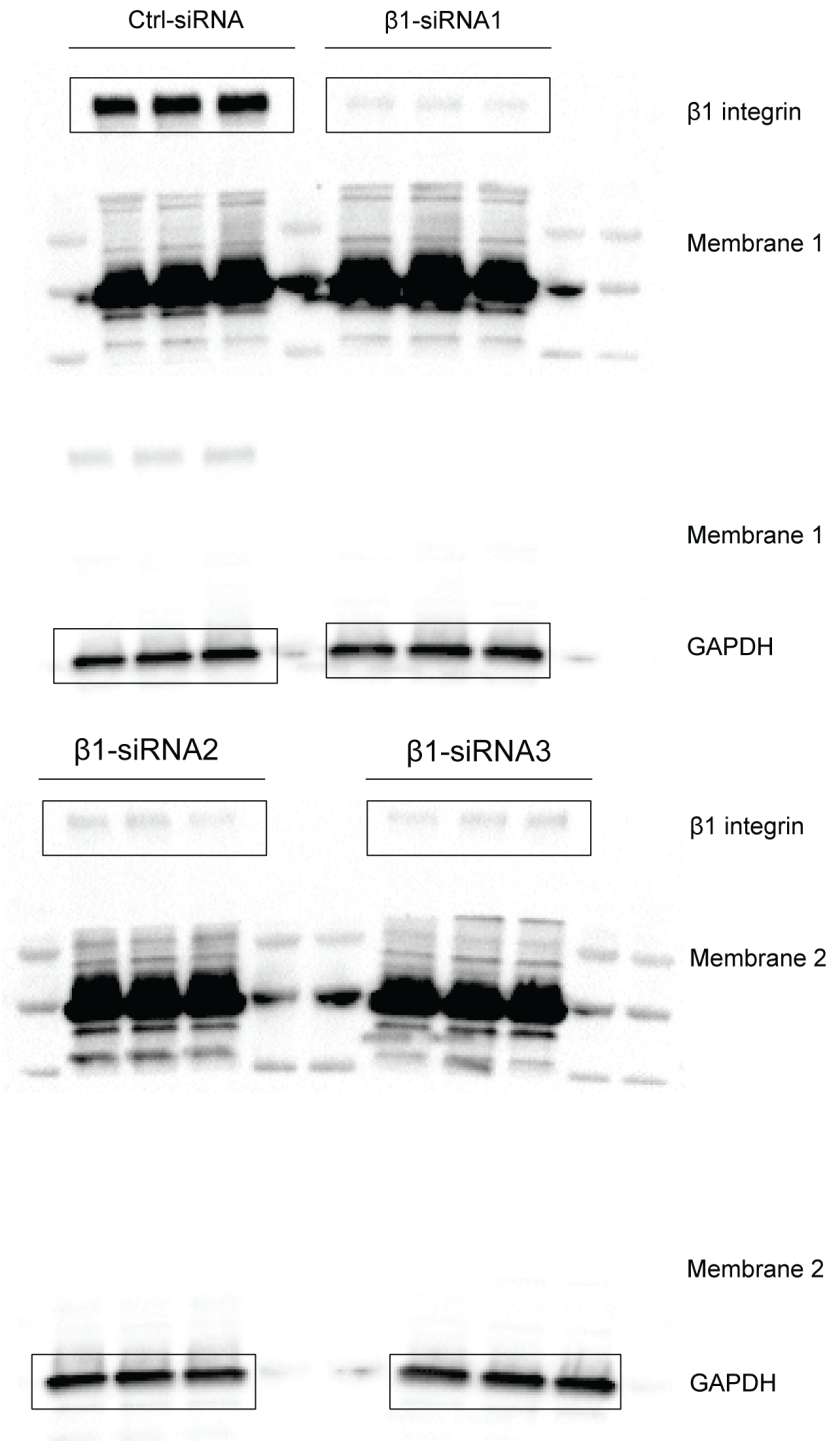

Supplementary Figure 1: Uncropped Western blot images used for Fig. 3.23.
Cropped regions are indicated by black frames.

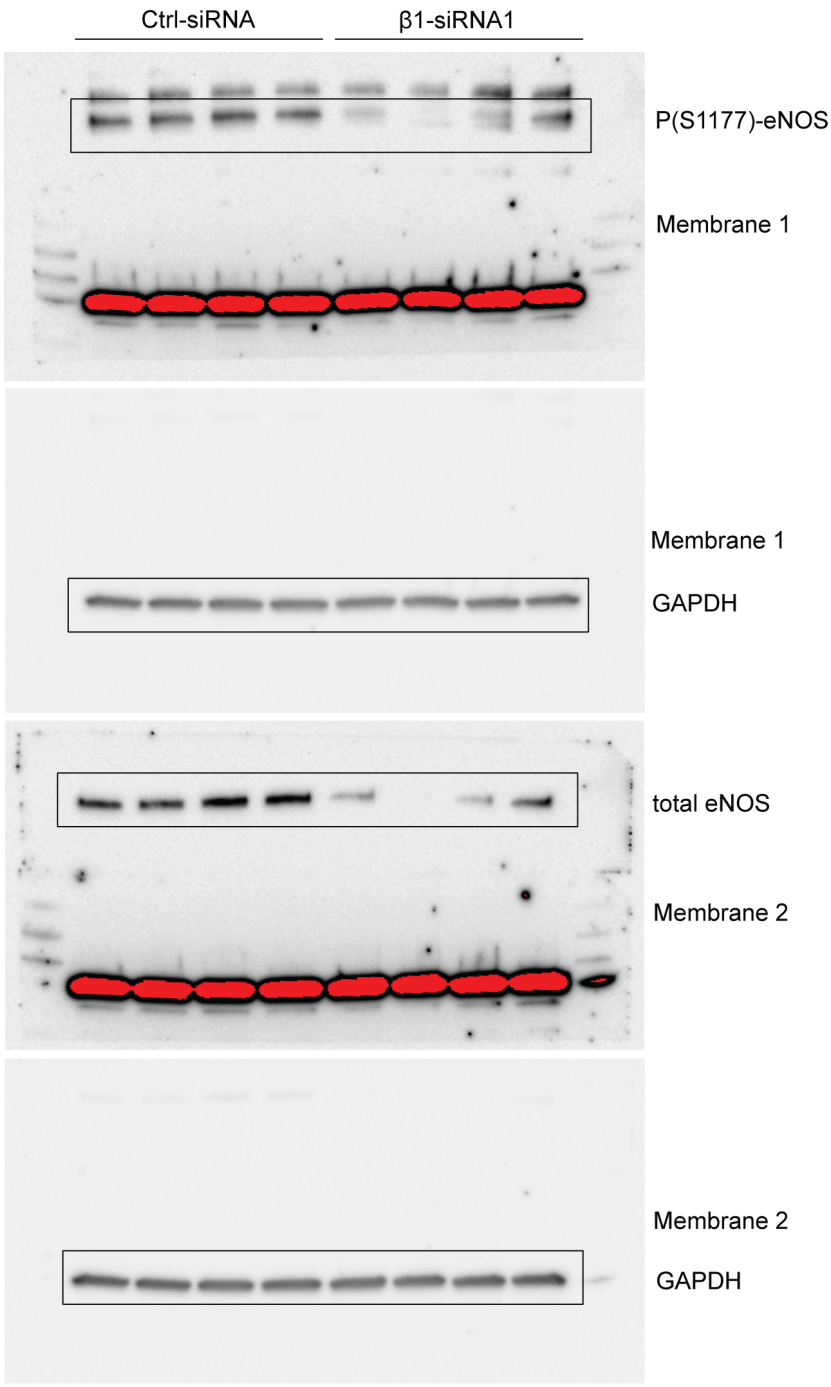

Supplementary Figure 2: Uncropped Western blot images used for Fig 3.25.
Cropped regions are indicated by black frames. Oversaturated pixels due to the long exposure were automatically labeled red.

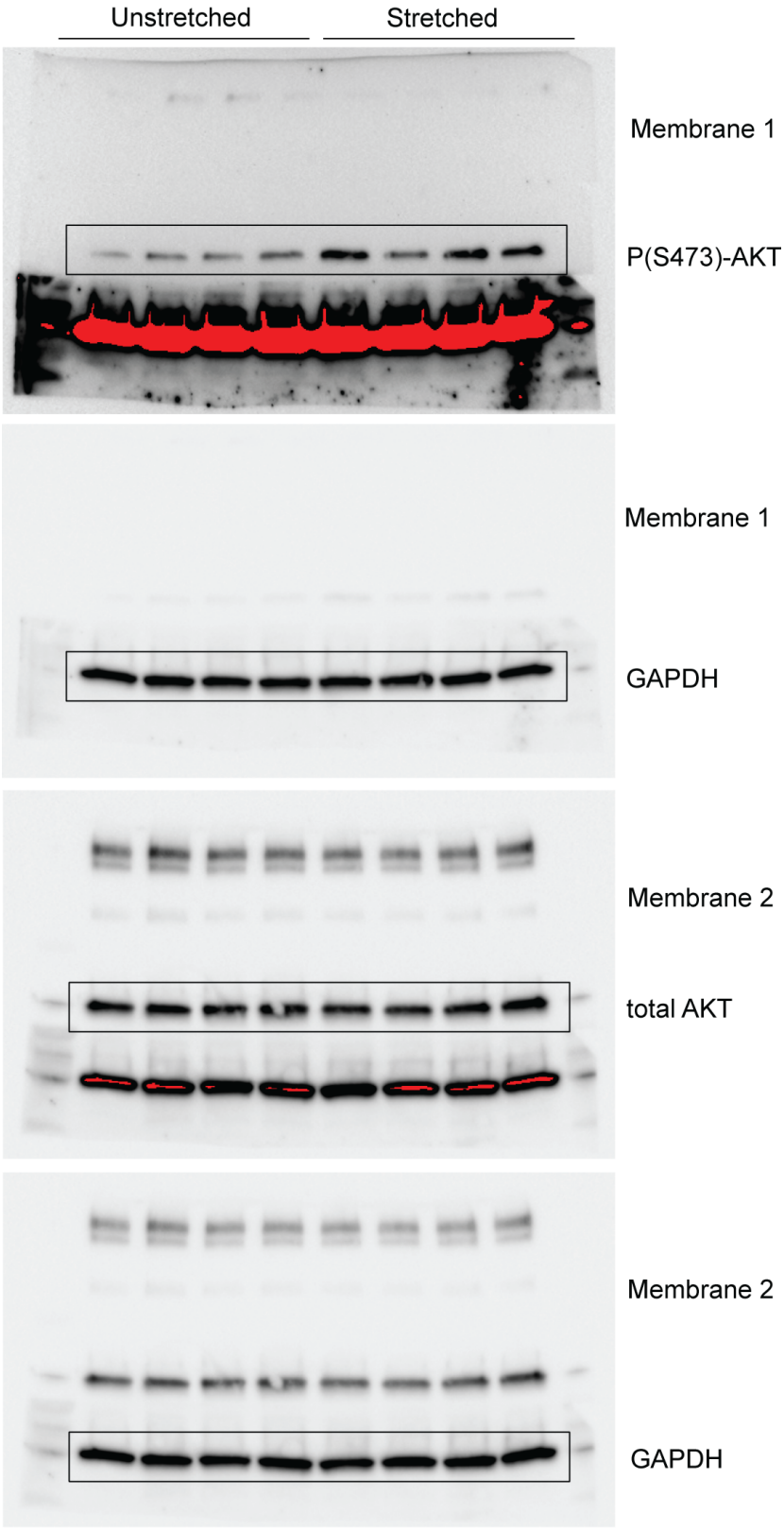

Supplementary Figure 3: Uncropped Western blot images used for Fig. 3.29.
Cropped regions are indicated by black frames. Oversaturated pixels due to the long exposure were automatically labeled red.

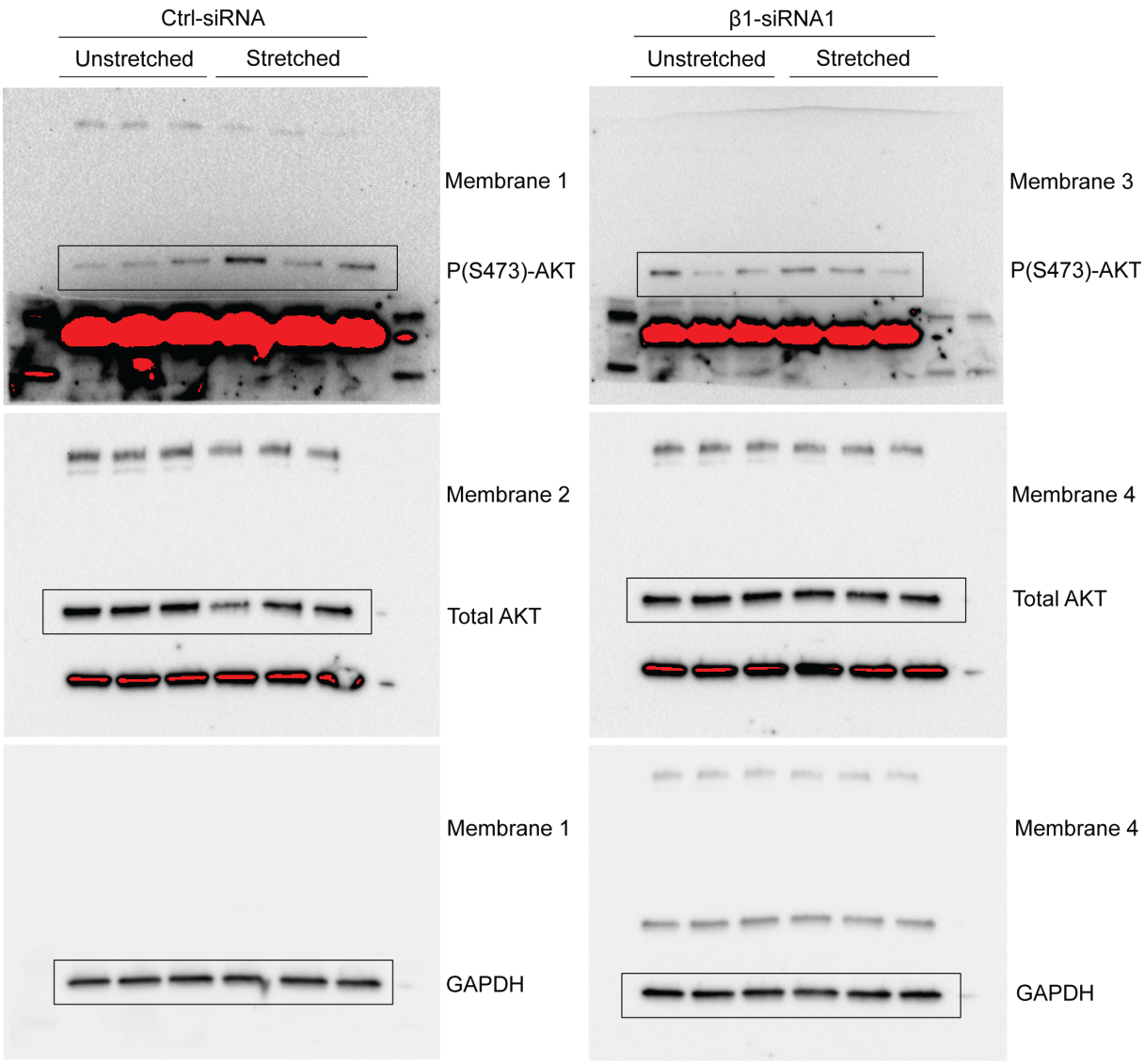

Supplementary Figure 4: Uncropped Western blot images used for Fig. 3.30.
Cropped regions are indicated by black frames. Oversaturated pixels due to the long exposure were automatically labeled red.

Statutory declaration

I herewith declare that I have composed the present dissertation independently and without use of any other than cited sources and aids in compliance with “Grundsätze zur Sicherung guter wissenschaftlicher Praxis an der Heinrich-Heine-Universität Düsseldorf”. This thesis, in the same or a similar form, has not been submitted to any other academic institution. I further declare that I did not absolve any promotion attempts before.

Düsseldorf,

_____

Anna Branopolski

Eidesstattliche Erklärung

Hiermit erkläre ich an Eides Statt, dass ich die vorliegende Dissertation selbständig und ohne Benutzung anderer als der angegebenen Quellen und Hilfsmittel unter Beachtung der "Grundsätze zur Sicherung guter wissenschaftlicher Praxis an der Heinrich-Heine Universität Düsseldorf" verfasst habe. Diese Arbeit ist - in gleicher oder ähnlicher Form - bei keiner anderen wissenschaftlichen Einrichtung eingereicht worden. Ich erkläre ferner, dass ich zuvor keine Promotionsversuche unternommen habe.

Düsseldorf,

_____

Anna Branopolski

Danksagung

Als Erstes möchte ich mich bei meinem Doktorvater Eckhard Lammert dafür bedanken, dass er mir ermöglicht hat, diese Dissertation in seinem Institut zu verwirklichen. Ich bin sehr dankbar für seine kontinuierliche Unterstützung sowie die vielen konstruktiven Anregungen und Denkanstöße in wissenschaftlicher und menschlicher Hinsicht.

Des Weiteren danke ich Malte Kelm für die Übernahme des Zweigutachters, für seine Unterstützung im Projekt und unsere konstruktiven Gespräche.

Ich möchte mich bei Christian Heiss als meinem Co-Betreuer für die vielen konstruktiven Gespräche, seine wertvollen Tipps und Unterstützung bedanken.

Bei Uli Flögel bedanke ich mich für die Ermöglichung und liebevolle Begleitung der MR-Versuche sowie den wissenschaftlichen Austausch. In diesem Zusammenhang danke ich auch Sebastian Haberkorn für die kompetente Einführung in die MRT-Technik.

Mein herzlicher Dank gilt allen aktuellen und ehemaligen Mitgliedern des Instituts für Stoffwechselphysiologie für das entspannte, humorvolle und zugleich professionelle Arbeitsklima sowie ihre Hilfsbereitschaft und Zuverlässigkeit. Besonders danke ich meiner Projektpartnerin und Freundin Carina H. für die tolle Zusammenarbeit, die wissenschaftlichen Besprechungen und jahrelange Unterstützung; Gemeinsam haben wir Erfolgsmomente erlebt, aber auch wichtige Hürden gemeistert. Bei Sofia U. bedanke ich mich herzlich für die Freundschaft und Unterstützung in menschlicher und wissenschaftlicher Hinsicht. Barbara B., Silke J. und Andrea K. danke ich für die große Unterstützung in technischer und menschlicher Hinsicht. Außerdem danke ich: Haiko K. für die tollen Mensa-Meetings und den musikalischen Austausch; Daniel E. für die wissenschaftlichen Gespräche, ausführliche Erklärungen von statistischen Methoden und kreative jazzige Einheiten; Esther H. für ihre Hilfe und fürs Zuhören; Oksana L. für die verantwortungsvolle Übernahme der Experimente. Ich danke auch allen anderen Institutsmitgliedern, die meine Promotionszeit bereichert haben, vor allem Linda G.-S., Okka S., Jessi M., Laura W., Silke O., Jennifer A., Laura H., Fatma D., Angela P., Tobi B. und Paula F.

Ich bedanke mich bei dem gesamten SFB 1116 dafür, dass ich an diesem Programm sowie an diversen interessanten Veranstaltungen teilnehmen durfte.

Außerdem bedanke ich mich bei meinen Freunden für die jahrelange Freundschaft, fürs Lachen und die vielen unvergesslichen Momente.

Vom ganzen Herzen bedanke ich mich bei meiner Familie, insbesondere bei meinem Mann, meiner Schwerster, meinen Eltern und Schwiegereltern, für die große Unterstützung und den Glauben an mich. Abschließend danke ich meinem Sohn für die wunderschönen Momente und einfach dafür, dass er da ist.